

# **Synthesis of a 7-Membered Biaryl Guanidine Catalyst and its Use in the Vinylogous Aldol Reaction**

B.Sc. (Honours), Brock University, 2011

Biotechnology

A thesis submitted in partial fulfillment of the requirements for the degree of  
Masters of Science

Faculty of Mathematics and Science, Brock University,  
St. Catharines Ontario

© Mohamed Hassan 2014

## **ABSTRACT:**

The present thesis outlines the preparation of a 7-membered guanidine. Initial efforts to obtain this guanidine via 2-chloro-1,3-dimethylimidazolinium chloride induced ring forming chemistry failed to provide the target in a reproducible fashion. Changing strategies, we were able to obtain the desired guanidine through CuCl mediated amination of a 7-membered thiourea intermediate to arrive at the target. In addition, the catalytic activity of this compound was evaluated in a vinylogous aldol reaction of dibromofuranone and four aromatic aldehydes to generate chiral  $\gamma$ -butenolides with modest to good enantiomeric excess. It was found that electron-poor aldehydes resulted in higher, 81% ee, whereas electron rich aldehydes led to low, 41% ee, levels of enantiomeric excess.

## **ACKNOWLEDGMENTS:**

First and foremost, I would like to thank my supervisor and mentor, Professor Travis Dudding, for supporting me and investing his time in developing my understanding of organic chemistry. His continued guidance and insight have played a major role in increasing my appreciation for researching. I would also like to thank my examining committee members, Professors Metallinos and Van der Est. for their assistance during the course of this project. I would like to thank professor Metallinos for welcoming me into his lab to use his equipment. Completion of this project would not have been possible without your help, thank you.

To members of the Dudding group, it has been a wonderful learning experience working with you all. I am grateful for the countless thoughtful discussions we've shared in the lab. In particular, I would like to thank Lee Belding and Roya Mirabdolbaghi for setting an excellent example to follow. I wish you both the best of luck in your sure to be bright futures.

To my parents, I doubt that any language has words strong enough to express my gratitude for everything you have done for me. I would like to thank you both for your endless patience and motivation; your encouraging voices kept me going when my tank was empty.

## **TABLE OF CONTENTS**

<b>1.1: LIST OF TABLES:</b> .....	v
<b>1.2: LIST OF FIGURES:</b> .....	vi
<b>1.3: LIST OF SCHEMES:</b> .....	viii
<b>1.4: LIST OF ABBREVIATIONS:</b> .....	x
<b>2.0: INTRODUCTION</b> .....	1
2.1: Natural product synthesis and the butenolide motif.....	1
2.2: Synthesis of $\gamma$ -substituted butenolides .....	3
2.3: Vinylogous aldol reaction .....	8
2.4: Guanidine functionality.....	14
2.5: Guanidines as organocatalysts .....	17
2.6: Approaches towards guanidine synthesis.....	21
2.6.1: Classical methods of guanidine preparation .....	21
2.6.2: DMC induced cyclization .....	24
2.6.3: CuCl mediated chemistry.....	27
2.7: Study objectives .....	30
3.1: Synthesis of chiral auxiliary and DMC induced cyclization.....	34
3.2: Thiourea synthesis and CuCl mediated amination chemistry .....	41
3.3: Evaluation of catalytic guanidine core in vinylogous aldol reaction .....	45
<b>4.0: CONCLUDING REMARKS AND FUTURE WORK</b> .....	53
<b>5.0: EXPERIMENTAL</b> .....	56
5.1: Synthesis of 1,1'-biphenyl-2,2'-diamine ( <b>60</b> ) .....	57
5.2: Synthesis of ( <i>R</i> )-2-amino-3-phenylpropan-1-ol ( <b>56</b> ) .....	58
5.3: Synthesis of ( <i>R</i> )-1-(( <i>tert</i> -butyldimethylsilyl)oxy)-3-phenylpropan-2-amine ( <b>57</b> ) .....	59
5.4: Synthesis of ( <i>R</i> )- <i>tert</i> -butyl (2-isothiocyanato-3-phenylpropoxy)dimethylsilane ( <b>52</b> ) .....	60
5.5: Synthesis of ( <i>R</i> )-1-(2'-amino-[1,1'-biphenyl]-2-yl)-3-(1-( <i>tert</i> - butyldimethylsilyl)oxy)-3-phenylpropan-2-yl)thiourea ( <b>53</b> ) .....	61

5.7: General procedure of 2-chloro-1,3-dimethylimidazolinium chloride (DMC) preparation ( <b>45</b> ) .....	62
5.8: Synthesis of 5H-dibenzo[d,f][1,3]diazepine-6(7H)-thione ( <b>55</b> ) .....	63
5.9: Synthesis of ( <i>R</i> )-1-(( <i>tert</i> -butyldimethylsilyl)oxy)-N-(5H-dibenzo[d,f][1,3]diazepin-6(7H)-ylidene)-3-phenylpropan-2-amine ( <b>48</b> ) .....	64
5.10: 3, 4-dibromo-5-((4-bromophenyl)(hydroxy)methyl)furan-2(5H)-one ( <b>63</b> ). ....	67
5.11: 3, 4-dibromo-5-((4-chlorophenyl)(hydroxy)methyl)furan-2(5H)-one ( <b>64</b> ). ....	68
5.12: 3, 4-dibromo-5-((4-methoxyphenyl)(hydroxy)methyl)furan-2(5H)-one ( <b>65</b> ). ....	69
5.13: 3, 4-dibromo-5-(hydroxyl(phenyl)methyl)furan-2(5H)-one ( <b>66</b> ). ....	70
6.0: <b>REFERENCES</b> .....	71
7.0: <b>SELECTED SPECTRA</b> .....	76

## 1.1: LIST OF TABLES:

<b>Table 1:</b> Substrate scope for CuCl mediated amination of tartaric acid derivatives.....	29
<b>Table 2:</b> Yield optimization of phenylalanine reduction .....	35
<b>Table 3:</b> Temperature and time dependence of DMC induced cyclization .....	40
<b>Table 4:</b> Temperature dependence of thiourea forming reaction in pyridine. ....	42
<b>Table 5:</b> Time and temperature dependency of vinylogous aldol reaction of mucobromic acid and 4-bromobenzaldehyde catalyzed by point chiral guanidine <b>48</b> .....	47
<b>Table 6:</b> Catalytic activity of point chiral guanidine compound in vinylogous aldol reaction with varied aldehyde substrates. ....	49

## 1.2: LIST OF FIGURES:

<b>Figure 1:</b> General $\gamma$ - butenolide motif. ....	2
<b>Figure 2:</b> Biologically active butenolide core. ....	3
<b>Figure 3:</b> Chemical transformations of mucohalic acids to corresponding $\gamma$ -butenolides...	4
<b>Figure 4:</b> Ti (IV) salicylidene catalyst <b>12</b> and copper (II) fluoride catalyst <b>13</b> . ....	11
<b>Figure 5:</b> Terada's axially chiral guanidine catalyst. ....	12
<b>Figure 6:</b> Examples of the guanidine functionality in naturally occurring compounds. ...	14
<b>Figure 7:</b> Resonance stabilized guanidinium cation. ....	15
<b>Figure 8:</b> pKa of various guanidine groups in acetonitrile. ....	15
<b>Figure 9:</b> Proton sponge; 1,8-bis(dimethylamino)naphthalene (DMAN). ....	16
<b>Figure 10:</b> Classical guanidine synthesis. ....	21
<b>Figure 11:</b> Target guanidine architecture. ....	31
<b>Figure 12:</b> Favored <i>syn</i> and <i>anti</i> isomers based on literature optical rotation. ....	50
<b>Figure 13:</b> Proposed vinylogous aldol catalytic cycle. ....	51
<b>Figure 14:</b> Axially chiral derivative of parent guanidine catalyst. ....	53
<b>Figure 15:</b> Modification at nitrogens of thiourea towards varied guanidine cores. ....	54
<b>Figure 16:</b> $\gamma$ -butenolide isomers from the vinylogous aldol reaction catalyzed by <b>48</b> .....	65

<b>Figure 17:</b> $^1\text{H}$ and $^{13}\text{C}$ NMR spectra of <b>60</b> .....	76
<b>Figure 18:</b> $^1\text{H}$ and $^{13}\text{C}$ NMR spectra of <b>56</b> .....	77
<b>Figure 19:</b> $^1\text{H}$ and $^{13}\text{C}$ NMR spectra of <b>57</b> .....	78
<b>Figure 20:</b> $^1\text{H}$ and $^{13}\text{C}$ NMR spectra of <b>52</b> .....	79
<b>Figure 21:</b> $^1\text{H}$ and $^{13}\text{C}$ NMR spectra of <b>53</b> .....	80
<b>Figure 22:</b> $^1\text{H}$ and $^{13}\text{C}$ NMR spectra of <b>55</b> .....	81
<b>Figure 23:</b> $^1\text{H}$ and $^{13}\text{C}$ NMR spectra of point chiral guanidine catalyst <b>48</b> .....	82
<b>Figure 24:</b> $^1\text{H}$ and $^{13}\text{C}$ NMR spectra of <i>syn</i> <b>66</b> .....	83
<b>Figure 25:</b> $^1\text{H}$ and $^{13}\text{C}$ NMR spectra of <i>anti</i> <b>66</b> .....	84
<b>Figure 26:</b> $^1\text{H}$ and $^{13}\text{C}$ NMR spectra of <i>syn</i> <b>63</b> .....	85
<b>Figure 27:</b> $^1\text{H}$ and $^{13}\text{C}$ NMR spectra of <i>anti</i> <b>63</b> .....	86
<b>Figure 28:</b> $^1\text{H}$ and $^{13}\text{C}$ NMR spectra of <i>syn</i> <b>64</b> .....	87
<b>Figure 29:</b> $^1\text{H}$ and $^{13}\text{C}$ NMR spectra of <i>anti</i> <b>64</b> .....	88
<b>Figure 30:</b> $^1\text{H}$ and $^{13}\text{C}$ NMR spectra of <i>syn</i> <b>65</b> .....	89
<b>Figure 31:</b> $^1\text{H}$ and $^{13}\text{C}$ NMR spectra of <i>anti</i> <b>65</b> .....	90



### 1.3: LIST OF SCHEMES:

<b>Scheme 1:</b> Knoevenagel condensation.....	5
<b>Scheme 2:</b> Indium (III) triflate catalyzed Friedel-Crafts hydroxylalkylation .....	6
<b>Scheme 3:</b> Indium mediated allylation of mucoholic acid.....	7
<b>Scheme 4:</b> Iminium catalyzed 1,4- Mukaiyama-Michael addition. ....	8
<b>Scheme 5:</b> Regio and stereo chemical issues in the vinylogous reaction. ....	9
<b>Scheme 6:</b> Vinylogous aldol reaction catalyzed by chiral B and Ti complexes. ....	10
<b>Scheme 7:</b> Guanidine catalyzed vinylogous aldol reaction.....	13
<b>Scheme 8:</b> Guanidine catalyzed Michael additon .....	17
<b>Scheme 9:</b> Guanidine catalyzed nucleophilic epoxidation.....	19
<b>Scheme 10:</b> Guanidine catalyzed Diels-Alder reaction .....	20
<b>Scheme 11:</b> Rao's approach to cyclic guanidines. ....	22
<b>Scheme 12:</b> Chinchilla's approach to substituted guanidine motifs .....	23
<b>Scheme 13:</b> Homochiral guanidine synthesis via isocyanate intermediates. ....	24
<b>Scheme 14:</b> Guanidine synthesis via iminium chloride intermediates.....	25
<b>Scheme 15:</b> DMC mediated intramolecular guanidine formation from thiourea. ....	26
<b>Scheme 16:</b> Copper (I) promoted amination of thiourea .....	27
<b>Scheme 17:</b> Scope of CuCl mediated guanidine synthesis .....	28
<b>Scheme 18:</b> DMC approach towards 7-membered guanidine <b>48</b> .....	32
<b>Scheme 19:</b> CuCl mediated amination of aromatic thiourea .....	33
<b>Scheme 20:</b> Vinylogous aldol reaction of aromatic aldehydes and mucubromic acid.....	33
<b>Scheme 21:</b> Approach towards point chiral thioisocyanate. ....	34
<b>Scheme 22:</b> DMC preparation from commercially available imidazolidnone.....	36

<b>Scheme 23:</b> One pot synthesis thioisocyanate <b>52</b> mediated by DMC salt. ....	37
<b>Scheme 24:</b> Condensation of biaryl diamine backbone to the point chiral head group .....	38
<b>Scheme 25:</b> Sequence to catalyst ( <i>R</i> )- <b>48</b> through DMC induced cyclization. ....	39
<b>Scheme 26:</b> CuCl coupling of aromatic thiourea to point chiral auxiliary. ....	41
<b>Scheme 27:</b> Generation of reactive substrates for the CuCl mediated amination .....	43
<b>Scheme 28:</b> Potentially competing coupling reaction during CuCl mediated conditions..	44
<b>Scheme 29:</b> Vinylogous aldol reaction catalyzed by <b>48</b> . ....	46

## 1.4: LIST OF ABBREVIATIONS:

(CD <sub>3</sub> ) <sub>2</sub> SO	Deuterated dimethylsulfoxide	equiv.	equivalents
m.p	melting point	pyr	pyridine
conc.	concentration	e.r.	enantiomeric ratio
DMC	2-chloro-1,3-dimethylimidazolinium chloride	ppm	parts per million
dr	disastereomeric ratio	BINAM	1,1'-binaphthyl-2,2'-diamine
ee	enantiomeric excess	aq.	aqueous
EI	Electron ionization	OTf	trifluoromethanesulfonate
h	hour(s)	DIAD	Diisopropyl azodicarboxylate
HPLC	high performance liquid chromatography	TPP	triphenylphosphine
HRMS	high resolution mass spectroscopy	Boc	N- <i>tert</i> -butoxycarbonyl
Hz	Hertz	DMAN	1,8-bis(dimethylamino)naphthalene
M	molar concentration	Pd/C	palladium on carbon
MHz	Megahertz	MeCN	acetonitrile
min(s)	minutes(s)	CDCl <sub>3</sub>	deuterated chloroform
NMR	Nuclear magnetic resonance	<sup>i</sup> Pr	isopropyl
rt	room temperature	de	diastereomeric excess
TBAF	Tetra- <i>n</i> -butylammonium fluoride	EtOH	ethanol
TBDMS	<i>tert</i> -butyldimethylsilyl	MeOH	methanol
THF	tetrahydrofuran	TLC	Thin layer chromatography

## **2.0: INTRODUCTION**

### **2.1: Natural product synthesis and the butenolide motif**

Since the milestone achievement in organic chemistry marked by Wöhler's synthesis of urea, significant progress has been achieved in the discipline.<sup>1,2</sup> This unyielding progress was fuelled in large part by the pharmaceutical sector's demand for new methodologies and reagents for the synthesis of core structures of medicinally active natural products.

Often times, pharmaceutical drugs and natural products contain at least one chiral carbon center; complicating their preparation by traditional methods. Chirality, from a synthesis point of view, can be arrived at from limited avenues. Without exception, chirality in synthetic chemistry is achieved by using optically pure starting materials and reagents; namely, chiral auxiliaries, chiral reagents, or asymmetric synthesis. Optically active starting materials and reagents have customarily included sugars, amino acids, and metabolites isolated from biological sources. Through electronic and steric effects operating during the course of a reaction, these naturally occurring sources of chirality induce or transfer stereoselectivity to the intermediates and products of the reactions.

Arriving at enantiomerically pure pharmaceutical products has served as a prominent driving force in the pursuit of improved control over the stereochemical output of organic reactions. To this end, new catalysts, ligands, and their respective

applications are reported continuously to satisfy the need for wider ranges of reaction conditions and to improve the efficiency of existing asymmetric processes.

Of particular relevance to the present work, is the asymmetric synthesis of a class of biologically active lactones, which possess an unsaturated four-carbon cyclic ester scaffold, known as butenolides, specifically  $\gamma$ -butenolides (**Figure 1**). Complicating their construction is the creation of two adjacent stereo centers, the configuration of which will depend on the synthetic sequence and methodology used to obtain the motif.

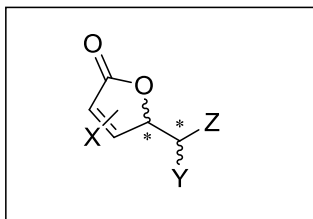


**Figure 1:** General  $\gamma$ - butenolide motif.

Reports of studies confirming that  $\gamma$ -butenolide containing natural products exhibited antibiotic,<sup>3</sup> antitumor,<sup>4</sup> and cytotoxic<sup>5</sup> activities have made the quest for methodologies to supply these promising modules worthwhile.

Examples of such natural products include the biologically active  $\gamma$ - substituted butenolide core include hirsutinolides **1** and **2** (**Figure 2**), isolated from the African plant *Vernonia staehelinoides*.<sup>6</sup> These motifs have been shown, through bio-assay guided fractionation, to possess antiplasmodial activity against a protozoan parasite, *Plasmodium falciparum*, accredited with triggering malaria.<sup>6</sup> The butenolide rings in these hirsutinolides were deduced to be the pharmacophores responsible for the

observed antiparasitic activity.<sup>6</sup> As a result of the biological activities associated with the butenolide structure and its many derivatives, great efforts have been devoted towards the development methodologies for their facile construction *en route* to natural product synthesis.

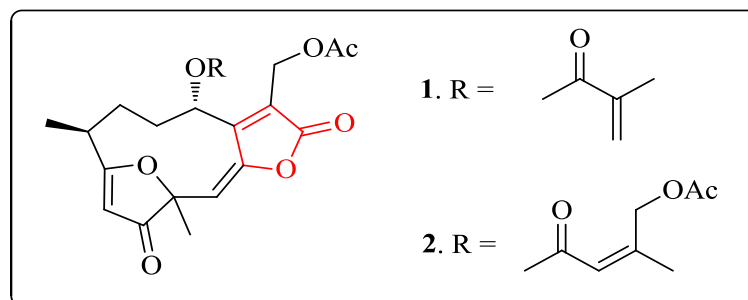


**Figure 2:** Biologically active butenolide core.

## 2.2: Synthesis of $\gamma$ -substituted butenolides

With representation in over 13,000 natural products, the  $\gamma$ - functionalized butenolide synthon, a prominent class of butenolides, has emerged as a valuable architectural platform for the development of new synthetic methodologies.<sup>7</sup> Recently, an array of reports have emerged outlining creative syntheses of  $\gamma$ -substituted butenolides from the relatively inexpensive and commercially available mucochloric and mucobromic acids (**Figure 3**), generically referred to as mucohalic acids.

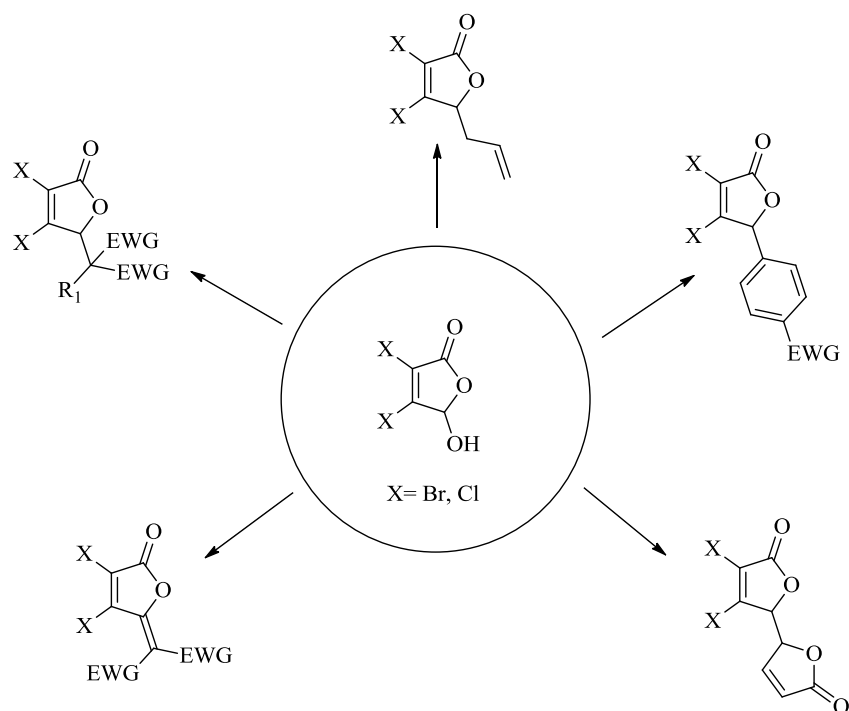
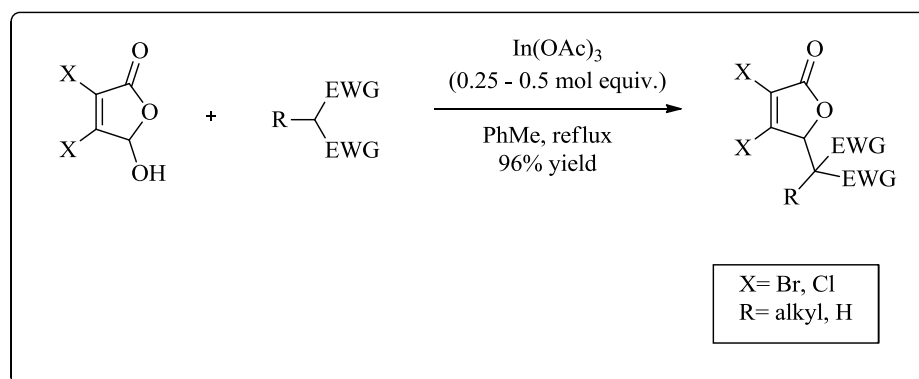


**Figure 3:** Chemical transformations of mucohalic acids to corresponding  $\gamma$ -butenolides.

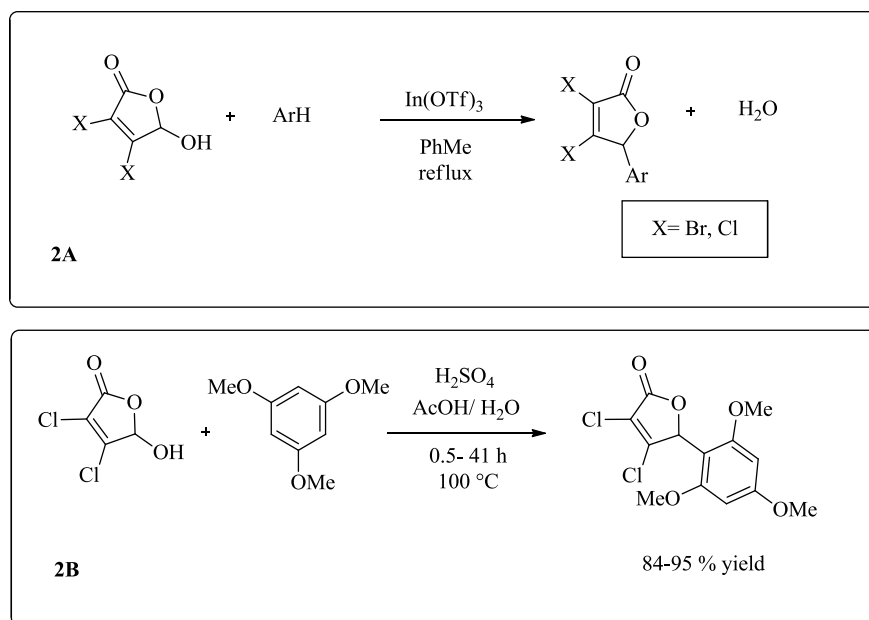
In 2005, Zangh and co-workers disclosed the use of Lewis acid (indium (III) salts) to catalyze the carbon-carbon bond forming Knoevenagel condensation (**Scheme 1**).<sup>8</sup> Performing the reaction in toluene, they used an *in situ* generated aldehyde from the open form mucohalic acid and an activated methylene compound to arrive at the corresponding butenolide. Although inherently lacking stereoselectivity, this methodology provided access to the desired targets in impressive yields.



**Scheme 1:** Knoevenagel condensation.

Another example of a procedure for preparing  $\gamma$ -substituted butenolides involved the indium (III) triflate catalyzed Friedel-Crafts hydroxylalkylation reported by Zhang in 2007.<sup>9</sup> In addition to the indium triflate mediated approach (**Scheme 2A**), Zhang and co-workers devised a more environmentally friendly metal free modification, with sulfuric acid as a catalyst, that had comparable yields and reaction times to the indium mediated process (**Scheme 2B**).



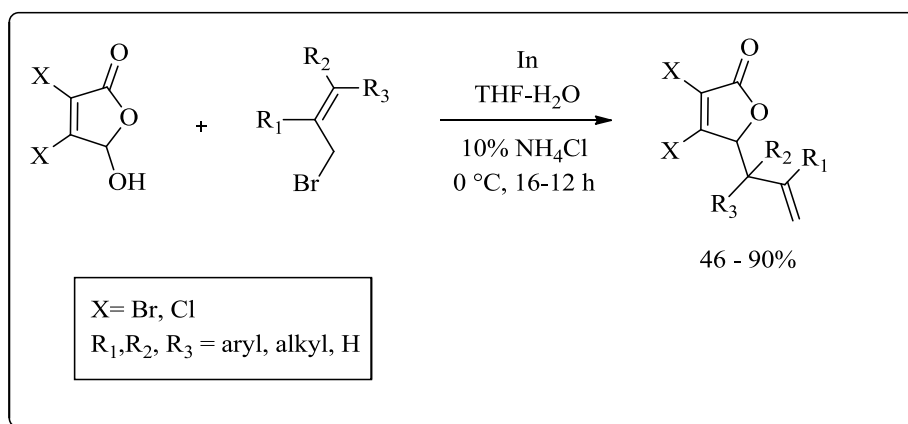


**Scheme 2:** Indium (III) triflate catalyzed Friedel-Crafts hydroxylalkylation.

Their disclosure employing sulfuric acid to catalyze the reaction between mucochloric acid and 1,3,5-trimethoxybenzene with high yield (84-95% yield) of the isolated product paved the road towards a green extension of this chemistry expanding the approaches towards  $\gamma$ -butenolide synthesis (**Scheme 2B**).<sup>9</sup>

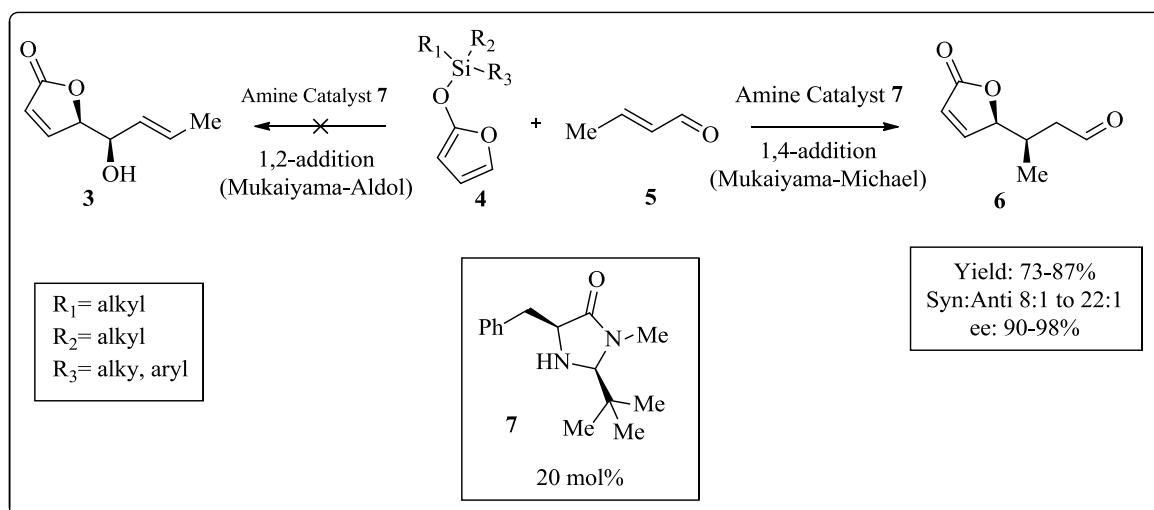
In a supplementary effort to exploit mucohalic acid derivatives as simple starting materials towards  $\gamma$ -functionalized butenolides, a report of the use of indium mediated allylation appeared.<sup>10</sup> This approach allows for generating the desired butenolides with an alkene handle at the  $\gamma$ -position of the unsaturated lactone rendering it a useful methodology to furnish key intermediates towards natural products. The methodology employs a THF-H<sub>2</sub>O solvent system and is mediated by indium in the presence of 10% NH<sub>4</sub>Cl (**Scheme 3**). Much like the previously outlined

avenues to furnish these  $\gamma$ -functionalized butenolides, this methodology fails to address stereo induction in the newly generated carbon-carbon bond.



**Scheme 3:** Indium mediated allylation of mucoholic acid.

The demand for a  $\gamma$ -butenolide generating reaction catalyzed by an organic molecule was met by efforts of the MacMillan group in 2003 when they revealed methodology identifying iminium catalysis as a valuable strategy for the asymmetric synthesis of  $\gamma$ -butenolide architecture from the coupling of simple  $\alpha$ ,  $\beta$ -unsaturated aldehydes **5** and silyloxy furans **4**.<sup>7</sup> Notably, by employing an imidazolidinone catalyst **7**, they were able to observe not only good diastereo and enantio induction but the reaction also favored the 1,4-Mukaiyama-Michael addition as opposed to the competing 1,2-Mukaiyama-aldol addition (**Scheme 4**).



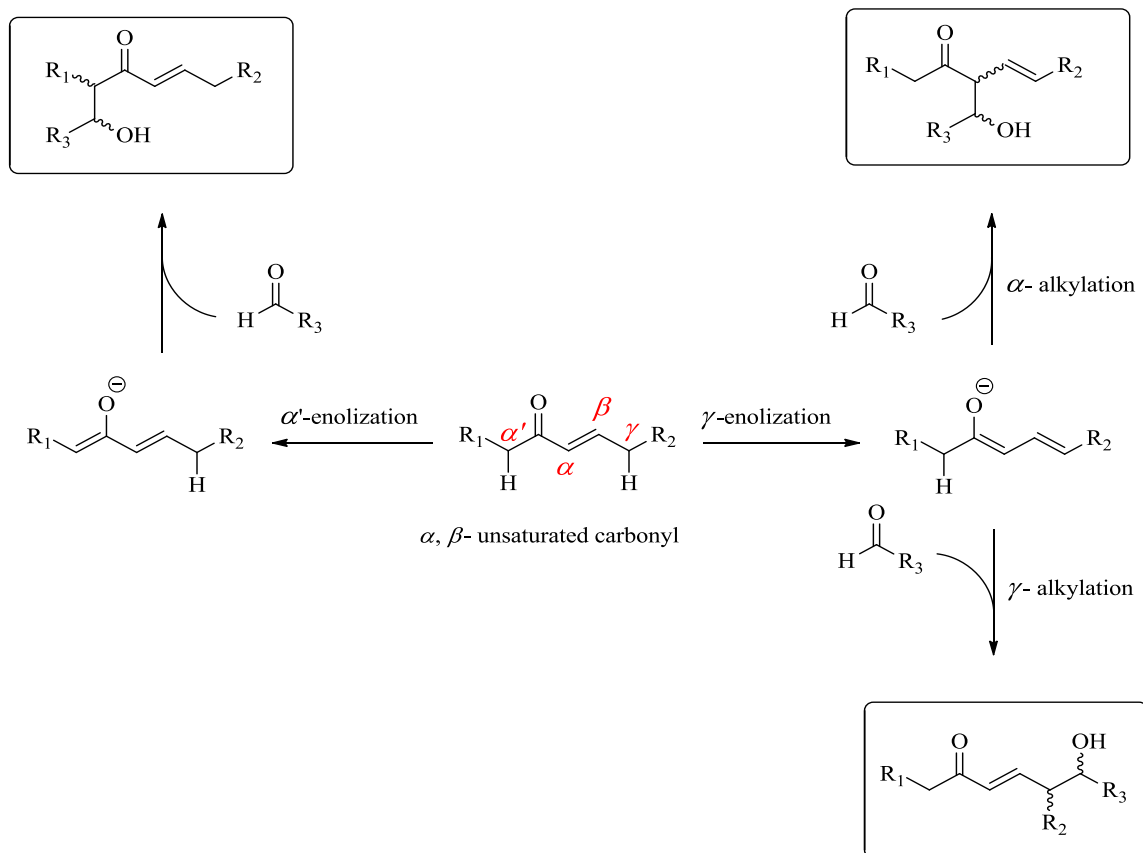
**Scheme 4:** Iminium catalyzed 1,4-Mukaiyama-Michael addition.

### 2.3: Vinylogous aldol reaction

Yet another potential approach towards the  $\gamma$ -substituted butenolide motif is the vinylogous aldol reaction, which is one of the most ubiquitous reactions in organic chemistry. Its vinylogous extension has been extensively investigated as it provides access to functionalized hydroxyl carbonyl compounds that contain a useful handle in the form of the double bond functionality.<sup>11</sup> Vinylogous reactions are known to proceed by the transmission of electronic effects through a conjugated  $\pi$ -system to the reactive center from which carbon-carbon bonds are to be formed.<sup>12</sup>

Historically, the achiral versions of vinylogous aldol reaction have been successfully catalyzed by metallic complexes, some of which included titanium, rhodium and copper catalytic cores.<sup>13-15</sup> However, the structural complexity achieved through the vinylogous aldol reaction and the variability of the alkylation patterns,  $\alpha$ -

alkylation vs.  $\gamma$ -alkylation (**Scheme 5**), have only recently begun to receive adequate attention as the effects of solvent, enolate counter ion, and temperature remain in need of further exploration. Pioneering attempts to resolve these difficulties and to expand the utility of the vinylogous aldol reaction employed chiral catalysts were introduced.

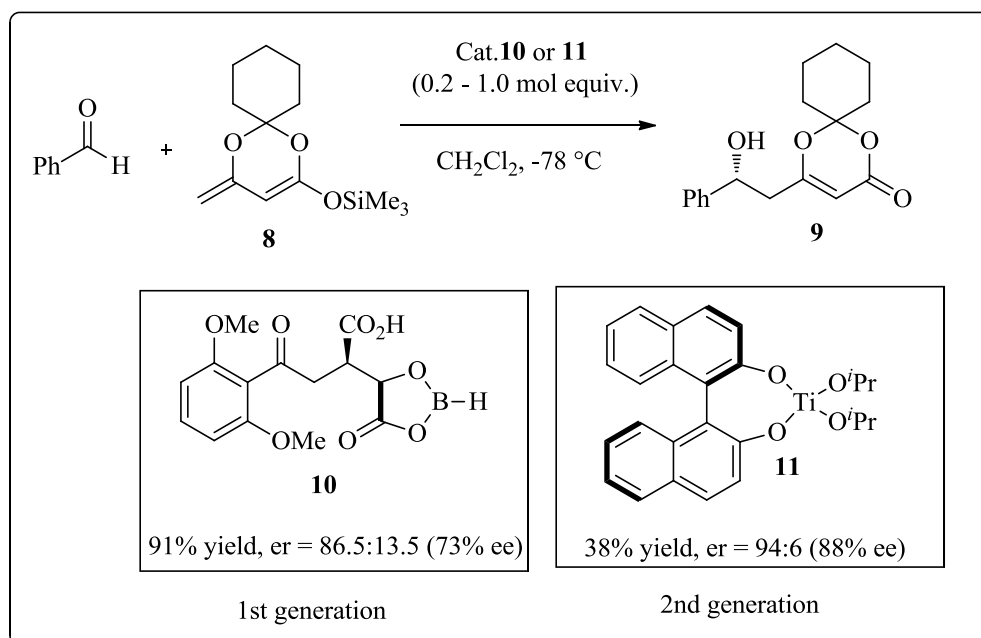


**Scheme 5:** Regio and stereo chemical issues in the vinylogous reaction.

Among the earliest efforts to target catalytic asymmetric vinylogous aldol reactions was the exploration of chiral borane species to control the cross addition of dienoxysilanes **8** to prochiral aldehydes. Although this approach (**Scheme 6**) provided

desired aldol product **9** at high yields and moderate enantiomeric excess, it required especially high loading of chiral borane reagent **10** rendering the approach inefficient.<sup>16</sup>

Disclosure by the same authors soon followed to provide an improved catalyst turnover number by making use of a titanium (IV) BINOL moiety **11** to catalyze the same reaction (**Scheme 6**). Although this alteration resulted in a significantly lowered catalytic loading and increased enantiomeric excess, it lead to an undesired decrease in reaction yield from 93% with the borane catalyst to 38% yield with the titanium species (**Scheme 6**).



**Scheme 6:** Vinylogous aldol reaction catalyzed by chiral B and Ti complexes.

Carreira and Singer developed the superior Ti (IV) -salicylidene binaphthyl catalyst **12** (**Figure 4**).<sup>17</sup> This report provided access to a collection of protected  $\delta$ -hydroxy acetoacetate adducts in high yields and very good asymmetric induction with enantiomeric excess ranging from 80-91%, although requiring 20 mol % catalytic loading. A more promising copper (II) fluoride catalyst **13** (**Figure 4**) was advanced a short time after Carreira's disclosure to furnish the same  $\delta$ -hydroxyl acetoacetate adducts in excellent yields and enantiomeric excess all the while maintaining a significantly lowered catalyst loading of 2 mol %.<sup>18</sup>

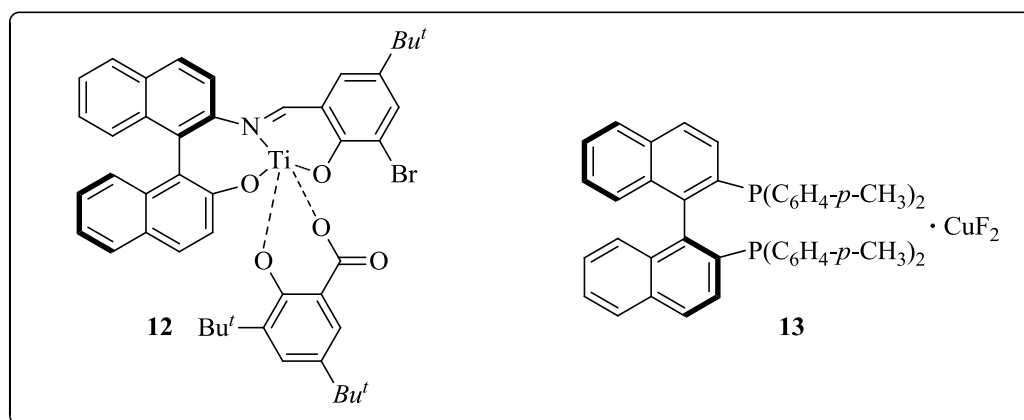


**Figure 4:** Ti (IV) salicylidene catalyst **12** and copper (II) fluoride catalyst **13**.

In summation to the deficiency in catalytic turn over observed with the bulk of the above mentioned metal complex catalyzed vinylogous aldol reactions and others reported in the literature,<sup>19-21,22</sup> and the inherent toxicity of metals and their relatively expensive nature, resulting from high catalyst loading, inspired interest in the development of analogous organic catalysts.

As such, methodologies towards the construction of the  $\gamma$ -substituted butenolide motif by way of vinylogous aldol reactions of butenolides and prochiral aldehydes (**Scheme 2**) asymmetrically catalyzed by the more basic guanidine core containing derivatives (**Figure 4**) began to appear in the literature.<sup>23</sup>

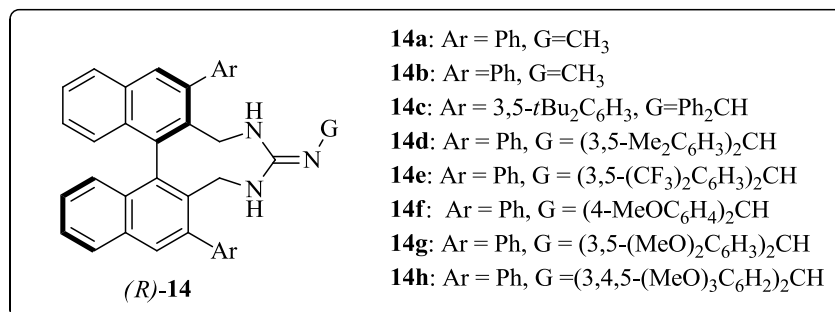
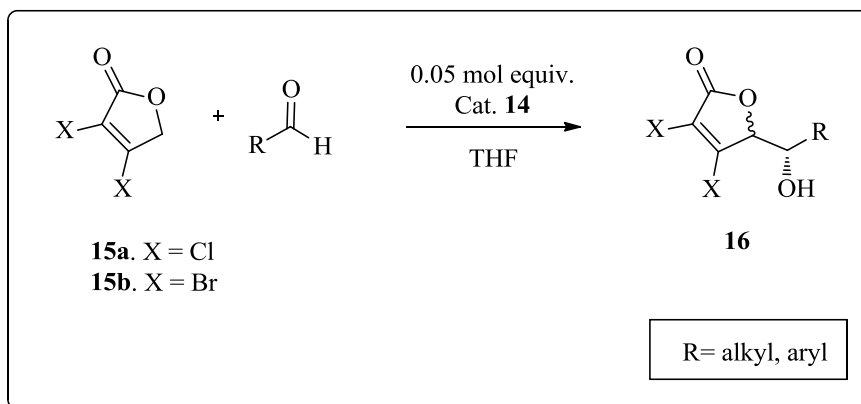


**Figure 5:** Terada's axially chiral guanidine catalyst.

A seminal example of a catalytic guanidine core being exploited towards the construction of  $\gamma$ -substituted butenolides was reported by Terada *et al.* in 2010.<sup>24</sup> Terada's work introduced a class of 9-membered axially chiral guanidine **14** (**Figure 5**) for the asymmetric vinylogous aldol reaction illustrated in **scheme 7**.

Derivatives of this catalyst were prepared by varying the steric bulk at the 3, 3'-positions (Ar in **Figure 5**) of the axially chiral backbone and the head group (G in **Figure 5**) to assess the effects of such steric and electronic modifications on the enantioselectivity of the reaction. Test reactions were carried out to determine the optimal solvent, temperature and catalyst loading from which it was found that the

yield and enantiomeric excess benefited from using THF as a solvent at -40 °C with 5 mol % catalyst loading.



**Scheme 7:** Guanidine catalyzed vinylogous aldol reaction.

By altering these structural and electronic elements, Terada was able to observe marked differences not only in the enantio- and diastereo-selectivity of the reaction, but also on the catalytic activities. The introduction of bulky benzyl substituents on the head guanidine nitrogen N (3) increased the catalytic activities and enantioselectivity when compared to those obtained with the sterically less-hindered methyl substituted guanidines.<sup>23,24</sup>

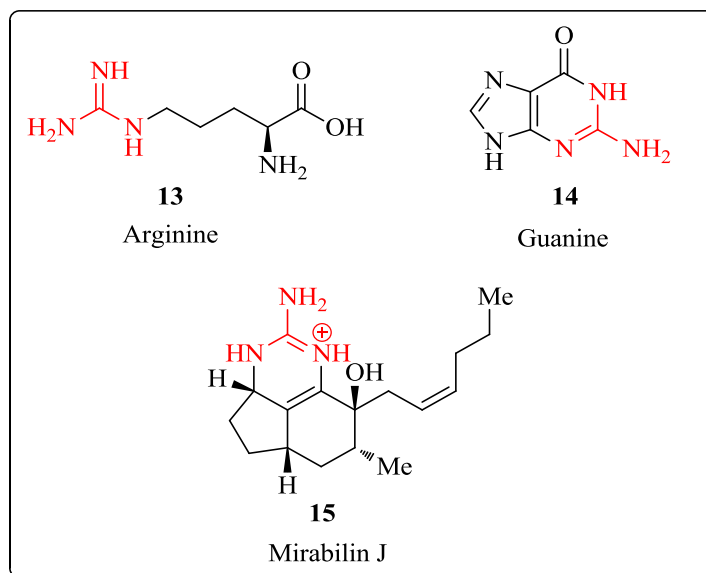
Interestingly, the favorable effects witnessed as a result of incorporation of steric bulk at the N(3) of the guanidine functionality were reversed when the steric bulk was introduced at the 3,3'-positions (in closer proximity to N(1) and N(2)) of the axially chiral binaphthyl backbone. Fine tuning the steric and electronic effects of this influential 9-membered guanidine catalyst delivered a suitable variant of the catalyst



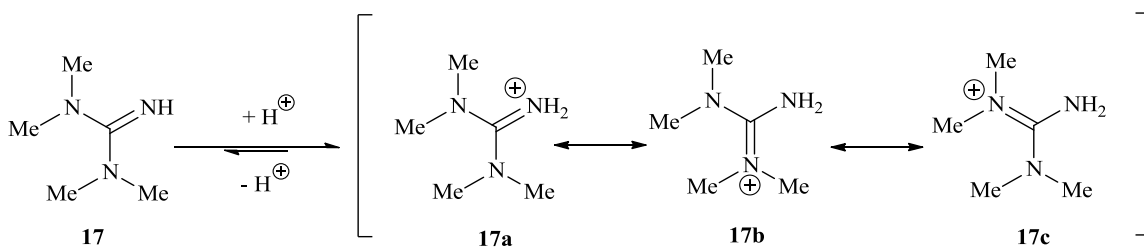
for probing the scope of the vinylogous aldol reaction. This variant, **14h** was substantially more electron rich than its structural analogues and thus more basic.<sup>23</sup>

## 2.4: Guanidine functionality

The guanidine functionality is found in countless molecules in nature from nucleotides and amino acids to secondary metabolites (**Figure 6**).<sup>25,26</sup> Its frame work consists of a central carbon bound to three nitrogen atoms. As a result of this unique distribution of electron rich atoms around a central carbon, the guanidinium cation is highly stabilized via resonance leading to the delocalization of positive charge (**Figure 7**).

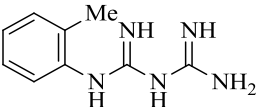
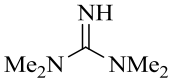
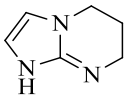
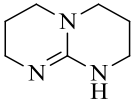


**Figure 6:** Examples of the guanidine functionality in naturally occurring compounds.



**Figure 7:** Resonance stabilized guanidinium cation.

As a consequence of this heightened guanidinium stability, the pKa of guanidines is generally high, and dwells in the neighborhood of 19-26 for some synthetically prepared analogs (**Figure 8**), designating them as potential superbases capable of remaining protonated over a wide pH range.<sup>27</sup>

				
pKa (MeCN)	19.43	23.30	25.45	25.96

**Figure 8:** pKa of various guanidine groups in acetonitrile.

It has been suggested by Ishikawa that there exists a discrepancy in the use of the term “superbase” to describe severe expression of basicity.<sup>28</sup> Often in these reports, the criteria justifying use of the term is ambiguous and dependent on the chemist who is reporting the work. One of the earliest definitions of the term super base comes from Caubere, who proposed that the term be kept for describing a base

that is the structural sum of two or more bases leading to new basic species with inherent new properties.<sup>28</sup>

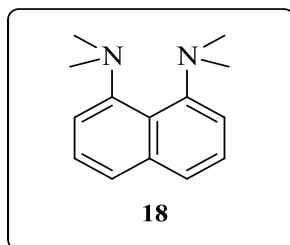


**Figure 9:** Proton sponge; 1,8-bis(dimethylamino)naphthalene (DMAN).

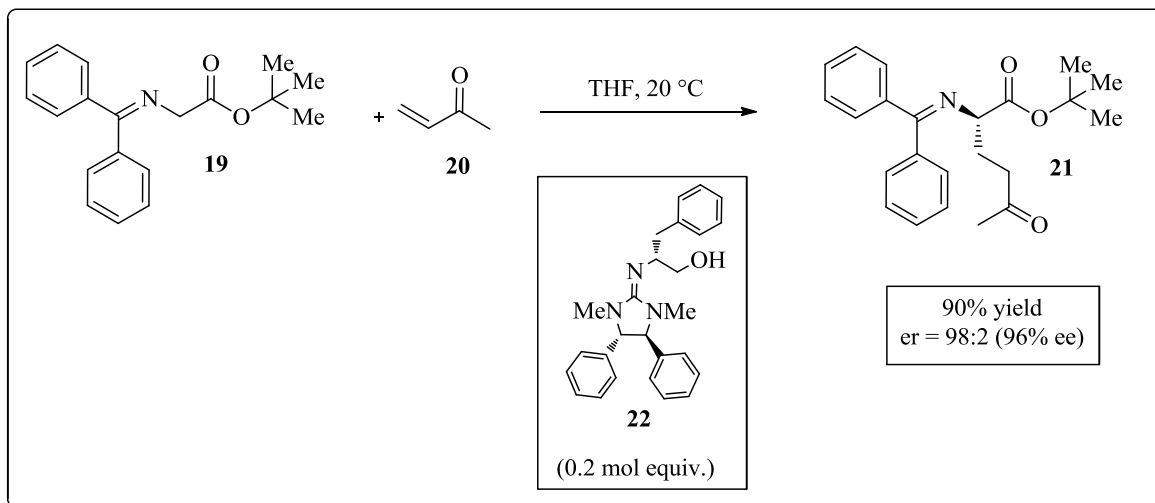
According to Caubere's definition, organic superbases should be a hybrid of two or more unique amine moieties and should express a new property not found in its parts.<sup>29</sup> A more modern and specific definition of the term was recently advanced by Ishikawa and it should be kept in mind when the term is used though out this work. Ishikawa defines a superbase as a nonionic powerful amine derivative with comparable to or higher basicity to that of the proton sponge (1,8-bis (dimethylamino) naphthalene; DMAN **18** in **Figure 9**).<sup>29</sup>

In addition to having unusually high lone-pair Lewis basicity, organic superbases are also commonly characterized by good kinetic activity in proton exchange processes and by the ability of their protonated forms to delocalize the positive charge via conjugation over two or more bonds (**Figure 6**), thus stabilizing the conjugate acid.<sup>30</sup> As such, guanidines are often categorized as superbases due to their strong basic nature and their ability to delocalize a positive charge. Superbase chemistry has been attracting increasing interest over the past two decades, from

synthetic and catalysis oriented investigators in hopes of further understanding and employing such systems as proton shuttles in asymmetric synthesis.

## 2.5: Guanidines as organocatalysts

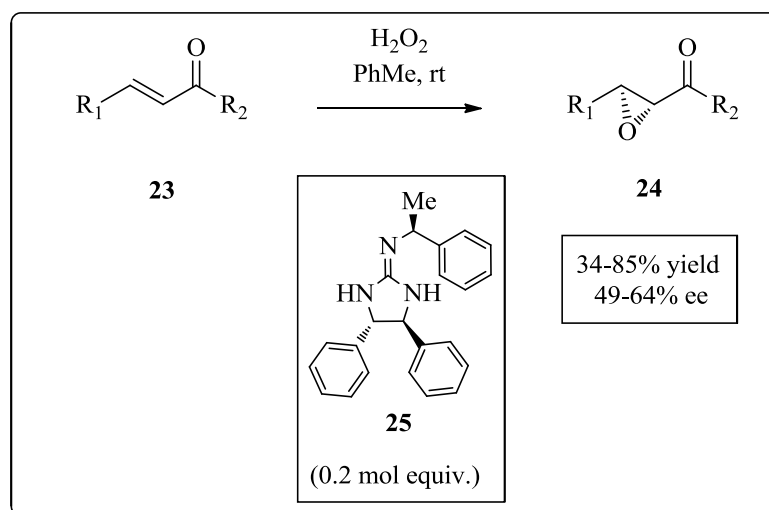
In the field of asymmetric organocatalysis, chiral guanidines represent a prominent class of molecules that have permitted a wide range of asymmetric organic transformations.<sup>31</sup> Branded as superbases, guanidines have been viewed as promising candidates to catalyze base-requiring organic reactions. Furthermore, they serve as promising catalysts from a green chemistry point of view as a result of their recycling potential and of projected ease of handling as well as the expected safety when compared to metal containing catalysts. Throughout this section a brief outline of historically significant examples of the use of guanidines to catalyze an array of asymmetric organic reactions will be presented.



**Scheme 8:** Guanidine catalyzed Michael addition.

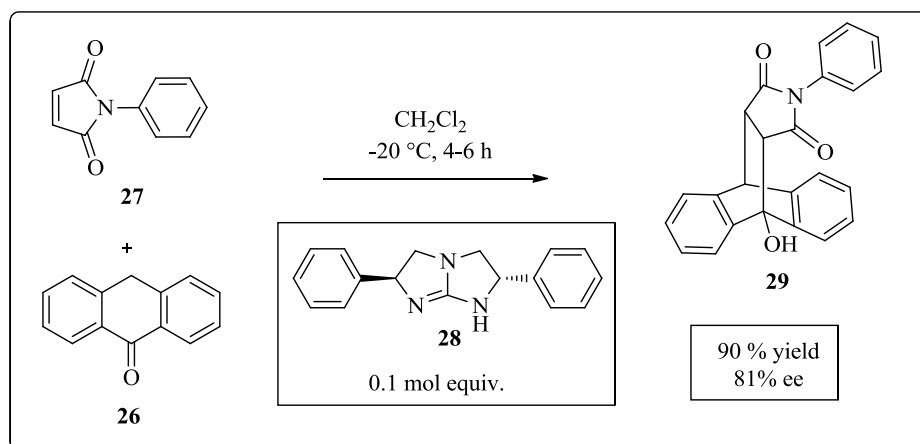
The Michael reaction has been targeted as an application for linear guanidine type catalysts by a number of groups in the late 1990's achieving varying levels stereo induction.<sup>32,33</sup> One of the earliest examples of a successful attempt at an asymmetric Michael addition with a monocyclic guanidine was reported by Isakawa and coworkers in 2001.<sup>34</sup> By reacting one equivalent of *t*-butyl diphenyliminoacetate **19** with 3.6 equivalents of methyl vinyl ketone **20** in the presence of 20 mol% of catalyst **22**, Isakawa was able to obtain addition adduct **21** (**scheme 8**) in 90% yield and an impressive 96% enantiomeric excess. Advances in the guanidine catalyzed Michael reaction paved way for the disclosure of other guanidine catalyzed variations of the reaction including the aza- Michael and phospho- Michael extensions.<sup>35,36</sup>

Similar 5-membered monocyclic guanidine skeletons have been employed towards asymmetric nucleophilic epoxidations of chalcone **23** (**Scheme 9**).<sup>37,38</sup> By treating the chalcone with 0.2 mole equivalents of guanidine catalyst **25** in toluene at room temperature the corresponding epoxide **24** was generated at good to high yields and moderate enantioselectivities. Predictably, the reaction was observed to proceed with lowered stereo induction at reflux temperatures although the yields improved.



**Scheme 9:** Guanidine catalyzed nucleophilic epoxidation.

Moreover, the utility of the Lewis base character of guanidines has been realized in the more widely used Diels-Alder reaction. Tan and coworkers provided a report outlining their success with an asymmetric guanidine catalyzed Diels-Alder reaction between maleimides **26** and substituted anthrones **27**.<sup>39,40</sup> By utilizing an optically active bicyclic guanidine catalyst **28**, this group was able to obtain reaction yields upwards of 85% (**Scheme 10**).



**Scheme 10:** Guanidine catalyzed Diels-Alder reaction.

Although the examples mentioned above are a select few with the intention of highlighting the diversity of organic reactions that have profited from the employment of guanidine catalysts, the recent literature is saturated with applications of guanidine catalysis. With such value in the field of asymmetric organocatalysis, it is of great importance to develop a repertoire of methodologies that will allow access to structurally and electronically varied guanidine modules.

## 2.6: Approaches towards guanidine synthesis

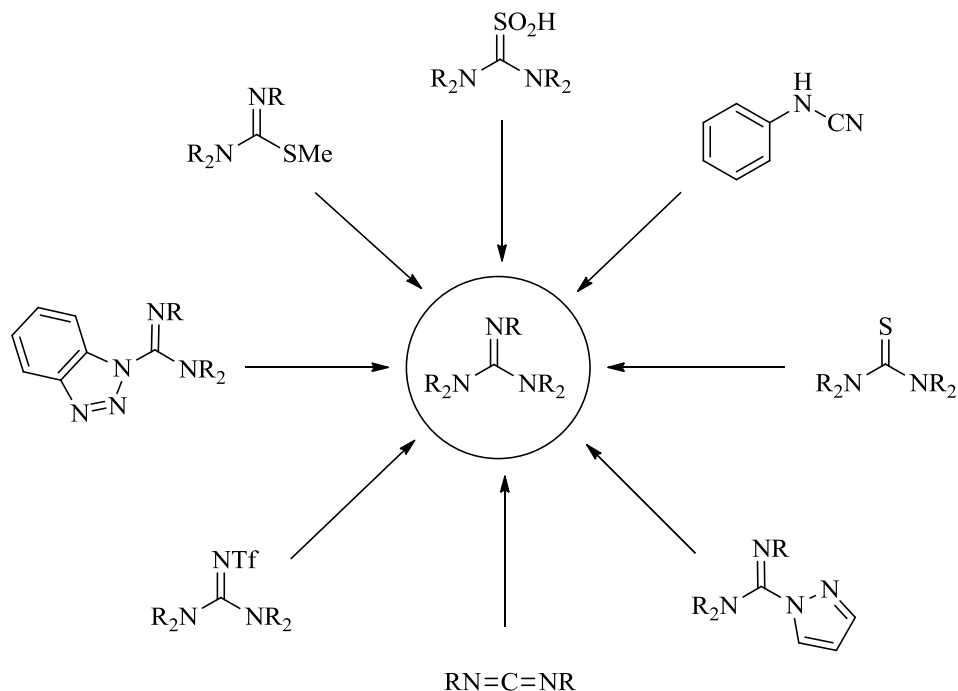
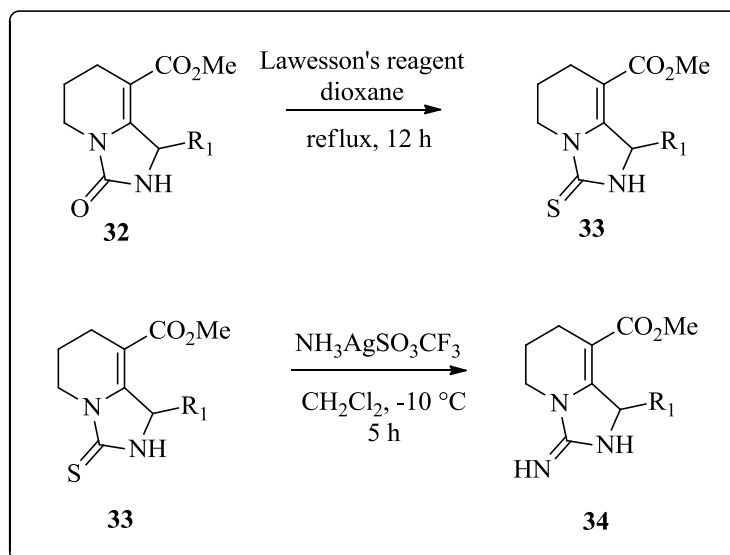


**Figure 10:** Classical guanidine synthesis.

### 2.6.1: Classical methods of guanidine preparation

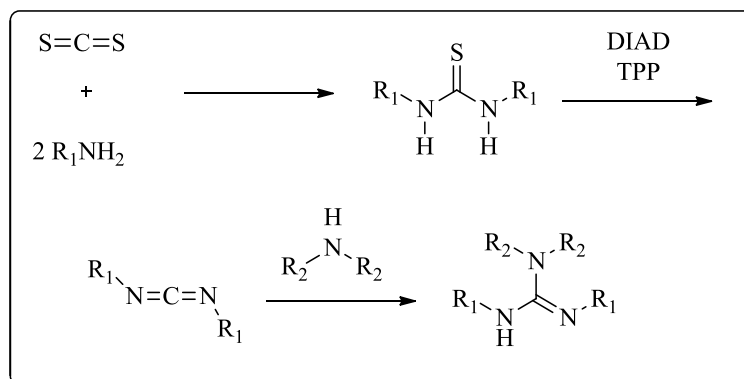
One of the earliest schemes towards guanidine functionality was advanced by Rao in pursuit of access to guanidine containing anti-viral drug leads.<sup>41</sup> This methodology proceeds through the key step of urea generation and conversion to the corresponding thiourea by refluxing in dioxane in the presence of Lawesson's reagent. Generation of the bicyclic guanidine **34** is achieved by subjecting the thiourea **33** to  $\text{NH}_3\text{AgSO}_3\text{CF}_3$  (**Scheme 11**).





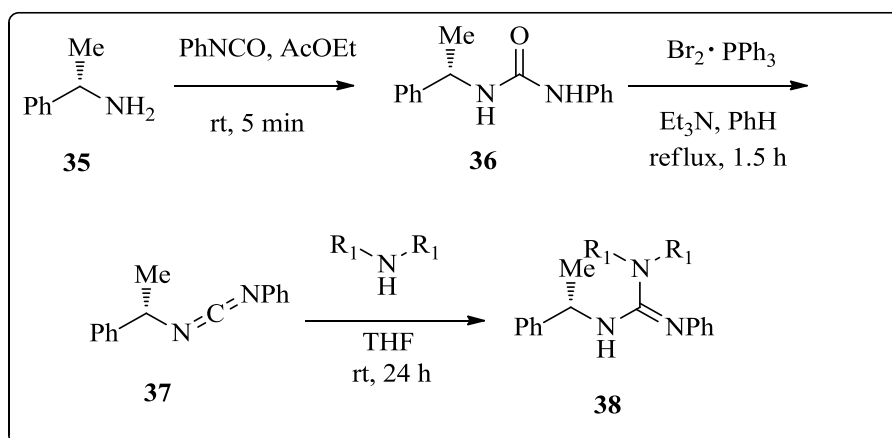
**Scheme 11:** Rao's approach to cyclic guanidines.

In the year following Rao's report, Chinchilla et al.<sup>42</sup> published an analogous study towards the generation of guanidines. Different from Rao's strategy, Chinchilla's approach exploits converting thiourea intermediate to a carbodiimide by treatment with diisopropyl azodicarboxylate (DIAD) and triphenylphosphine. The corresponding guanidine is then finally furnished by treatment of the carbodiimide with a secondary amine (**Scheme 12**).



**Scheme 12:** Chinchilla's approach to substituted guanidine motifs.

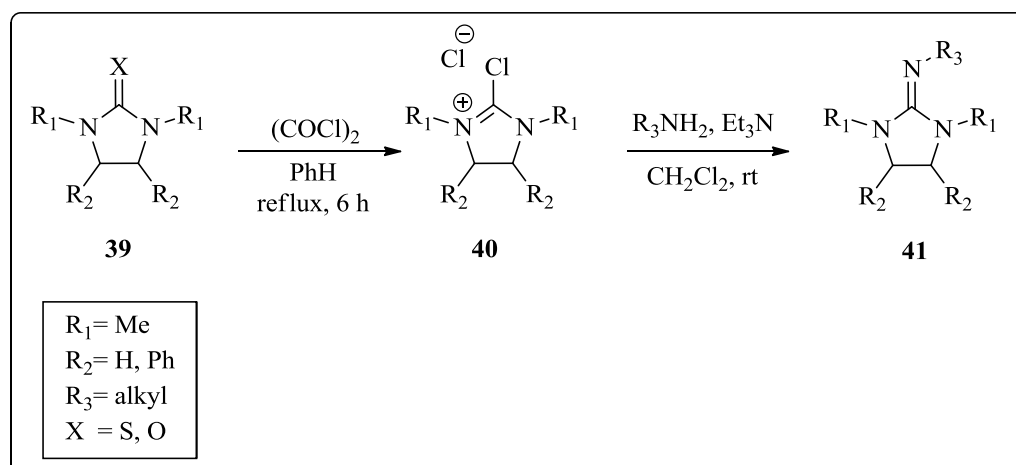
Pursuing homochiral guanidines, Chinchilla in the same study arrived at guanidine **38** by employing a similar procedure outlined in **Scheme 13**. This approach provided access to guanidines by reacting chiral primary amines **35** with a phenylisocyanate to provide a chiral urea **36** which was subsequently converted into carbodiimide **37** by bromotriphenylphosphonium bromide. The carbodiimide intermediate furnished the desired homochiral guanidine **38** upon treatment with an appropriate secondary amine.



**Scheme 13:** Homochiral guanidine synthesis via isocyanate intermediates.

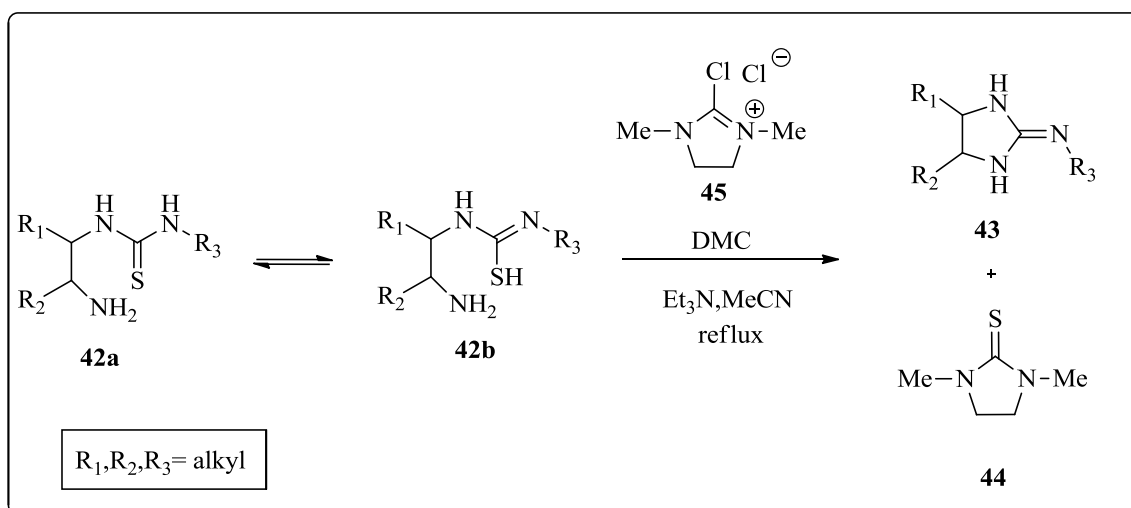
### 2.6.2: DMC induced cyclization

A procedure for the preparation of cyclic guanidines was established by Isobe et al.<sup>43</sup> In this approach cyclic diamines are converted to urea or thiourea precursors, and then treated with oxalyl chloride to provide the corresponding key iminium chloride intermediate **40**. Arriving at the cyclic guanidine target **41** is then achieved by treatment of the iminium salts with a desired primary or secondary amine in the presence of base (**Scheme 14**).



**Scheme 14:** Guanidine synthesis via iminium chloride intermediates.

Ishikawa, one of the figures responsible for popularizing DMC **45** (2-chloro-1,3-dimethyl-4,5-dihydro-1H-imidazol-3-ium chloride) has published several reports outlining the use of DMC induced cyclization in furnishing a number of guanidines including some of cyclic nature.<sup>44</sup> This reported work was essential in the field as it provided, for the first time, a direct route towards cyclic guanidines starting from a thiourea and either an intermolecular (**Scheme 14**) and intramolecular amine (**Scheme 15**).



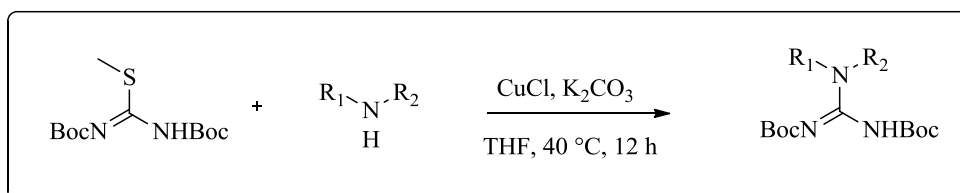
**Scheme 15:** DMC mediated intramolecular guanidine formation from thiourea.

DMC was originally introduced as a versatile reagent with several functions in synthetically useful reactions such as chlorinations, oxidations, reductions, and rearrangements in addition to dehydration reactions under nearly neutral conditions.<sup>45</sup> Furthermore, it was demonstrated that DMC reacted with various primary amines to give the corresponding 5-membered guanidine derivatives (**Scheme 15**). This methodology offers yet another potentially simple approach towards cyclic guanidines for a range of asymmetric synthesis after the introduction of chirality into the template. Further alkylation or direct amination with secondary amines provides the corresponding guanidinium salts. This DMC mediated approach introduced by Isakawa holds attractive benefits; one is the potential for modification of the cyclic core to include an array of chiral and achiral substituents. In addition, the versatile

nature of the DMC salt allows for the amination of thiourea to proceed in an intermolecular and intramolecular fashion.

### 2.6.3: CuCl mediated chemistry

Investigations by Keszler and co-workers employing copper (II) carbonate to promote the displacement of a thiomethyl moiety provided access to highly functionalized guanidine derivatives.<sup>46</sup> This work served as the inspiration behind utilizing the relatively non-toxic thiophilic copper salt. More recently, Ube et. al. ensued to build on Keszler's work with the aim of increasing the low to moderate yields afforded by the copper (II) carbonate methodology.<sup>47</sup> Ube's modification called for use of the more thiophilic copper (I) chloride as a promoter of thiourea amination in the presence of K<sub>2</sub>CO<sub>3</sub> (**Scheme 16**).



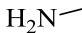
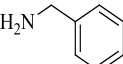
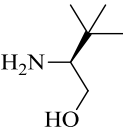
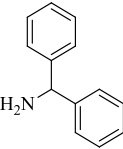
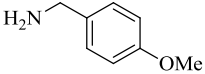
**Scheme 16:** Copper (I) promoted amination of thiourea.

Alternatively, Zou et al. made use of Ube's methodology to furnish chiral tartaric acid guanidine derivatives **47a- 47g**, demonstrating the expanded scope of the methodology.<sup>48</sup> This report was of particular interest to the focus of the study at hand



guanidines will with no doubt be evident in the increase of guanidine architecture application in times to come.

**Table 1:** Substrate scope for CuCl mediated amination of tartaric acid derivatives.

Entry	Substrate	Yield (%)
1		82
2		90
3		73
4		83
5		99



## 2.7: Study objectives

A central area of focus in our laboratories has been the development of a class of guanidine superbases to employ towards asymmetric syntheses, in particular the synthesis of  $\gamma$ -hydroxy butenolide derivatives through vinylogous aldol reactions of mucobromic acid and prochiral aromatic aldehydes (**Scheme 20**). The guanidine functionality provides the Lewis base character required in the catalytic steps of the reaction mechanism while steric and electronic factors in proximity of the guanidine core will dictate the stereochemical outcome of the products.

To this end, we envisioned utilizing a synthetically short and practical approach towards a point chiral guanidine module, such as (*R*)- **48**, that accommodates structural and electronic modification by simple changes in the choice of starting material without complicating the synthetic approach. Guided by literature precedence two synthetic routes will be explored; namely the DMC induced cyclization (**Scheme 15**) and the CuCl mediated amination approach (**Scheme 16**).<sup>43,48</sup> These strategies hold the potential of providing access to molecules featuring a common 7-membered guanidine core **48** with point chiral head groups and aromatic substituents (**Figure 9**) to influence the enantio and diastereo- selectivity outcomes of a vinylogous aldol reaction to furnish  $\gamma$ - functionalized butenolides (**Scheme 7**).

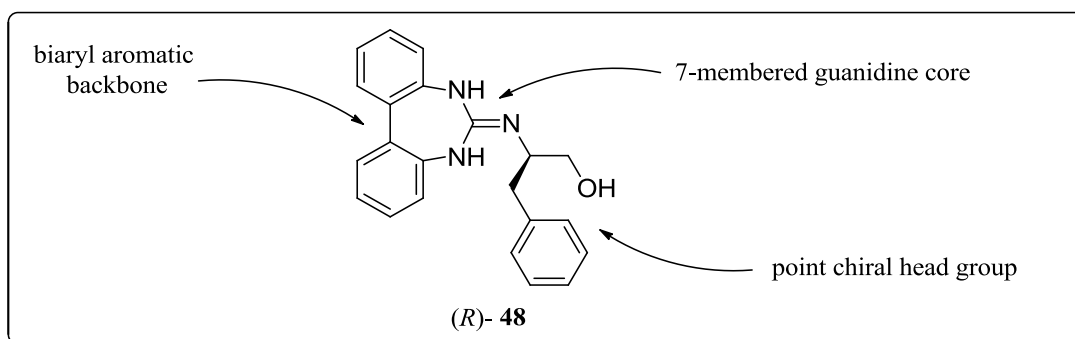
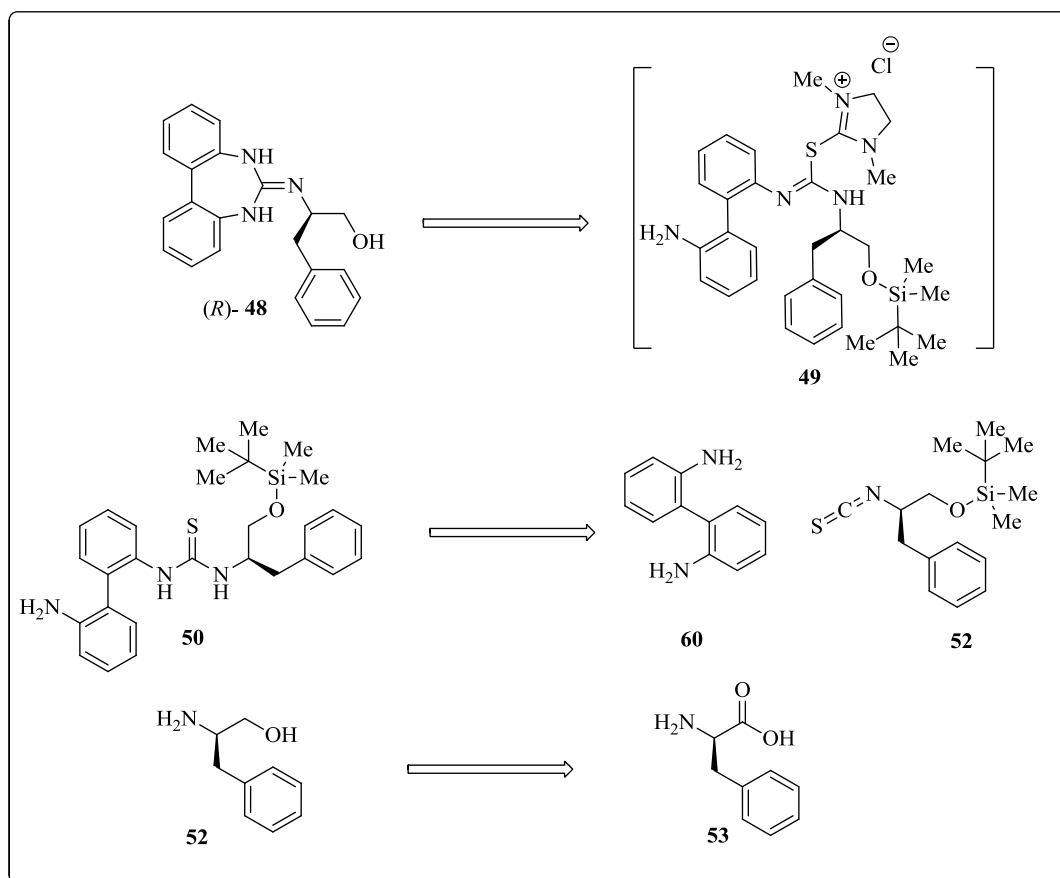


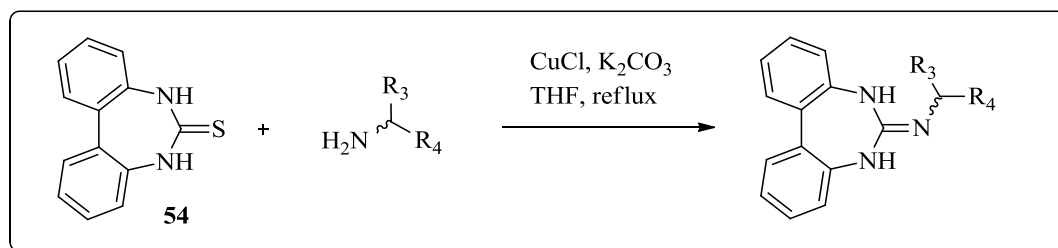
**Figure 11:** Target guanidine architecture.

Following the DMC approach towards our catalyst the desired parent chiral guanidine catalyst (*S*)-2-(5H-dibenzo[d,f][1,3]diazepin-6-(7H)-ylidenamino)-3phenylpropan-1-ol **48**, synthetic efforts will be divided into three major parts as outlined in **Scheme 18**: preparation of the chiral auxiliary ligand **52** from (*R*)-phenylalanine **53**; formation of a thiourea intermediate **50** by coupling of the aromatic backbone **60** to the chiral auxiliary **52**; and finally DMC induced cyclization to arrive at the target **48**.



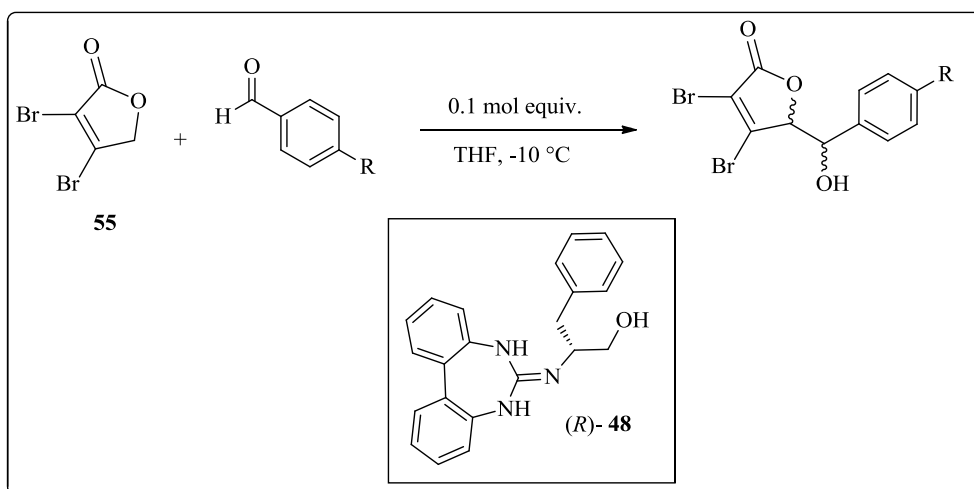
**Scheme 18:** DMC approach towards 7-membered guanidine **48**.

On the other hand, a shorter sequence inspired by the CuCl induced amination (**Scheme 19**) will also be explored as a mean towards the preparation of 7-membered guanidine core. If successful, this approach will allow for structural adjustment based on the choice of starting material.



**Scheme 19:** CuCl mediated amination of aromatic thiourea.

Furthermore, with a practical synthetic sequence by which to access our unique 7-membered guanidine (**Figure 9**) in hand, our focus will shift towards evaluating its catalytic activity in the vinylogous aldol reaction. Exploration of the guanidine catalyzed coupling of aromatic aldehydes and the unsaturated lactone **55** to provide enantiomerically enriched  $\gamma$ -substituted butenolides will be carried out to complete the study.

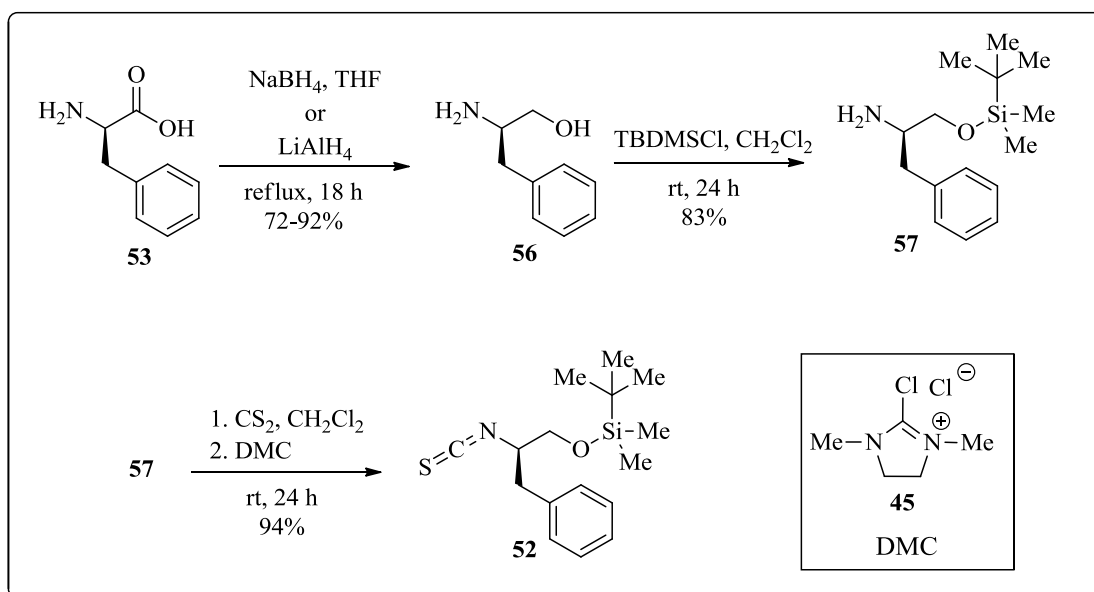


**Scheme 20:** Vinylogous aldol reaction of aromatic aldehydes and 3,4-dibromofuranone.

### 3.0: RESULTS AND DISCUSSION

#### 3.1: Synthesis of chiral auxiliary and DMC induced cyclization

It was of interest to develop methodologies for introducing point chirality adjacent to the guanidine core. This was achieved by converting an optically active amino acid, (*R*)-phenylalanine, to its corresponding thioisocyanate **52** in three steps (Scheme 21).



**Scheme 21:** Approach towards point chiral thioisocyanate.

(*R*)-Phenylalanine **53** was reduced from the carboxylic acid to the corresponding alcohol **56** using a methodology reported by Zaideh et al.<sup>49</sup> utilizing sodium borohydride as the reducing agent. This reaction was reported to furnish the reduced amino acid in 60% yield.

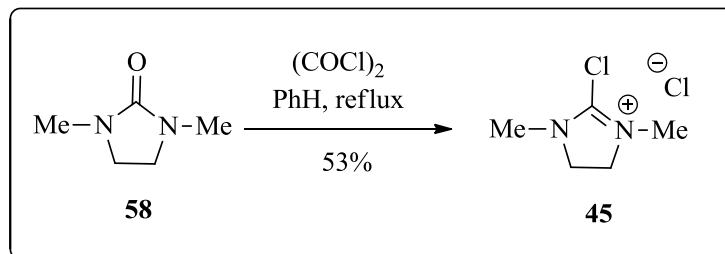
Although acceptable, this 72% yield would compound with subsequent reactions to reduce the yields of the overall synthetic sequence. As such, we set out to optimize this transformation by exploring alternative reaction conditions and reagents. It was found that increasing the reaction time from 4 hours to 24 hours, supplied amino alcohol **56** at a 72% yield in our best effort (**Table 2**). Further experimentation with reducing agents revealed that more desirable results can be achieved by using  $\text{LiAlH}_4$  to obtain the corresponding amino alcohol **56** in 86% yield (**Table 2**).

**Table 2:** Yield optimization of phenylalanine reduction

Entry	Reagent	Time (h)	Yield (%)
1	$\text{NaBH}_4$	4	60
2	$\text{NaBH}_4$	24	72
3	$\text{LiAlH}_4$	6	71
4	$\text{LiAlH}_4$	24	86

With (*R*)-phenylalinalol, **56**, obtained through the lithium aluminum hydride reduction, we carried out the TBDMS protection of the alcohol moiety. Since the subsequent transformations in this sequence invoke use of the DMC salt and the knowledge that DMC salts have been known to act as a chlorinating agents in the presence of alcohols, we were forced to introduce a step to our sequence for masking the alcohol functionality.<sup>43</sup> This would eliminate the potential for competition between the nucleophilic alcohol and the primary amine leading to thioisocyanate **52** formation and ensuring that DMC used in the cyclization step is used up only for inducing ring

closure as opposed to chlorination. The bulk associated with the TBDMS protecting group ensured that both of the above requirements were met. TBDMS protected **57** was obtained at 88% yield, a good result for a protection reaction but low when compared to the quantitative yields reported by Isobe and coworkers.

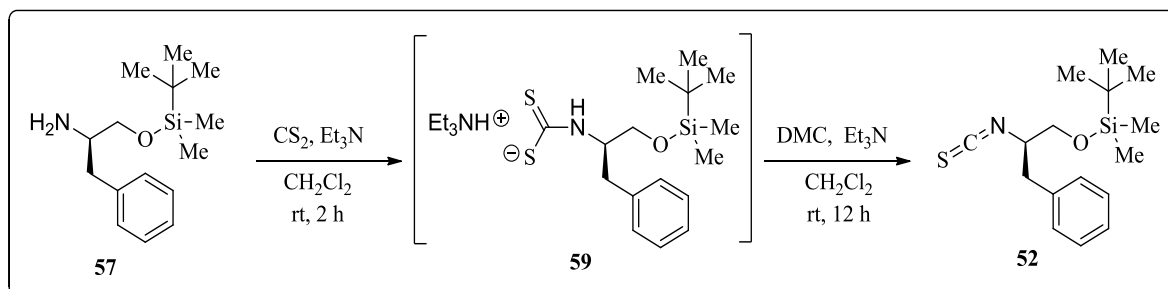


**Scheme 22:** DMC preparation from commercially available imidazolidnone.

It was of paramount importance to utilize freshly prepared DMC salt **45** as it is well known to decompose in the presence of moisture to the corresponding urea.<sup>50</sup> This was avoided by preparing a fresh batch of the salt for immediate subsequent use. DMC was generated by treatment of treatment of 1,3-dimethylimidazolidin-2-one **58** in benzene with oxalyl chloride and refluxing in benzene for 6 hours. Upon completion the reaction, DMC product was washed with dry benzene and ether until the remaining fine solid **45** became clear and colorless. This approach, as described by Isobe *et al.*, provided mediocre yields often as a result of product loss during the purification steps.

With a fresh supply of DMC in hand, we carried out preparation of isothiocyanate **52** (**Scheme 23**). Construction of isothiocyanate **52** was done by

treatment of **57** with carbon disulfide in the presence of catalytic triethylamine to produce the triethylammonium dithiocarbamate intermediate **59** (**Scheme 23**), which was then converted to isothiocyanate **52** by a DMC induced dehydrosulfide process. This sequence was carried out in one pot without the isolation of the triethylammonium dithiocarbamate **59**. Upon completion of the reaction, the product was isolated and purified in greater than 90% yields. Once the highly polar protected amino alcohol was converted to the corresponding thioisocyanate the polarity was decreased significantly, as a result of masking the polar amine group. Pure isothiocyanate **52** product was obtained readily by column using 10:1 hexanes to ethyl acetate as an elutant.



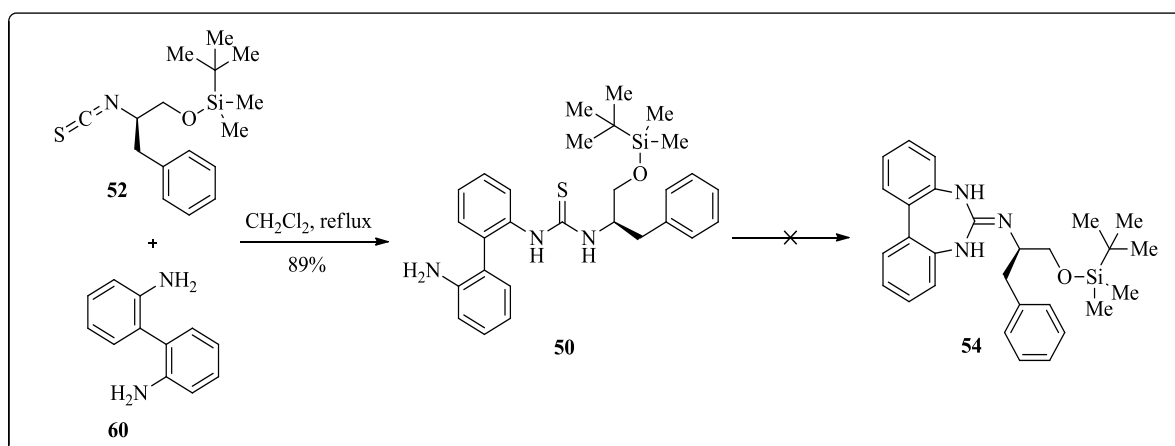
**Scheme 23:** One pot synthesis thioisocyanate **52** mediated by DMC.

In the subsequent reaction, electrophilic thioisocyanate **52** was subjected to nucleophilic attack by the Biaryl diamine lone pair electrons of **60** (**scheme 24**). The thiourea product of this reaction was confirmed to be **53** by NMR and mass spectroscopy. The desired thiourea **53** was isolated as clear oil. Yields obtained for



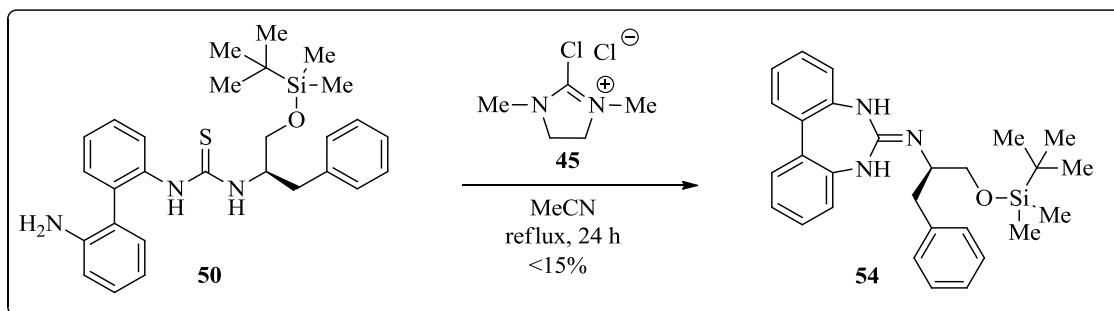
this reaction, 84%, were on average lower than the 96% obtained by Isobe and coworkers, which is likely due to loss of some product in transfer as the oil is very viscous and hard to remove off surfaces.

It is of interest to note that this reaction reaches a standstill once the thiourea product is generated. Condensation of the free aromatic amine to the chiral auxiliary was not followed by intramolecular ring closure to generate the guanidine core **54**. This was due to the moderate nucleophilicity of aromatic amines which can be attributed to its resonance contribution into the appended aromatic ring system. As such, further activation of the electrophile was required in order to complete the transformation and append both aryl amines to the chiral auxiliary furnishing the guanidine functionality (**Scheme 24**).



**Scheme 24:** Condensation of biaryl diamine backbone to the point chiral head group.

To this end, an attractive solution from the recent literature was to employ the DMC salt **45** to further activate (**Scheme 15**) thiourea **53** by DMC; rendering it sufficiently electrophilic for generating the corresponding target.



**Scheme 25:** Desulfonation sequence leading to protected guanidine **54**.

Although TLC and NMR analysis of the DMC induced cyclization appeared to indicate formation of the guanidine moiety, isolation and purification of the newly formed product proved difficult. Numerous attempts to optimize purification techniques (solvent choice for flash chromatography, triethylamine concentrations and crystallization conditions) failed to generate pure DMC induced ring closing product **54**.

Examination of reaction conditions allowed for marginal increase in yield when the temperature was increased to the point of reflux for acetonitrile for 24 hours (Entry 6 **table 3**). Initially, we attempted the reaction at room temperature to avoid decomposition of the sensitive DMC reagent which is known to decompose at higher temperatures. To our regret, room temperature reactions failed to provide the desired

7-membered guanidine. Further attempts to reduce the temperature also gave similar results of no product and unreacted starting materials and DMC salt.

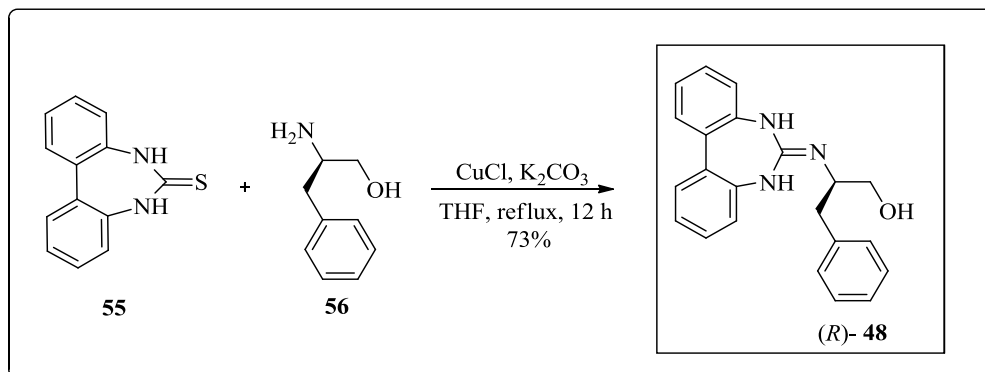
**Table 3:** Temperature and time dependence of DMC induced cyclization

Entry	Time (h)	Temperature ( °C)	Yield (%)
1	6	0	0
2	24	0	0
3	6	rt	0
4	24	rt	5
5	6	reflux	7
6	24	reflux	15

Since the DMC salt was not decomposing during the reaction as indicated by NMR studies, we turned our attention to a more fundamental problem with the procedure. To the best of our knowledge, the DMC induced cyclic guanidine formation has never been employed towards the construction of 7-membered cyclic architecture. Our search of the literature provided examples of 5- and 6-membered ring systems which are known to be the more thermodynamically favored in contrast to the 7-membered construct. Struck by this new found limitation associated with the DMC chemistry we abandoned this approach towards our target guanidine and began revising our synthetic sequence.

### 3.2: Thiourea synthesis and CuCl mediated amination chemistry

At the outset of this study we aimed at arriving at a unique 7-membered guanidine core **48** through a short and practical sequence. This goal was met with difficulties associated with the DMC chemistry and the inherent troubles of forming a cyclic system of thermodynamically unfavored size. As such, copper mediated chemistry held a potential solution in the form of a potentially shorter sequence that would benefit from the construction of a 7-membered cyclic thiourea **55** prior to guanidine formation from a suitable biaryl diamine such as **60**. With the diamine derived thiourea in hand we envisioned a smooth amination through protocol described by Wang to furnish the desired guanidine core **48**.<sup>48</sup> Excited by the potential of shortening the synthetic sequence by eliminating redundant steps such as protection and deprotection of an alcohol moiety we pressed ahead preparing the required thiourea backbone **55** and the corresponding amino alcohol **56** for CuCl induced amination (**Scheme 26**).



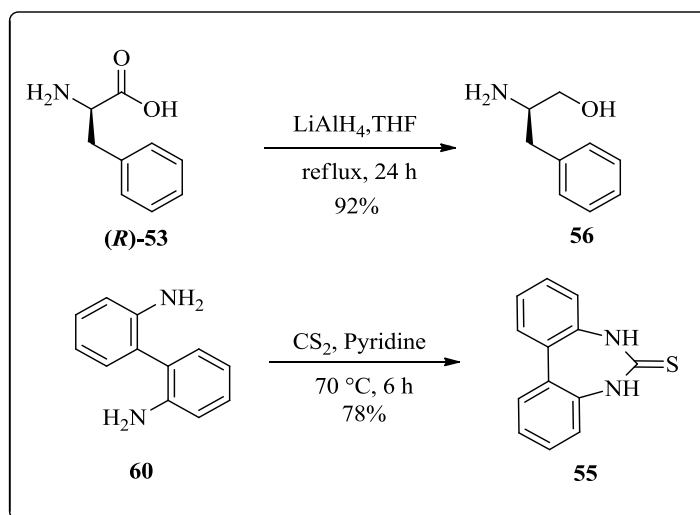
**Scheme 26:** CuCl coupling of aromatic thiourea to point chiral auxiliary.

Armed with an optimized procedure for attaining pure amino alcohol (**Scheme 27**) and biphenyl diamine we set out to furnish the required thiourea. Thiourea synthesis involved exposing the aromatic diamine to carbon disulfide in the presence of pyridine as a reaction solvent. Dependency of product formation on temperature was explored in **Table 4**. The original reports attempt the conversion at 75 °C and for 6 hours to provide the thiourea product at 60% yield.

At an optimal temperature of 90 °C for 6 hours we achieved the highest yield for this reaction (Entry 5 **Table 4**). Purification of the thiourea product **55** was carried out smoothly by acidifying the reaction mixture followed by a water wash to remove pyridinium and then extracting the product with dichloromethane. Crystallization of the product was done in ethanol to provide pure white crystals of thiourea **55**.

**Table 4:** Temperature dependence of thiourea forming reaction in pyridine.

Entry	Temperature ( °C)	Time (h)	Yield (%)
1	r.t	6	27
2	45	6	41
3	50	6	55
4	75	6	77
5	90	6	79

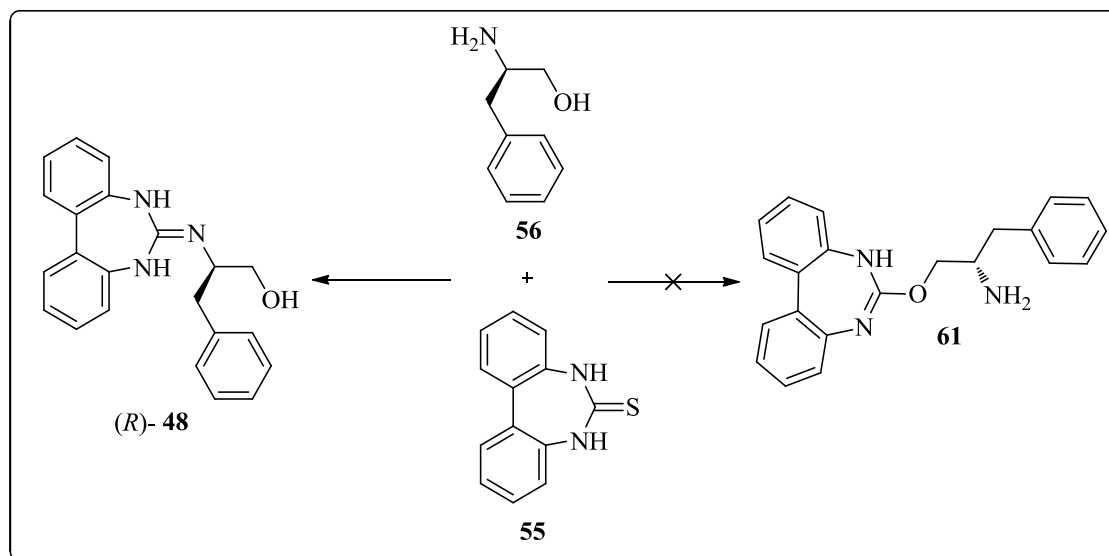


**Scheme 27:** Generation of reactive substrates for the CuCl mediated amination.

With the desired thiourea **55** and amino alcohol fragment **56** in hand, an exploration of the CuCl mediated guanidine formation ensued. Upon addition of the solvent to the CuCl and thiourea, the reaction mixture underwent a color change from white to a bright green color. Gradually, the green color became less intense as the dark brown CuS byproduct was generated. The reaction was monitored by TLC and was quenched with ammonium chloride upon completing. The end point of the reaction was always marked by the reaction mixture changing color to dark brown. An acidic work up followed by column purification smoothly supplied the guanidinium salt, which was then deprotonated by stirring in a 2M NaOH solution for 3 hours.

It is worthwhile to note that this reaction favored the formation of the guanidine moiety **48** as opposed to oxydiazepin **61** that would result from a nucleophilic attack on the thiourea by the hydroxyl functionality of the amino alcohol

fragment. This was the result of the primary amine being a better nucleophile than the hydroxyl group (**Scheme 28**).



**Scheme 28:** Potentially competing coupling reaction during CuCl mediated conditions.

Purification of guanidine **48** proved much simpler through the CuCl mediated process than the DMC induced cyclization pathway. This may have been the result of several factors, the first being that the CuCl process employs inorganic reagents that could simply be removed by aqueous washes. The DMC- induced cyclization pathway invokes the use of organic reagents that require separation from the product, and unfortunately in this particular example the major impurity spot, a thiourea byproduct, happened to run at the same R.F. value as the desired compound for the solvents explored.

We were pleased to arrive at the guanidine target 48 through the CuCl induced amination of an appropriate thiourea. This technology allowed us to shorten our synthetic route from seven transformations to no more than three depending on the starting materials chosen.

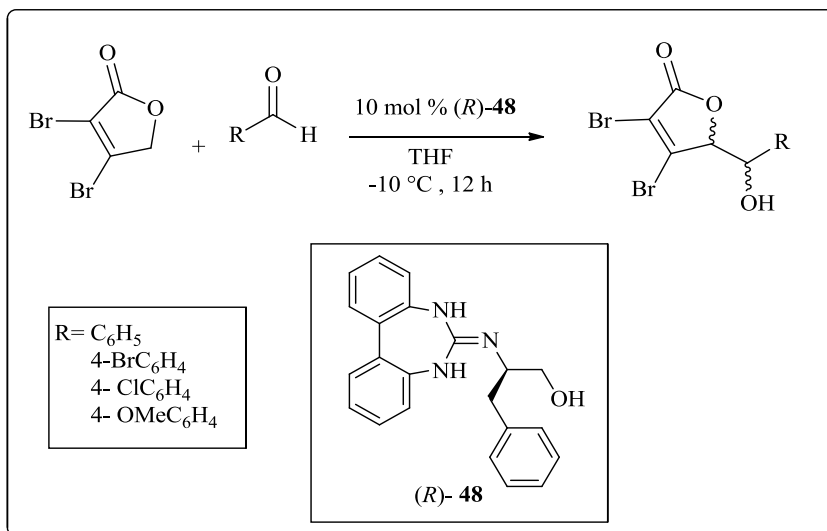
### 3.3: Evaluation of catalytic guanidine core in vinylogous aldol reaction

In our attempt to explore and gauge the proficiency of our newly arrived at 7-membered guanidine catalysts we set our sights on the vinylogous aldol reaction between aromatic aldehydes and  $\gamma$ -substituted unsaturated lactones (**Scheme 30**). With guidance from the literature,<sup>23</sup> we were able to identify this reaction as a suitable testing ground. Electing to follow in the footsteps of Terada, who obtained promising results in this type of vinylogous aldol catalyzed by an axially chiral 9-membered guanidine, we began screening reaction conditions (**Table 5**).

In reported examples of guanidine catalyzed reaction of this type, THF was found to be the most suitable solvent so we began our experiments with THF as a solvent.<sup>23</sup> Reaction conditions were relatively mild; atmospheric pressure and low temperatures with 10% catalyst loading (**Scheme 30**). The aldehyde of choice for preliminary testing was 4-bromobenzaldehyde as it was an activated crystalline aldehyde.<sup>51</sup> Initially reaction were monitored by TLC in order to determine an end point, but it was soon realized that the reaction proceeded sluggishly and thus required



a minimum of 12 hours before any appreciable amount of the desired  $\gamma$ -butenolide could be formed.



**Scheme 29:** Vinylogous aldol reaction catalyzed by **48**.

The effects of time and temperature on yield were investigated for the vinylogous aldol reaction catalyzed by parent guanidine compound **48**. The temperatures chosen were all  $-10\text{ }^{\circ}\text{C}$  degrees Celsius or below in order to maintain stereo control of the reaction outcome. As one might expect, it was observed that the highest reaction yields obtained were those where the reaction mixture was kept at 0 degree (Entry 2, 4, 7 in **Table 5**). Although this temperature was optimal, we carried out our asymmetric reactions at  $-10\text{ }^{\circ}\text{C}$  to avoid corrosion of enantio induction. It was also observed that the reaction produced greater yield up to 12 hours, at which point the effects of diminishing returns were witnessed (Entries 1, 3, 6, and 8 in **Table 5**).

**Table 5:** Time and temperature dependency of vinylogous aldol reaction of mucobromic acid and 4-bromobenzaldehyde catalyzed by point chiral guanidine **48**.

Entry	Time (h)	Temperature ( °C)	Yield (%)
1	4	-10	37
2	4	0	44
3	6	-10	50
4	6	0	47
5	12	-20	39
6	12	-10	54
7	12	0	63
8	24	-10	59
9	24	0	66

Somewhat discouraged with the subpar yields achieved through the 7-membered guanidine core when compared to the yields obtained by Terada's 9-membered catalytic core we turned to the structural differences between the two moieties (**Figure 14**).

The reaction conditions used by our group and those used by Terada were identical with the only differences in the architecture of the catalyst. The first and most obvious of these differences is the chirality of the catalysts; our catalyst **48** possesses a point chiral head group and that used by Terada possesses an axially chiral binaphthyl backbone (**Figure 10**). Although significant, this dissimilarity should not result in differences in yields but instead in the degree of stereo induction.

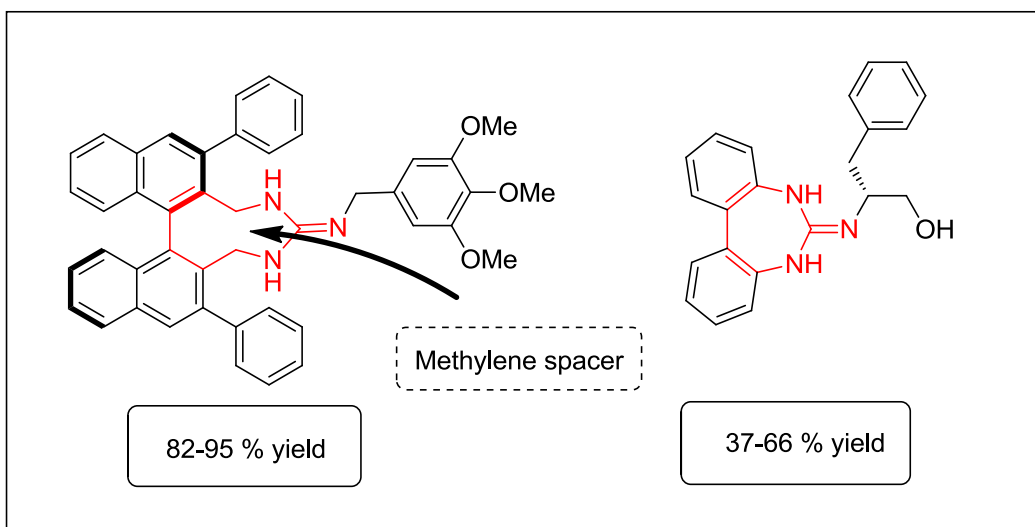


**Figure 10:** Comparison of 9- and 7-membered guanidine catalyst architectures and their respective achieved yields in the vinylogous aldol reaction.

The second of these structural differences is the number of carbons separating the guanidine functionality from the aromatic backbone. In our point chiral catalyst **48** the guanidine moiety is directly appended to the aromatic backbone giving these nitrogens similar basicity to aniline derivatives. In contrast, the guanidine group of Terada's catalyst **14h** is detached from the aromatic backbone by a methylene group creating an overall more electron rich and thus more basic moiety. This marked difference in turn leads to major differences in basicity and thus the difference in reactivity of the two analogs witnessed in their respective product conversion during the vinylogous aldol reaction (**Figure 10**).

To further explore stereinduction effects imparted on the  $\gamma$ -butenolide by catalyst **48**, we performed the reaction with other *p*-substituted aldehydes under the same condition, -10 °C and 10 mol % catalytic loading (**Table 6**).

**Table 6:** Catalytic activity of point chiral guanidine compound in vinylogous aldol reaction with varied aldehyde substrates.

Entry	Aldehyde (R)	Yield (%)	d.r. * ( <i>syn:anti</i> )	e.r. (ee %)**	
				<i>syn</i>	<i>anti</i>
1	C <sub>6</sub> H <sub>5</sub>	47	69:31	80.5:19.5 (61.0%)	69:31 (38.3%)
2	4-ClC <sub>6</sub> H <sub>4</sub>	54	74:26	89:11 (78.1%)	63:37 (26.3%)
3	4-BrC <sub>6</sub> H <sub>4</sub>	59	90:10	90.5:9.5 (80.6%)	54:46 (7.8%)
4	4-OMeC <sub>6</sub> H <sub>4</sub>	46	62:38	71:29 (41.6%)	57.5:42.5 (15.4%)

\* d.r. was obtained by <sup>1</sup>H NMR

\*\* ee was obtained by HPLC analysis

We were pleased to observe some degree of selectivity in the  $\gamma$ -butenolides synthesized by guanidine **48** catalyzed vinylogous aldol reaction (**Table 6**). For all of the aldehyde substrates tested it was observed that our catalyst favored the *syn* isomer over the *anti*. The highest level of diastereomeric selectivity towards the *syn* isomer was observed in the case of electron deficient aldehydes 90:10 and 74:26, 4-bromobenzaldehyde and 4-chlorobenzaldehyde respectively (entries 2 and 3 in **Table 6**). Electron rich aldehyde 4-methoxybenzaldehyde showed milder selectivity 69:31 (entry 1 in **Table 6**), but continued the general trend of favoring the *syn* isomer. Comparable to d.r. obtained from the electron rich 4-methoxybenzaldehyde substrate in entry 1 was the d.r. achieved with the benzaldehyde substrate (entry 4 **Table 6**).

Enantiomeric excess was measured for both the *syn* and *anti*-isomer obtained from each substrate. A distinct drop in enantiomeric excess is observed when comparing the *syn* to the *anti* isomers (**Table 6**). Generally, the same trend of electron poor aldehyde substrates providing the highest levels of diastereomeric selectivity was observed when considering enantiomeric excess. Electron deficient 4-bromobenzaldehyde and 4-chlorobenzaldehyde substrates provided the highest enantiomeric excess 81% and 78% (entries 2 and 3 in **Table 6**) respectively for the major *syn* isomer (**Figure10**). The lowest enantiomeric excess observed was 42% in the case of the electron rich 4-methoxybenzaldehyde while the substituted benzaldehyde substrate gave an enantiomeric excess of 61% (entries 1 and 4 **Table 6**). Enantiomeric excess for the *anti*-isomers were markedly lower than those observed in the *syn* isomers, ranging from 7% to 38%.

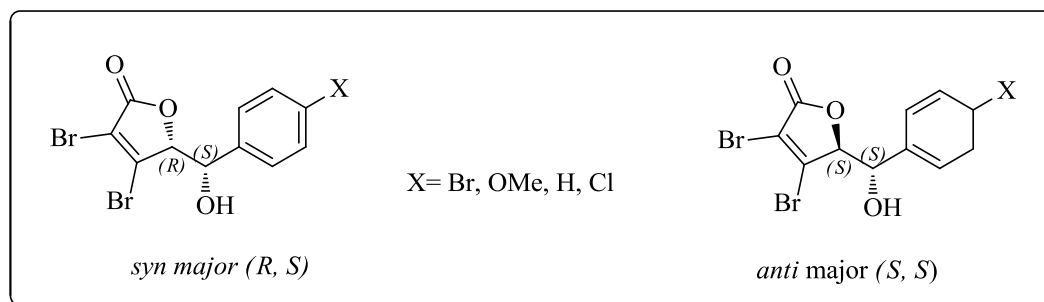


**Figure 12:** Favored *syn* and *anti* isomers based on literature optical rotation.

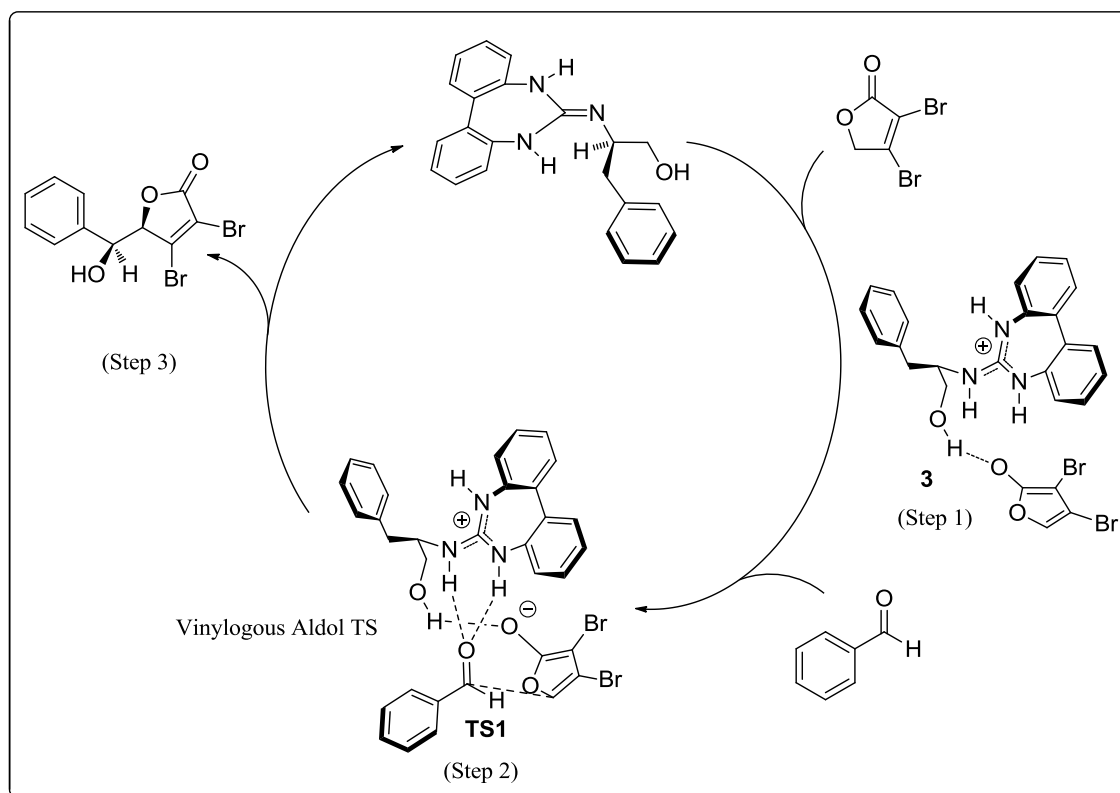


**Figure 13:** Proposed vinylogous aldol catalytic cycle.

Through preliminary computational modeling, we were able to propose the above catalytic cycle to rationalize the experimentally observed stereo induction. In this model, our guanidine catalyst deprotonates the acidic 2,3-dibromofuranone generating the guanidinium stabilized enolate. This complex is stabilized by a hydrogen bonding interaction between the negatively charged oxygen of the conjugated enolate and the hydroxyl group of the chiral moiety of the catalyst. During this time, the aldehyde added to the reaction mixture is positioned in proximity to the activated enolate and stabilized by two hydrogen bonding interactions between the protonated guanidinium nitrogens and the aldehydes carbonyl oxygen (**Figure 13**). In

the subsequent step, the catalyst is regenerated as electron density is pushed down to the  $\gamma$ -position of the vinylogous substrate to result in an attack on the alcohol coordinated aldehyde to furnish the *syn* isomer of the  $\gamma$ -substituted butenolide.

## 4.0: CONCLUDING REMARKS AND FUTURE WORK

The preceding study encapsulated our recent efforts in two areas of research; the development of methodology towards guanidine superbases, and the utility of such organic molecules in the production of  $\gamma$ -butenolides via the vinylogous aldol reaction.

We have outlined a practical synthetic route to the facile construction of a 7-membered guanidine core which allows for simple modification of electronic and steric components of the catalyst. Arriving at the catalyst entailed transformation of biaryl diamines into an electrophilic 7-membered cyclic thiourea. This was then subjected to CuCl mediated nucleophilic amination by phenylalanine derived amino alcohol to generate the guanidinium chloride salt which is then converted to the free base to arrive at the target. This methodology proved to be versatile in terms of nucleophilic amine choice, and in turn, allows for having control over the nature of the point chiral auxiliary, as well as the aromatic backbone.

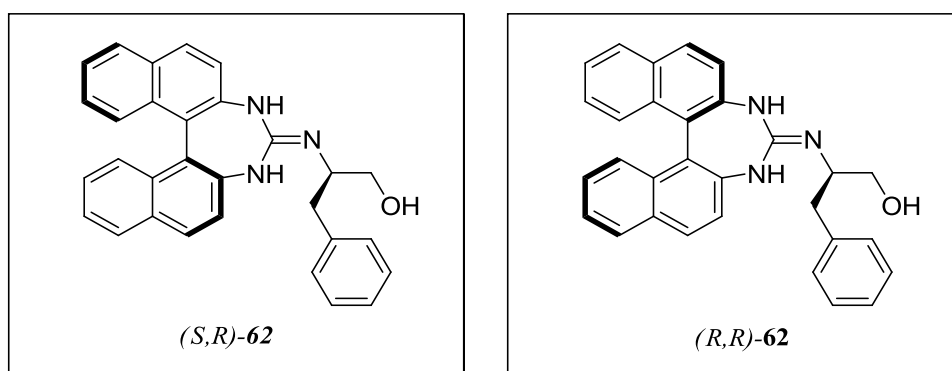


**Figure 14:** Axially chiral derivative of parent guanidine catalyst.



With tested methodology in hand for the construction of 7-membered guanidine cycles it would be of future interest to explore an array of modifications to arrive at a library of related guanidine architectures. One such alteration would provide axially chiral derivatives of the parent guanidine, by subjecting a BINAM derived cyclic urea to CuCl amination (**Figure 12**). This exciting possibility would create a set of diastereomers (match and mismatch partners) that may prove to be beneficial in probing the vinylogous aldol reaction.

Other avenues of work in this area will include exploring a wider range of auxiliaries with varying electronic and steric properties. Possible suitors may include an array of naturally occurring amino acids with varying desirable characteristics. Considering the lowered enantiomeric excess obtained in test runs of the catalyst, it would be of worth exploring modifications at the aryl backbone. Some of these modifications will include the incorporation of steric bulk at the 3,3'-position. The proximity of such modifications to the catalytic guanidine core may very well increase the catalyst selectivity in stereinduction.

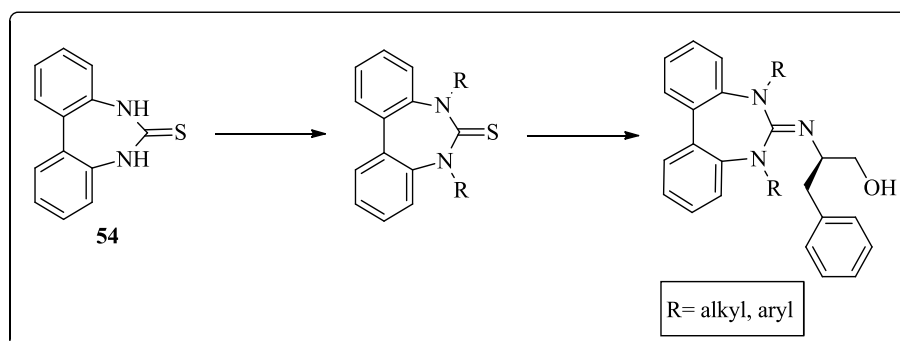


**Figure 15:** Modification at nitrogens of thiourea towards varied guanidine cores.

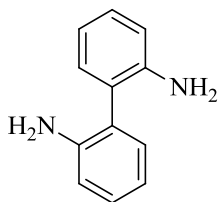
Testing and reaction screening of our guanidine catalyst would also serve to further our work in the field of organic superbases. It is fathomable that this class of catalysts would be better suited for reactions not explored in this work as a consequence of their increased pKa's making them appropriate for proton shuttle responsibilities. Towards this goal, the base requiring electrophilic amination reactions,<sup>52</sup> asymmetric Strecker,<sup>53</sup> use in Claisen rearrangement,<sup>54,55</sup> or use as guanidinium ylide reagents in aziridination reaction<sup>56,57</sup> would all be worthwhile grounds of exploration.

## 5.0: EXPERIMENTAL

### General:

Materials were obtained from commercial suppliers (Sigma-Aldrich) and were used without further purification. Dry ( $\text{CH}_2\text{Cl}_2$ ) dichloromethane, THF (tetrahydrofuran), and toluene were obtained by Puresolv MD 5 purification system. All reactions were performed under an inert atmosphere. Reactions were monitored by thin layer chromatography (TLC) using TLC silica gel 60 F254, EMD Merck. Flash column chromatography was performed over Silicycle ultrapure silica gel (230-400 mesh). NMR spectra were obtained with a Bruker DPX-300 ( $^1\text{H}$  300 MHz,  $^{13}\text{C}$  75.5 MHz) in  $\text{CDCl}_3$  or DMSO. The chemical shifts are reported as  $\delta$  values (ppm) relative to tetramethylsilane. Enantiomeric excess was measured on an Agilent 1100 series high pressure liquid chromatography (HPLC) with (OD-H or AS-H) column, wavelength = 245 nm. Mass spectra were obtained on an MSI/Kratos concept IS Mass spectrometer. Optical rotations were recorded on a Perkin elmer 341 with sodium lamp polarimeter. FT-IR spectra were obtained on an ATI Mattson

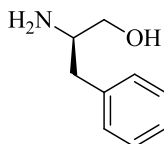
### 5.1: Synthesis of 1,1'-biphenyl-2,2'-diamine (**60**)



**60**

To a dried 100 mL RBF 2,2'-dinitro-1,1'-biphenyl (8.19mmol, 2.000g) and 10% Pd/C (0.2003g) were added and flushed with nitrogen gas. The resulting mixture was dissolved in 30 mL of abs EtOH and it was heated to 60 °C. A solution of 65% Hydrazine hydrate was then added drop wise to the hot EtOH mixture in 4 portions (total of 6.25mL or 1.56 mL/portion). The reaction mixture was allowed to reflux for 15 hours, cooled to room temperature and subsequently filtered over celite. The filtrate was concentrated to about 10 mL and then diluted with 30mL of distilled water. The resulting cloudy solution was allowed to sit for 3 hours. The solution was then filtered and dried under vacuum to obtain **60** (1.159g, 77%) as white solid.  $^1\text{H}$  NMR ( $\text{CDCl}_3$ , 300 MHz)  $\delta$  = 7.15-7.24 (m, 4H), 6.84-6.91 (m, 4H), 3.88 (s, 4H);  $^{13}\text{C}$  NMR ( $\text{CDCl}_3$ , 75.5 MHz)  $\delta$  = 143.5, 131.1, 128.8, 124.8, 119.2, 115.9.

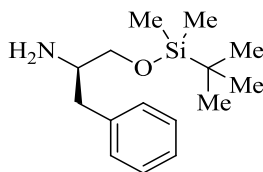
## 5.2: Synthesis of (*R*)-2-amino-3-phenylpropan-1-ol (**56**)



**56**

A flame dried 250 mL RBF was charged with  $\text{LiAlH}_4$  (65.68 mmol, 2.4925 g) and THF (100 mL) in an ice bath. The resulting mixture was treating with *R*-phenylalanine (32.0879 mmol, 5.000g) in 6 portions then the whole was allowed to stir for 1 hour while warming up to room temperature. This mixture was then set to reflux for 15 hours. The reaction was cooled to room temperature and quenched with 2M NaOH. The THF- $\text{H}_2\text{O}$  mixture was decanted out of the reaction vessel and an additional 40 mL of THF was used to extract any remaining product from the white residue remaining in the reaction vessel. The solvent was combined and evaporated under reduced pressure. The product was extracted from the aqueous mixture with  $\text{CH}_2\text{Cl}_2$  and dried over  $\text{MgSO}_4$ . The organic layer was concentrated under vacuum. Consequent recrystallizing furnished **56** (4.4636 g, 92% yield) as colorless crystals.  $^1\text{H}$  NMR ( $\text{CDCl}_3$ , 300 MHz)  $\delta$  = 7.32 (m, 2H), 7.22 (m, 3H), 3.66 (d,  $J$  = 8.3 Hz, 1H), 3.44 (dd,  $J$  = 7.2, 3.7 Hz, 1H), 3.19 (s, 1H), 2.82 (dd,  $J$  = 13.7, 5.6 Hz, 1H), 2.63 (dd,  $J$  = 8.2, 5.2 Hz, 1H), 2.48 (s, 3H);  $^{13}\text{C}$  NMR ( $\text{CDCl}_3$ , 75.5 MHz)  $\delta$  = 138.2, 129.4, 128.5, 126.6, 65.7, 54.2, 40.2.

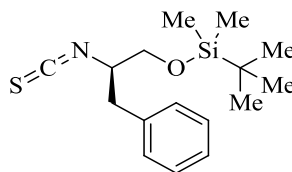
**5.3: Synthesis of (*R*)-1-((*tert*-butyldimethylsilyl)oxy)-3-phenylpropan-2-amine (**57**)**



**57**

A solution of TBDMSCl (6.3920 mmol, 0.9635 g) in CH<sub>2</sub>Cl<sub>2</sub> (7.2 mL) was added drop wise to a stirring suspension of (*R*)-2-amino-3-phenylpropan-1-ol **56** (6.3910 mmol, 0.9665 g), Et<sub>3</sub>N (12.7850 mmol, 1.2937 g), and DMAP (1.2790 mmol, 0.1562 g) in CH<sub>2</sub>Cl<sub>2</sub> (9.75 mL). The whole was allowed to stir at room temperature for 19 hours then poured in water. The crude product was extracted from the water with CH<sub>2</sub>Cl<sub>2</sub> then dried over MgSO<sub>4</sub>. Flash chromatography (hexanes: ethyl acetate = 4:1) furnished **57** (1.4084 g, 83% yield) as a clear colorless oil. <sup>1</sup>H NMR (CDCl<sub>3</sub>, 300 MHz). δ = 7.29-7.34 (m, 2H), 7.21-7.25 (m, 3H), 0.08 (s, 6H), 0.94 (s, 9H), 1.71 (s, 2H), 2.52- 2.59 (dd, *J* = 7.8, 5.3 Hz, 2H), 3.58- 3.63 (d, *J* = 8.1 Hz, 1H), 3.44-3.50 (dd, *J* = 7.2, 3.5 Hz, 1H), 3.12-3.14 (m, 1H), 2.81- 2.85 (dd, *J* = 12.9, 5.5 Hz, 1H); <sup>13</sup>C NMR (CDCl<sub>3</sub>, 75.5 MHz). δ = 139.1, 129.2, 128.4, 126.2, 67.4, 54.3, 40.4, 25.9, 18.2, -5.3.

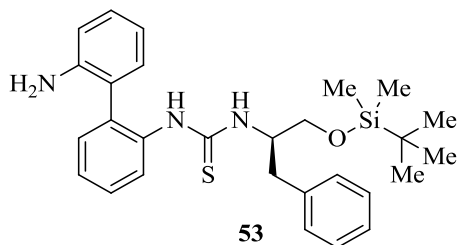
**5.4:** Synthesis of (*R*)-*tert*-butyl (2-isothiocyanato-3-phenylpropoxy)dimethylsilane (**52**)



**52**

A flame dried RBF was charged with (*R*)-1-((*tert*-butyldimethylsilyl)oxy)-3-phenylpropan-2-amine **57** (3.9660 mmol, 1.0529 g), Et<sub>3</sub>N (9.5184 mmol, 0.9632 g) and CH<sub>2</sub>Cl<sub>2</sub> (10.5 mL). To this mixture was added CS<sub>2</sub> (4.7592 mmol, 0.29 mL) drop wise. The resulting mixture was allowed to stir for 2 hours at room temperature. A solution of DMC (4.7590 mmol, 0.8045 g) in CH<sub>2</sub>Cl<sub>2</sub> (4.5 mL) was added drop wise to the stirring solution of protected alcohol. The resulting mixture was stirred at room temperature for an additional 24 hours. The resulting mixture was filtered and the solvent was removed under vacuum. Flash chromatography (hexanes to ethyl acetate = 10:1) provided thioisocyanate **52** (1.1450 g, 94% yield) as a clear colorless oil. <sup>1</sup>H NMR (CDCl<sub>3</sub>, 300 MHz) δ = 7.31- 7.35 (m, 3H), 7.23- 7.25 (m, 2H), 3.84- 3.91 (m, 1H), 3.69- 3.71 (m, 1H), 2.95- 3.07 (dd, *J* = 8.2, 5.4 Hz, 1H ), 2.88- 2.92 (dd, *J* = 7.9, 5.9 Hz, 1H), 0.96 (s, 9H), 0.12 (s, 6H); <sup>13</sup>C NMR (CDCl<sub>3</sub>, 75.5 MHz) δ = 136.5, 129.3, 128.6, 127.0, 64.3, 61.1, 38.1, 25.8, 18.2, -5.4.

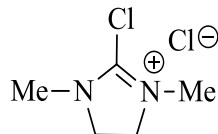
**5.5:** Synthesis of (*R*)-1-(2'-amino-[1,1'-biphenyl]-2-yl)-3-(1-(*tert*-butyldimethylsilyl)oxy)-3-phenylpropan-2-yl)thiourea (**53**)



A flame dried RBF was charged with 1,1'-biphenyl-2,2'-diamine **60** (1.3460 mmol, 0.2480 g) and (*R*)-*tert*-butyl(2-isothiocyanato-3-phenylpropoxy)dimethylsilane **52** (1.2240 mmol, 0.3759g) and CH<sub>2</sub>Cl<sub>2</sub> (2 mL). This mixture was set to reflux for 24 hours. The resulting mixture was cooled to room temperature and the solvent was evaporated under reduced pressure. Flash chromatography (hexanes: ethyl acetate = 2:1) provided thiourea product **53** (0.6020 g, 89% yield) as a viscous clear oil. <sup>1</sup>H NMR (DMSO, 300 MHz). δ = 8.82- 8.88 (d, *J* = 19.4 Hz, 1H), 7.18- 7.44 (m, 10H), 7.05-7.06 (t, *J* = 13.8 Hz, 1H), 6.93- 6.95 (t, *J* = 14.7 Hz, 1H), 6.75- 6.80 (m, 1H), 6.61- 6.66 (m, 1H), 4.64- 4.71 (d, *J* = 19.8 Hz, 2H), 4.56 (brs, 1H), 3.51 (brs, 2H), 2.80-2.85 (m, 2H), 0.87 (brs, 9H), 0.02 (brs, 6H); <sup>13</sup>C NMR (DMSO, 75.5 MHz) δ = 181.4, 146.0, 138.8, 137.0, 135.6, 131.5, 131.0, 129.5, 128.8, 128.7, 127.8, 126.5, 117.2, 116.0, 115.5, 63.1, 57.1, 56.7, 36.2, 26.2, 18.3, , - 4.9, - 4.9. HRMS (EI): *m/z* calcd for C<sub>28</sub>H<sub>37</sub>N<sub>3</sub>OSSi (M<sup>+</sup>): 491.2427; found 491.2417.



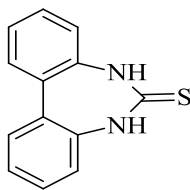
**5.7:** General procedure of 2-chloro-1,3-dimethylimidazolinium chloride (DMC) preparation (**45**)



**45**

To a solution of 1,3-dimethyl-2-imidazolidinone **58** (5.3012 g, 46.441 mmol) in benzene (20ml) was added oxalyl chloride (8.18 mL, 95.3201 mmol) and 2 drops of DMF. The resulting mixture was refluxed for 18 hours. The reaction mixture was allowed to cool to room temperature then it was filtered under inert atmosphere. The filtrate was washed with dry benzene then dried under vacuum to afford DMC **45** (3.062, 39% yield) as beige powder. Spectral data was in full agreement with a genuine example from the literature.<sup>43</sup>

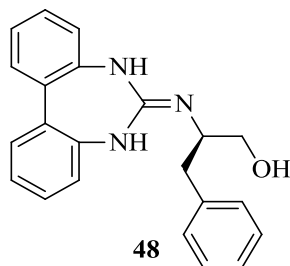
### 5.8: Synthesis of 5H-dibenzo[d,f][1,3]diazepine-6(7H)-thione (**55**)



**55**

A flame dried RBF was charged with 1,1'-biaryl-2,2'diamine **60** (5.5812 mmol, 1.0275 g) and pyridine (9.3 mL). To the dissolved diamine was added CS<sub>2</sub> drop wise then whole was heated to 70 °C for 6 hours. The reaction mixture was allowed to cool to room temperature before it was poured into a mixture of CH<sub>2</sub>Cl<sub>2</sub>-H<sub>2</sub>O (2:1). The pH of this mixture was adjusted to 2 with 1M HCl. The crude product was then extracted with CH<sub>2</sub>Cl<sub>2</sub> (3 X 30 mL). The organic layer was dried over NaSO<sub>4</sub> then the solvent was removed under reduced pressure. Recrystallization from EtOH furnished thiourea **55** (0.9852 g, 78 % yield) as white needles. <sup>1</sup>H NMR (DMSO, 300 MHz) δ = 10.08 (s, 2H), 7.41- 7.44 (d, *J* = 7.9 Hz, 2H), 7.28- 7.31 (t, *J* = 14.9 Hz, 2H), 7.22- 7.24 (t, *J* = 15.1 Hz, 2H), 7.08- 7.11 (dd, *J* = 7.3, 1.1 Hz, 2H); <sup>13</sup>C NMR (DMSO, 75.5 MHz) δ = 141.4, 130.4, 129.6, 125.9, 121.9; m.p. = 243-244 °C.

**5.9:** Synthesis of (*R*)-1-((*tert*-butyldimethylsilyl)oxy)-*N*-(5H-dibenzo[*d,f*][1,3]diazepin-6(7H)-ylidene)-3-phenylpropan-2-amine (**48**)



A flame dried RBF was charged with CuCl (2.319 mmol, 0.2319 g), K<sub>2</sub>CO<sub>3</sub> (4.6862 mmol, 0.6480g) and 5H-dibenzo[*d,f*][1,3]diazepine-6(7H)-thione **55** (0.9372 mmol, 0.2120 g) and THF (4 mL). This mixture was allowed to stir at room temperature for 1 hour. To the resulting mixture was added (*R*)-2-amino-3-phenylpropan-1-ol **56** (1.1247 mmol, 0.1700 g) and the whole was setup to reflux for 10 hours. The reaction was quenched with saturated aqueous NH<sub>4</sub>Cl and then allowed to stir for 1 hour. The aqueous mixture was extracted with CH<sub>2</sub>Cl<sub>2</sub> (3 X 15 mL). The organic extracts were washed with brine and dried over MgSO<sub>4</sub>. The organic layer was filtered through a pad of celite then concentrated under reduced pressure. Flash chromatography provided the guanidinium salt product (MeOH to CH<sub>2</sub>Cl<sub>2</sub>, 4: 96). The free guanidine base was generated by dissolving the salt in CH<sub>2</sub>Cl<sub>2</sub> and stirring with 2N NaOH (4 mL) for 4 hr. The organic residue was extracted with CH<sub>2</sub>Cl<sub>2</sub> (3 X 8 mL) then dried over K<sub>2</sub>CO<sub>3</sub>. The solvent was then removed under reduced pressure and dried in vacuum to provide guanidine **48** (0.2350 g, 73 % yield) as white solid. <sup>1</sup>H NMR (CDCl<sub>3</sub>, 300 MHz) δ = 7.37- 7.40 (dd, *J* = 7.5, 1.6 Hz, 2H), 7.13- 7.26 (m, 9H), 6.92-

6.94 (d,  $J = 5.5$  Hz, 2H), 5.67 (brs, 3H), 3.92- 3.94 (q,  $J = 6.9$  Hz, 1H), 3.68- 3.71 (d,  $J = 9.8$  Hz, 1H), 3.48- 3.54 (t,  $J = 18.6$  Hz, 1H), 2.82- 2.89 (m, 1H), 2.66- 2.73 (m, 1H).  $^{13}\text{C}$  NMR ( $\text{CDCl}_3$ , 75.5 MHz)  $\delta = 158.5, 144.3, 137.7, 131.7, 129.5, 129.1, 128.6, 128.5, 126.7, 124.7, 67.1, 57.3, 37.3$ .  $[\alpha]_{\text{D}}^{17} = -63.93$  ( $c$  0.61,  $\text{CHCl}_3$ ); m.p. = 115-116 °C. HRMS (ED):  $m/z$  calcd for  $\text{C}_{22}\text{H}_{21}\text{N}_3\text{O}$  ( $\text{M}^+$ ) = 344.1685; found = 344.1711.

### Vinylogous aldol reaction:

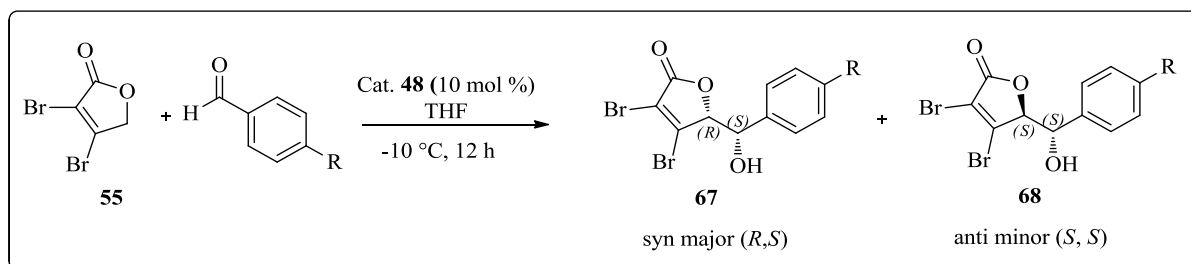


**Figure 16:**  $\gamma$ -butenolide isomers from the vinylogous aldol reaction catalyzed by **48**.

### General vinylogous aldol procedure catalyzed by (*R*)- **48**:

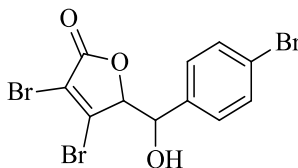
To a flame dried 5mL round bottom flask containing guanidine catalyst (*R*)-1-((tert-butyl dimethylsilyl)oxy)-N-(5H-dibenzo[d,f][1,3]diazepin-6(7H)-ylidene)-3-phenylpropan-2-amine **48** (1 mmol) was added (10 mmol) of benzaldehyde. This mixture was dissolved in dry THF (1.5 mL) and stirred in a -10 °C sodium chloride/ice (1:3) bath for 1 hour. To the resulting mixture was added dibromo butenolide **55** (11 mmol) and the whole was allowed to stir for 12 hours. The reaction was quenched with  $\text{NH}_4\text{Cl}$  and the product extracted with  $\text{CH}_2\text{Cl}_2$  (3 X 10 mL). the organic layer was washed with brine (10 mL) then dried over  $\text{Na}_2\text{SO}_4$ . The solvent was evaporated under

reduced pressure. Flash chromatography (hexanes to ethylacetate = 4:1) provided pure *syn* and *anti*  $\gamma$ -butenolide products **63-66**.

### Stereochemical assignment:

Based on the work of Terada et al.<sup>23</sup> we assigned the absolute configuration of the major *syn*  $\gamma$ -butenolide isomer 3,4-dibromo-5-(hydroxy(phenyl)methyl)furan-2(5H)-one **66**:  $[\alpha]_D^{18} +205.88$  (*c* 0.52, CHCl<sub>3</sub>) as the (*R,S*) configuration. Previously, Terada reported that the major *syn* isomer of 3,4-dibromo-5-(hydroxyl(phenyl)methyl)furan-2(5H)-one obtained through his 9-membered guanidine catalyzed vinylogous aldol reaction had the absolute stereochemistry of (*S,R*) with an optical rotation of  $[\alpha]_D^{20} -150.0$  (*c* 1.00, CHCl<sub>3</sub>). The absolute configurations all of our *syn* derivatives (*syn* **63-66**) are assumed to have the same stereochemistry of **67**. The stereochemistry of the major *anti* isomer of 3,4-dibromo-5-(hydroxy(phenyl)methyl)furan-2(5H)-one:  $[\alpha]_D^{18} +20.60$  (*c* 0.34, CHCl<sub>3</sub>) assigned was as (*S,S*) since it was the antipode of the *anti* major reported by Terada. The absolute stereochemical configuration of all our *anti* derivatives (*anti* **63-66**) was assumed to be the same as **68**.

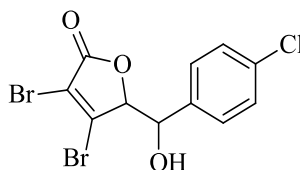
**5.10: 3,4-dibromo-5-((4-bromophenyl)(hydroxy)methyl)furan-2(5H)-one (63)**



**63**

59% yield; *syn:anti* = 90:10; HPLC analysis Chiralpak AD-3 (hexane/<sup>i</sup>PrOH = 90/10, 1.0 mL/min, 220 nm, 30 °C) ; 18.29 (*syn*, major), 25.03 (*syn*), 17.60 (*anti*, major), 25.95 (*anti*) min; 80.6% ee (*syn*), 7.8% ee (*anti*); *syn* isomer: (*R*)-3,4-dibromo-5-((*S*)-(4-bromophenyl)(hydroxy)methyl)furan-2(5H)-one; white solid;  $[\alpha]_D^{18} +228$  (*c* 0.52, CHCl<sub>3</sub>); <sup>1</sup>H NMR (300 MHz, CDCl<sub>3</sub>)  $\delta$  = 7.55- 7.58 (d, *J* = 8.1 Hz, 2H), 7.35- 7.38 (d, *J* = 8.3 Hz, 2H), 5.15 (s, 1H), 5.08 (s, 1H), 2.19 (brs, 1H). <sup>13</sup>C NMR (CDCl<sub>3</sub>, 75.5 MHz)  $\delta$  = 165.8, 144.7, 136.9, 132.0, 128.4, 123.1, 116.2, 86.7, 71.4; *anti* isomer: (*S*)-3,4-dibromo-5-((*S*)-(4-bromophenyl)(hydroxy)methyl)furan-2(5H)-one; white solid;  $[\alpha]_D^{19} +190$  (*c* 0.1, CHCl<sub>3</sub>); <sup>1</sup>H NMR (300 MHz, CDCl<sub>3</sub>)  $\delta$  = 7.51- 7.54 (d, *J* = 8.3 Hz, 2H), 7.26-7.29 (d, *J* = 5.2 Hz, 2H), 5.33 (s, 1H), 5.27-5.32 (s, 1H), 2.51 (brs, 1H); <sup>13</sup>C NMR (CDCl<sub>3</sub>, 75.5 MHz)  $\delta$  = 166.0, 144.8, 132.0, 129.1, 128.5, 128.4, 126.6, 87.1, 73.7.

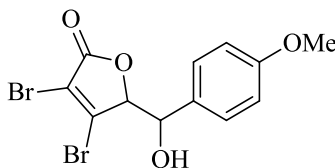
**5.11: 3,4-dibromo-5-((4-chlorophenyl)(hydroxy)methyl)furan-2(5H)-one (64)**



**64**

54% yield; *syn:anti* = 74:26; HPLC analysis Chiralpak AD-3 (hexane/*i*PrOH = 90/10, 1.0 mL/min, 220 nm, 30 °C) ; 16.75 (*syn*, major), 22.07 (*syn*), 17.60 (*anti*, major), 25.95 (*anti*) min; 78.1% ee (*syn*), 26.3% ee (*anti*); *syn* isomer: (*R*)-3,4-dibromo-5-((*S*)-(4-chlorophenyl)(hydroxy)methyl)furan-2(5H)-one; white solid;  $[\alpha]_D^{18} +166.7$  (*c* 0.54, CHCl<sub>3</sub>); <sup>1</sup>H NMR (300 MHz, CDCl<sub>3</sub>)  $\delta$  = 7.39-7.44 (m, 4H), 5.16 (brs, 1H), 5.08 (d, *J* = 2.3 Hz, 1H), 2.22 (brs, 1H); <sup>13</sup>C NMR (300 MHz, CDCl<sub>3</sub>)  $\delta$  = 165.9, 144.7, 136.4, 135.0, 129.0, 128.2, 116.2, 86.7, 71.4; *anti* isomer: (*S*)-3,4-dibromo-5-((*S*)-(4-bromophenyl)(hydroxy)methyl)furan-2(5H)-one; white solid;  $[\alpha]_D^{19} +79.1$  (*c* 0.42, CHCl<sub>3</sub>); <sup>1</sup>H NMR (300 MHz, CDCl<sub>3</sub>)  $\delta$  = 7.32- 7.39 (4H, m), 5.32-5.33 (d, *J* = 2.8 Hz, 1H), 5.28-5.29 (d, *J* = 2.7 Hz, 1H), 2.62 (brs, 1H); <sup>13</sup>C NMR (CDCl<sub>3</sub>, 75.5 MHz)  $\delta$  = 165.5, 143.4, 135.0, 134.1, 128.8, 128.0, 116.7, 86.8, 73.0.

**5.12:** 3,4-dibromo-5-((4-methoxyphenyl)(hydroxy)methyl)furan-2(5H)-one  
(**65**)

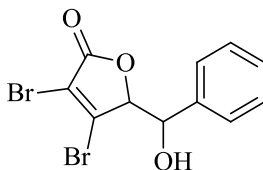


**65**

46% yield; *syn:anti* = 72:38; HPLC analysis Chiralpak AD-3 (hexane/<sup>i</sup>PrOH = 90/10, 1.0 mL/min, 220 nm, 30 °C) ; 23.99 (*syn*, major), 28.64 (*syn*), 19.19 (*anti*, major), 28.46 (*anti*) min; 40.6% ee (*syn*), 15.4% ee (*anti*); *syn* isomer: (*R*)-3,4-dibromo-5-((*S*)-(4-methoxyphenyl)(hydroxy)methyl)furan-2(5H)-one; white solid;  $[\alpha]_D^{19} +155.2$  (*c* 0.29, CHCl<sub>3</sub>); <sup>1</sup>H NMR (300 MHz, CDCl<sub>3</sub>)  $\delta$  = 7.40-7.43 (d, *J* = 8.6 Hz, 2H), 6.93-6.96 (d, *J* = 8.2 Hz, 2H), 5.08- 5.09 (d, *J* = 2.7 Hz, 1H), 5.12 (s, 1H), 2.08- 2.09 (brs, 1H), 3.85 (s, 3H); <sup>13</sup>C NMR (CDCl<sub>3</sub>, 75.5 MHz)  $\delta$  = 166.1, 160.1, 145.2, 130.0, 128.2, 115.9, 114.1, 87.0, 71.8, 55.3; *anti* isomer: (*S*)-3,4-dibromo-5-((*S*)-(4-methoxyphenyl)(hydroxy)methyl)furan-2(5H)-one; white solid;  $[\alpha]_D^{19} +61.7$  (*c* 0.47, CHCl<sub>3</sub>); <sup>1</sup>H NMR (300 MHz, CDCl<sub>3</sub>)  $\delta$  = 7.28- 7.31 (m, 2H), 6.88- 6.90 (m, 2H), 5.33- 5.34 (d, *J* = 2.8 Hz, 1H), 3.82 (s, 3H), 5.24 (brs, 1H), 2.41- 2.43 (brs, 1H); <sup>13</sup>C NMR (CDCl<sub>3</sub>, 75.5 MHz)  $\delta$  = 165.7, 160.1, 143.9, 128.0, 127.4, 116.4, 113.9, 87.0, 73.6, 55.2.



**5.13: 3, 4-dibromo-5-(hydroxyl(phenyl)methyl)furan-2(5H)-one (66)**



**66**

47% yield; *syn:anti* = 69:31; HPLC analysis Chiralpak AD-3 (hexane/<sup>i</sup>PrOH = 90/10, 1.0 mL/min, 220 nm, 30 °C) ; 20.17 (*syn*, major), 22.99 (*syn*), 20.50 (*anti*, major), 26.26 (*anti*) min; 61.0% ee (*syn*), 38.3% ee (*anti*); *syn* isomer: (*R*)-3,4-dibromo-5-((*S*)-(hydroxy(phenyl)methyl)furan-2(5H)-one; white solid;  $[\alpha]_D^{18} + 205.88$  (*c* 0.34, CHCl<sub>3</sub>); <sup>1</sup>H NMR (300 MHz, CDCl<sub>3</sub>)  $\delta$  = 7.42-7.51 (m, 5H), 5.17- 5.18 (d, *J* = 2.2 Hz, 1H), 5.12 (d, *J* = 2.3 Hz, 2H), 2.19 (s, 1H); <sup>13</sup>C NMR (CDCl<sub>3</sub>, 75.5 MHz)  $\delta$  = 166.0, 145.1, 138.0, 129.1, 128.8, 126.7, 116.0, 86.9, 72.0; *anti* isomer: (*S*)-3,4-dibromo-5-((*S*)-( hydroxyl(phenyl)methyl)furan-2(5H)-one; white solid;  $[\alpha]_D^{17} + 20.6$  (*c* 0.34, CHCl<sub>3</sub>); <sup>1</sup>H NMR (300 MHz, CDCl<sub>3</sub>)  $\delta$  = 7.35-7.45 (m, 5H), 5.35- 5.36 (d, *J* = 3 Hz, 1H), 5.29- 5.30 (d, *J* = 2.9 Hz, 1H), 2.19 (s, 1H); <sup>13</sup>C NMR (CDCl<sub>3</sub>, 75.5 MHz)  $\delta$  = 165.7, 143.7, 135.5, 129.1, 128.6, 126.6, 116.5, 87.0, 73.7.

## 6.0: REFERENCES

1. Corey, E. J.; Cheng, X. *The logic of chemical synthesis*; John Wiley New York: 1989.
2. ApSimon, J. *The total synthesis of natural products*; John Wiley & Sons: 2009; Vol. 7.
3. Miao, S.; Andersen, R. J. *J. Org. Chem.* **1991**, 56, 6275-6280.
4. Ortega, M. J.; Zubía, E.; Ocaña, J. M.; Naranjo, S.; Salvá, J. *Tetrahedron* **2000**, 56, 3963-3967.
5. Jung, J.; Pummangura, S.; Chaichantipyuth, C.; Patarapanich, C.; Fanwick, P.; Chang, C.; McLaughlin, J. *Tetrahedron* **1990**, 46, 5043-5054.
6. Pillay, P.; Vleggaar, R.; Maharaj, V. J.; Smith, P. J.; Lategan, C. A.; Chouteau, F.; Chibale, K. *Phytochemistry* **2007**, 68, 1200-1205.
7. Brown, S. P.; Goodwin, N. C.; MacMillan, D. W. *J. Am. Chem. Soc.* **2003**, 125, 1192-1194.
8. Zhang, J.; Sarma, K. D.; Curran, T. T.; Belmont, D. T.; Davidson, J. G. *J. Org. Chem.* **2005**, 70, 5890-5895.
9. Zhang, J.; Blazecka, P. G.; Curran, T. T. *Tetrahedron Lett.* **2007**, 48, 2611-2615.
10. Zhang, J.; Blazecka, P. G.; Berven, H.; Belmont, D. *Tetrahedron Lett.* **2003**, 44, 5579-5582.
11. Evans, D. A.; Kozlowski, M. C.; Murry, J. A.; Burgey, C. S.; Campos, K. R.; Connell, B. T.; Staples, R. *J. Am. Chem. Soc.* **1999**, 121, 669-685.

12. Casiraghi, G.; Zanardi, F.; Appendino, G.; Rassu, G. *Chem. Rev.* **2000**, *100*, 1929-1972.
13. Pichon, M.; Jullian, J.; Figadère, B.; Cavé, A. *Tetrahedron Lett.* **1998**, *39*, 1755-1758.
14. Szlosek, M.; Franck, X.; Figadère, B.; Cavé, A. *J. Org. Chem.* **1998**, *63*, 5169-5172.
15. Lee, S.; Chan, T. *Tetrahedron* **1984**, *40*, 3611-3616.
16. Casiraghi, G.; Zanardi, F.; Appendino, G.; Rassu, G. *Chem. Rev.* **2000**, *100*, 1929-1972.
17. Singer, R. A.; Carreira, E. M. *J. Am. Chem. Soc.* **1995**, *117*, 12360-12361.
18. Krüger, J.; Carreira, E. M. *J. Am. Chem. Soc.* **1998**, *120*, 837-838.
19. Singer, R. A.; Carreira, E. M., *J. Am. Chem. Soc.* **1995**, *117*, 12360-12361.
20. Krüger, J.; Carreira, E. M. *J. Am. Chem. Soc.* **1998**, *120*, 837-838.
21. Taylor, S. J.; Duffey, M. O.; Morken, J. P. *J. Am. Chem. Soc.* **2000**, *122*, 4528-4529.
22. Evans, D. A.; Tregay, S. W.; Burgey, C. S.; Paras, N. A.; Vojkovsky, T. *J. Am. Chem. Soc.* **2000**, *122*, 7936-7943.
23. Ube, H.; Shimada, N.; Terada, M. *Angew. Chem. Int. Ed.* **2010**, *49*, 1858-1861.
24. Ube, H.; Shimada, N.; Terada, M. *Angew. Chem. Int. Ed.* **2010**, *49*, 1858-1861.
25. Berlinck, R. G.; Burtoloso, A. C. B.; Kossuga, M. H. *Nat. Prod. Rep.* **2008**, *25*, 919-954.

26. Berlinck, R. G.; Kossuga, M. H. *Nat. Prod. Rep.* **2005**, *22*, 516-550.
27. Taylor, J. E.; Bull, S. D.; Williams, J. M. *Chem. Soc. Rev.* **2012**, *41*, 2109-2121.
28. Caubere, P. *Chem. Rev.* **1993**, *93*, 2317-2334.
29. Ishikawa, T. *Superbases for organic synthesis: guanidines, amidines and phosphazenes and related organocatalysts*; Wiley Online Library: 2009.
30. Raczyńska, E. D.; Cyrański, M. K.; Gutowski, M.; Rak, J.; Gal, J.; Maria, P.; Darowska, M.; Duczmal, K. *J. Phys. Org. Chem.* **2003**, *16*, 91-106.
31. Leow, D.; Tan, C. *Asian J. Chem.* **2009**, *4*, 488-507.
32. Ma, D.; Cheng, K. *Tetrahedron: Asymmetry* **1999**, *10*, 713-719.
33. Corey, E.; Zhang, F. *Org. Lett.* **2000**, *2*, 4257-4259.
34. Ishikawa, T.; Araki, Y.; Kumamoto, T.; Seki, H.; Fukuda, K.; Isobe, T. *Chem. Commun.* **2001**, 245-246.
35. Martín-Portugués, M.; Alcázar, V.; Prados, P.; de Mendoza, J. *Tetrahedron* **2002**, *58*, 2951-2955.
36. Fu, X.; Jiang, Z.; Tan, C. *Chem. Commun.* **2007**, 5058-5060.
37. Kita, T.; Shin, B.; Hashimoto, Y.; Nagasawa, K. *Heterocycles* **2007**, *73*, 241-247.
38. Shin, B.; Tanaka, S.; Kita, T.; Hashimoto, Y.; Nagasawa, K. *Heterocycles* **2008**, *76*, 801-810.
39. Shen, J.; Nguyen, T. T.; Goh, Y.; Ye, W.; Fu, X.; Xu, J.; Tan, C. *J. Am. Chem. Soc.* **2006**, *128*, 13692-13693.

40. Shen, J.; Tan, C. *Org. Biomol. Chem.* **2008**, *6*, 4096-4098.
41. Rao, A.; Gurjar, M.; Islam, A. *Tetrahedron Lett.* **1993**, *34*, 4993-4996.
42. Chinchilla, R.; Nájera, C.; Sánchez-Agulló, P. *Tetrahedron: Asymmetry* **1994**, *5*, 1393-1402.
43. Isobe, T.; Fukuda, K.; Tokunaga, T.; Seki, H.; Yamaguchi, K.; Ishikawa, T. *J. Org. Chem.* **2000**, *65*, 7774-7778.
44. Isobe, T.; Fukuda, K.; Yamaguchi, K.; Seki, H.; Tokunaga, T.; Ishikawa, T. *J. Org. Chem.* **2000**, *65*, 7779-7785.
45. Isobe, T.; Ishikawa, T. *J. Org. Chem.* **1999**, *64*, 5832-5835.
46. Wityak, J.; Gould, S. J.; Hein, S. J.; Keszler, D. A. *J. Org. Chem.* **1987**, *52*, 2179-2183.
47. Ube, H.; Uruguchi, D.; Terada, M. *J. Organomet. Chem.* **2007**, *692*, 545-549.
48. Zou, L.; Wang, B.; Mu, H.; Zhang, H.; Song, Y.; Qu, J. *Org. Lett.* **2013**, *15*, 3106-3109.
49. Zaideh, B. I.; Saad, N. M.; Lewis, B. A.; Brenna, J. T. *Anal. Chem.* **2001**, *73*, 799-802.
50. Isobe, T.; Ishikawa, T. *J. Org. Chem.* **1999**, *64*, 6984-6988.
51. Kjell, D. P.; Slattery, B. J.; Semo, M. J. *J. Org. Chem.* **1999**, *64*, 5722-5724.
52. Terada, M.; Nakano, M.; Ube, H. *J. Am. Chem. Soc.* **2006**, *128*, 16044-16045.
53. Becker, C.; Hoben, C.; Schollmeyer, D.; Scherr, G.; Kunz, H. *Eur. J. Org. Chem.* **2005**, *2005*, 1497-1499.

54. Martin Castro, A. M. *Chem. Rev.* **2004**, *104*, 2939-3002.
55. Uyeda, C.; Jacobsen, E. N. *J. Am. Chem. Soc.* **2008**, *130*, 9228-9229.
56. Haga, T.; Ishikawa, T. *Tetrahedron* **2005**, *61*, 2857-2869.
57. Hada, K.; Watanabe, T.; Isobe, T.; Ishikawa, T. *J. Am. Chem. Soc.* **2001**, *123*, 7705-7706.

## 7.0: SELECTED SPECTRA

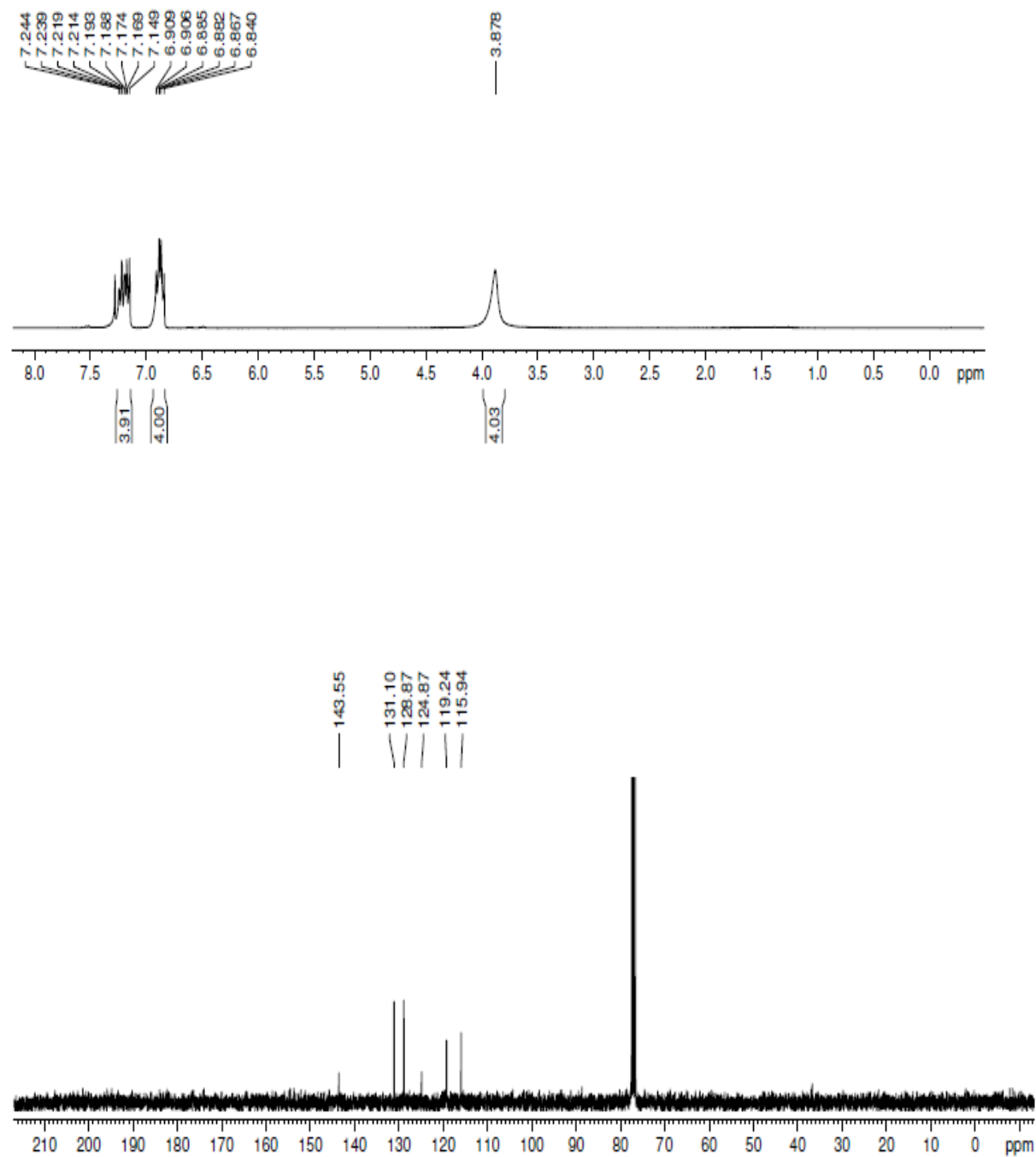


**Figure 17:**  $^1\text{H}$  and  $^{13}\text{C}$  NMR spectra of **60**

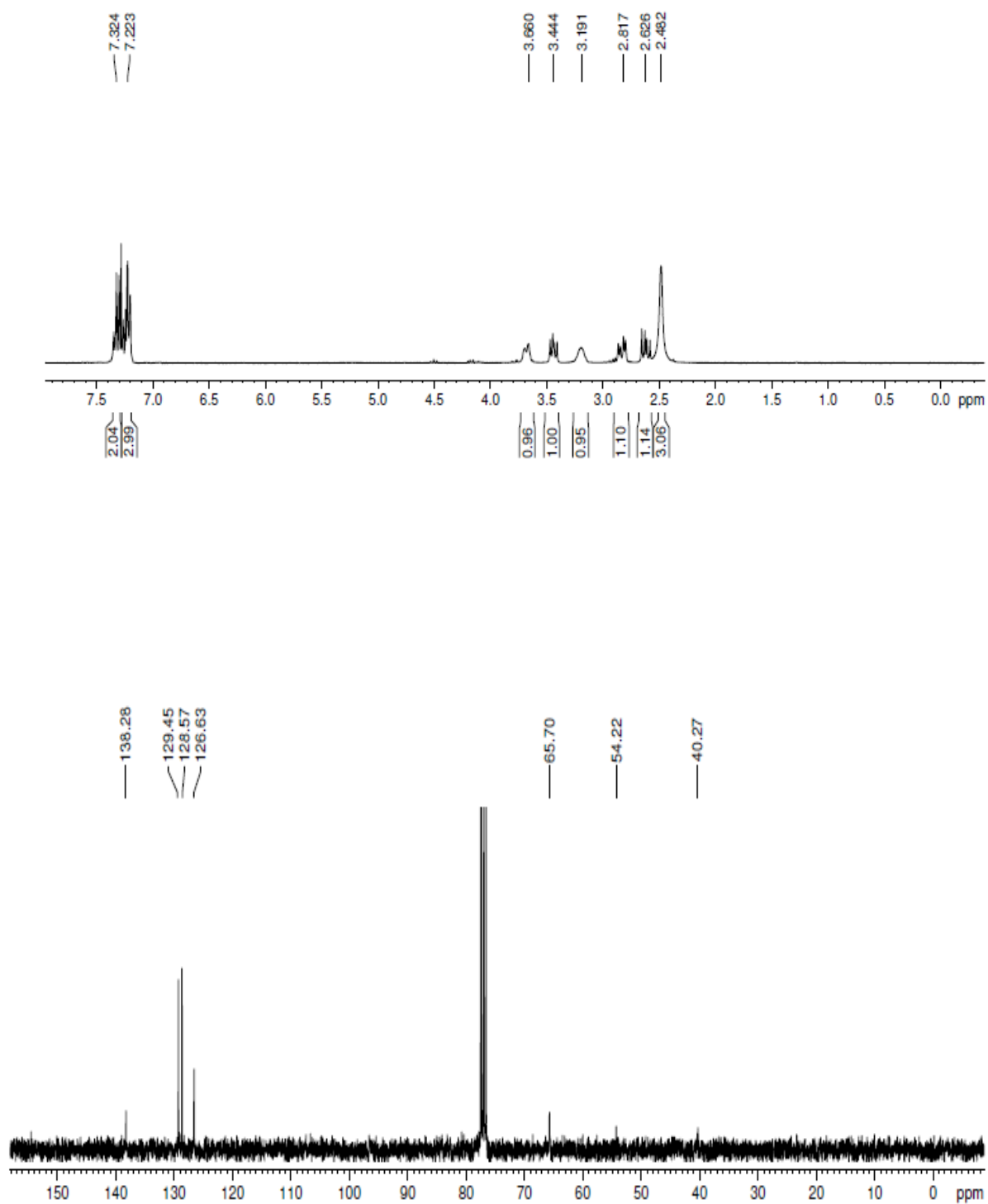


**Figure 18:**  $^1\text{H}$  and  $^{13}\text{C}$  NMR spectra of **56**



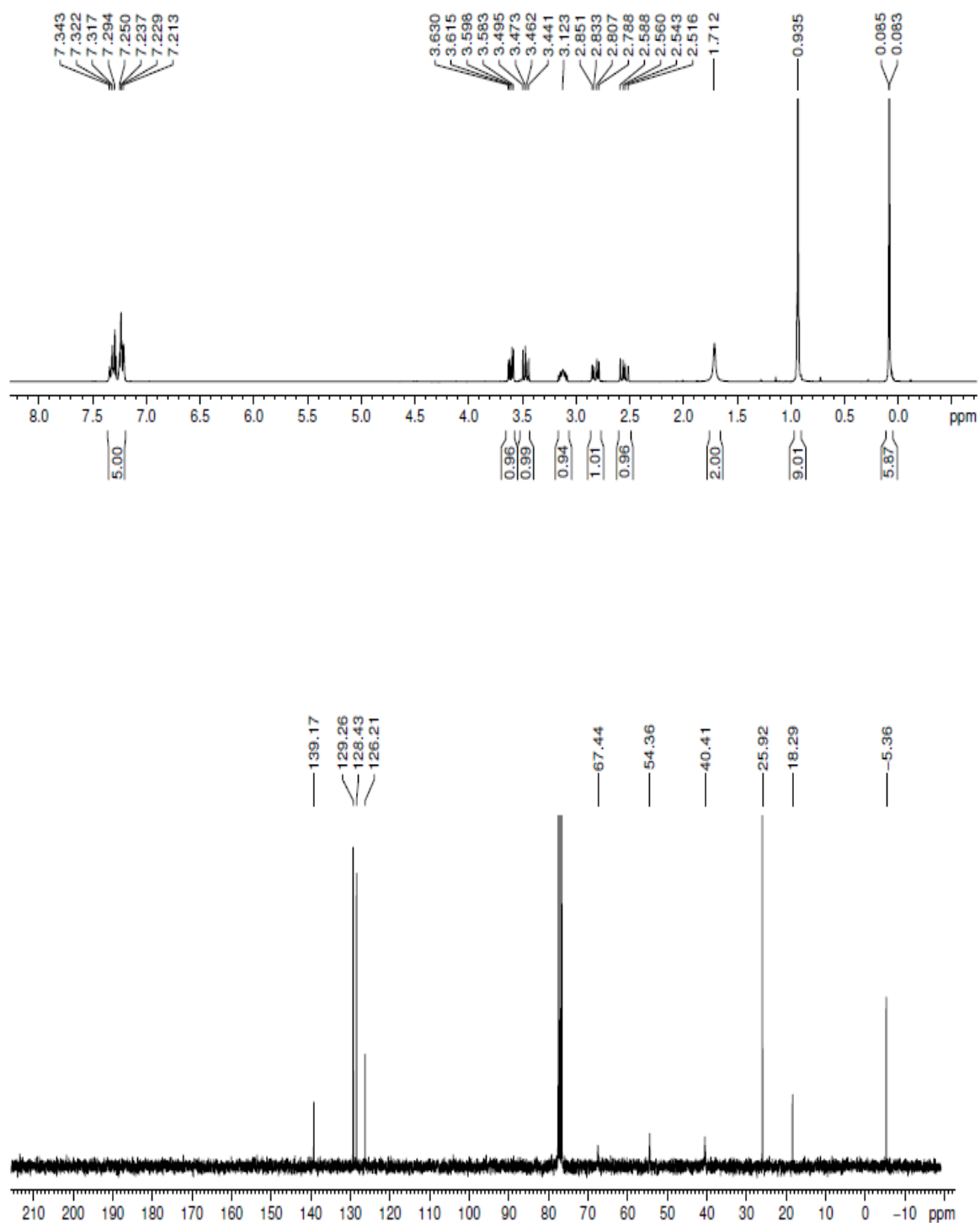


**Figure 19:** <sup>1</sup>H and <sup>13</sup>C NMR spectra of **57**

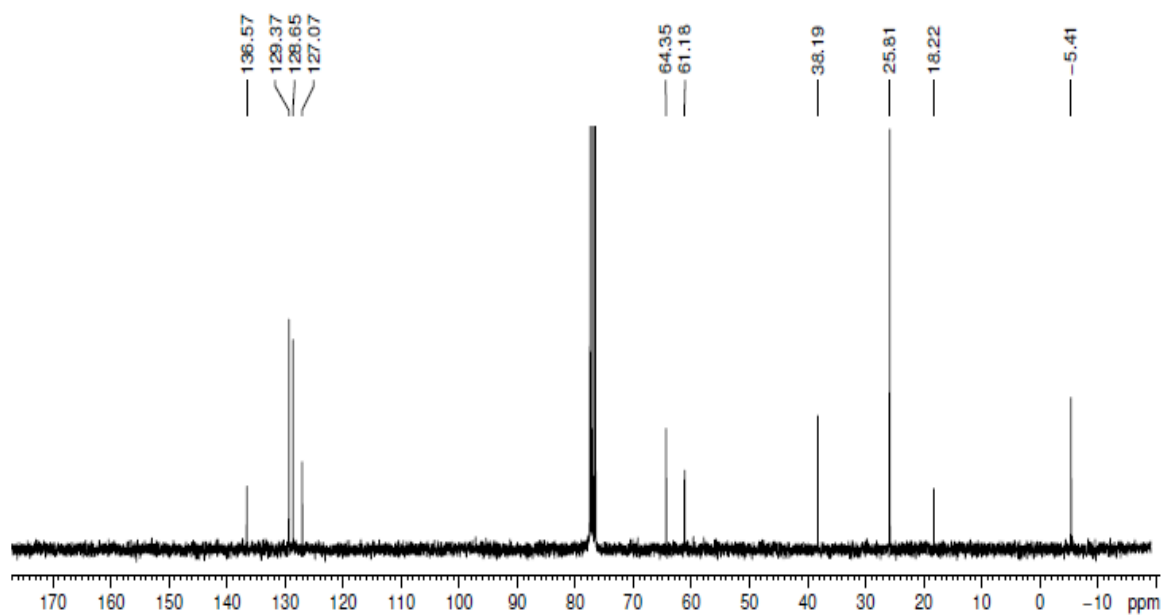
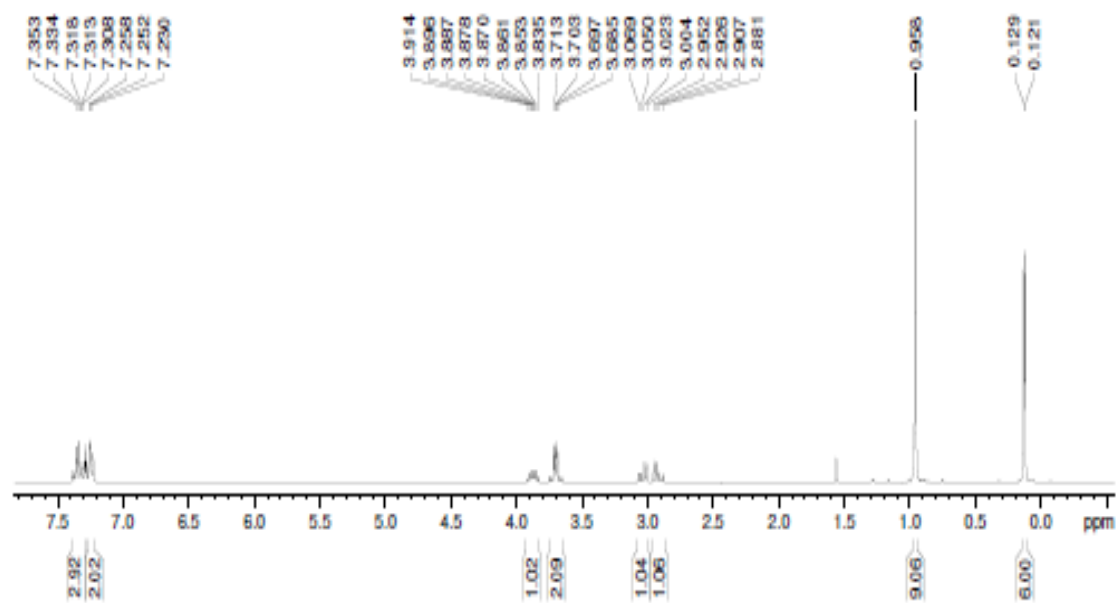


**Figure 20:** <sup>1</sup>H and <sup>13</sup>C NMR spectra of **52**

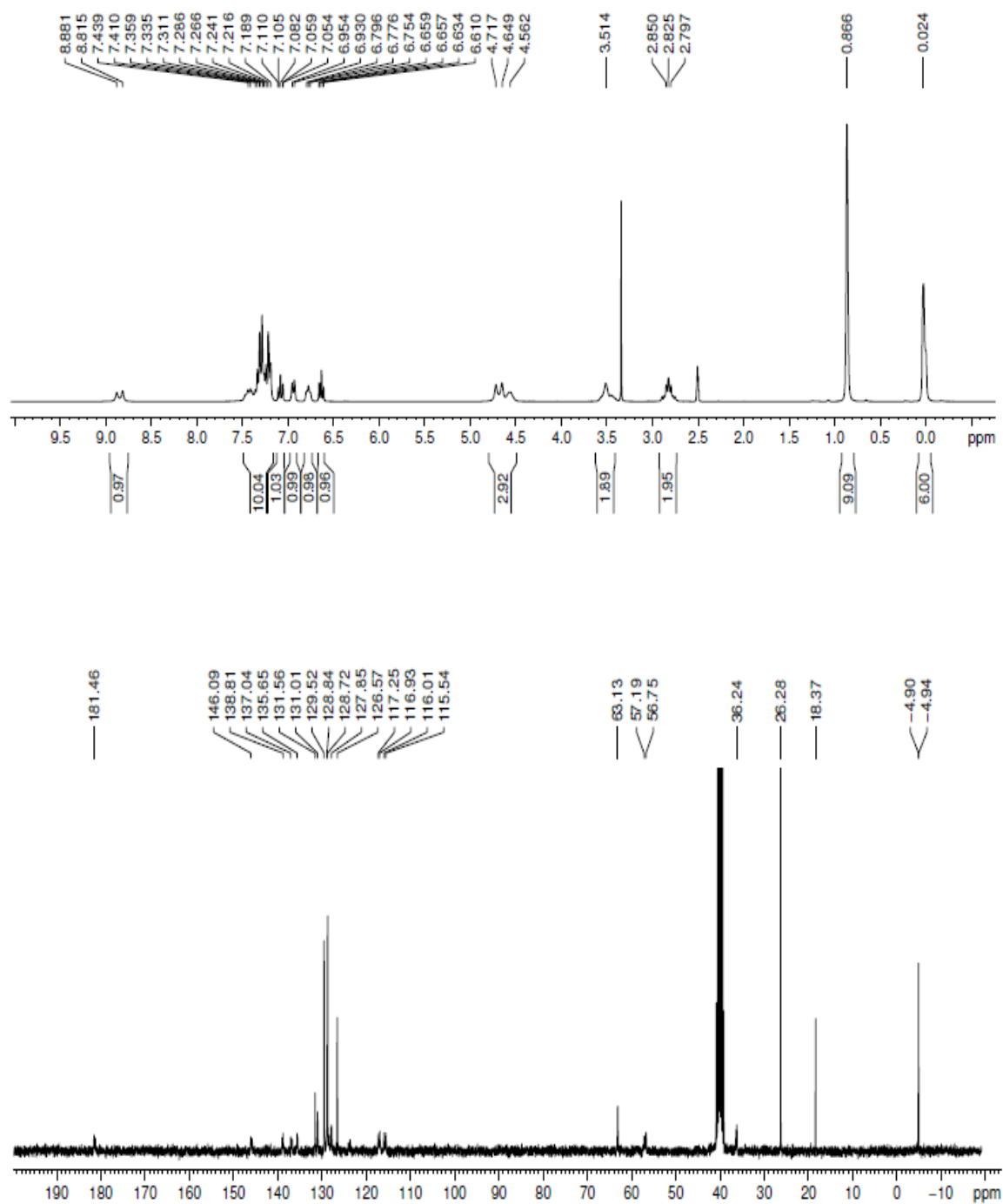


**Figure 21:**  $^1\text{H}$  and  $^{13}\text{C}$  NMR spectra of **53**

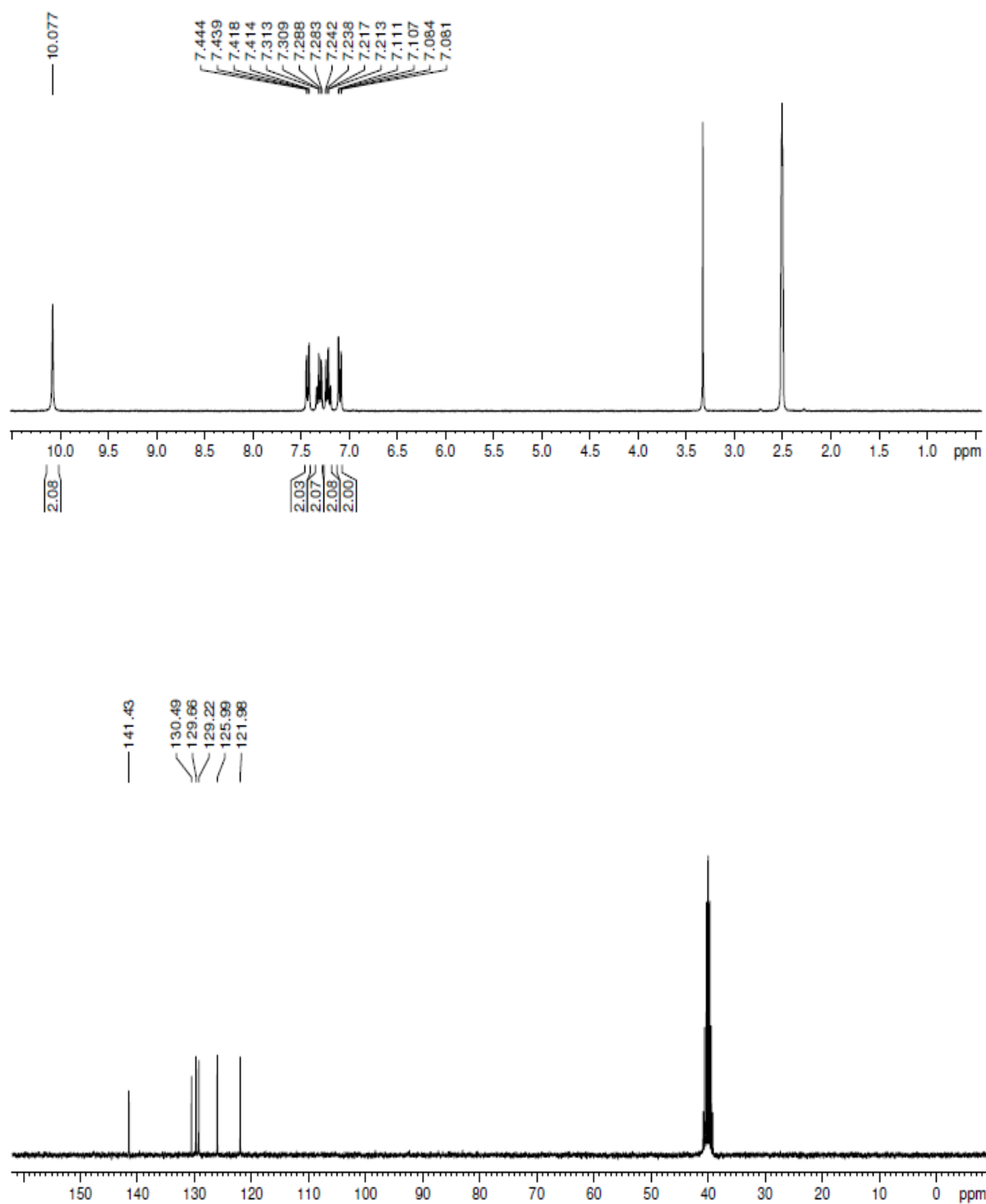


**Figure 22:**  $^1\text{H}$  and  $^{13}\text{C}$  NMR spectra of **55**

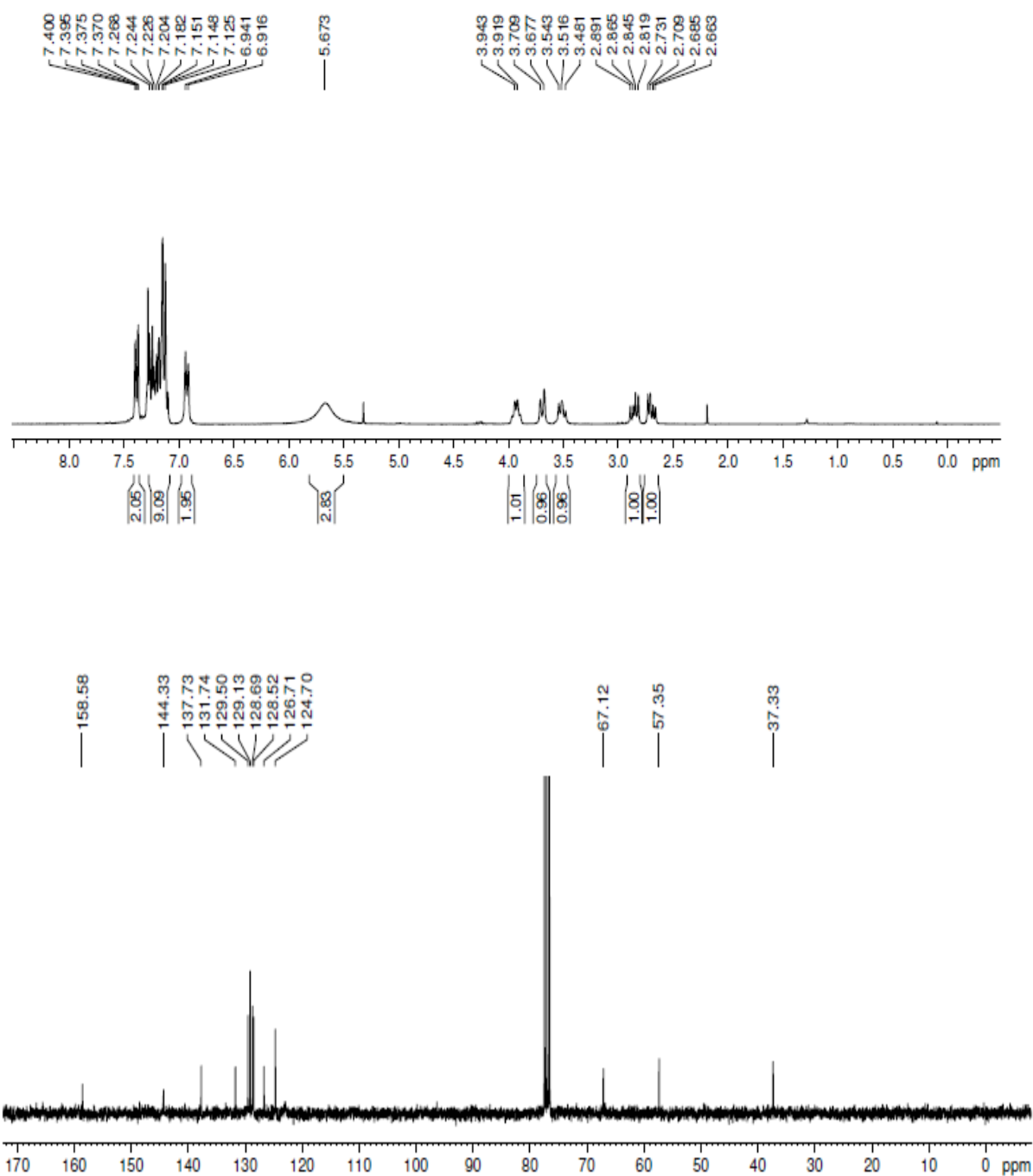


**Figure 23:**  $^1\text{H}$  and  $^{13}\text{C}$  NMR spectra of point chiral guanidine catalyst **48**

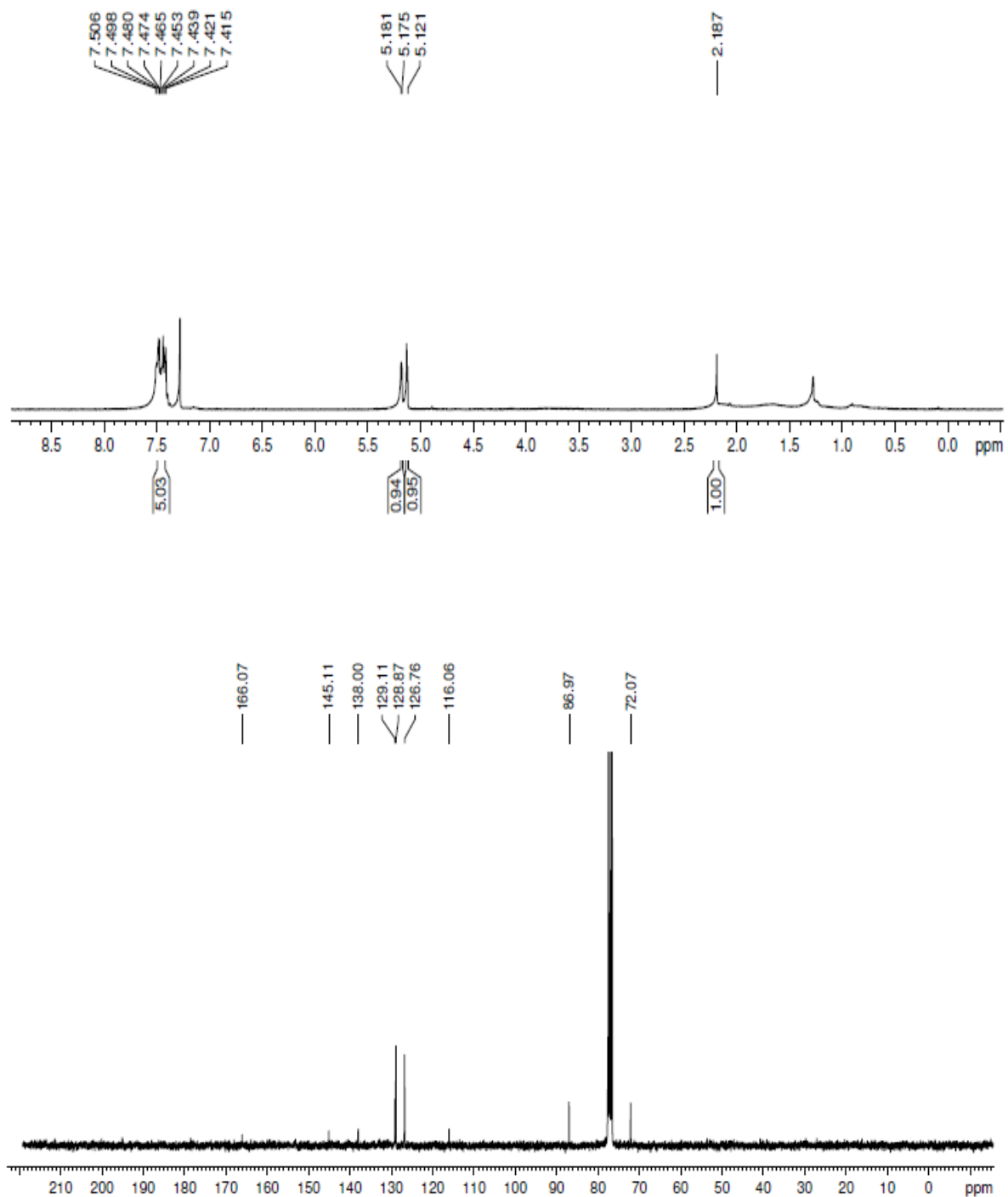


**Figure 24:**  $^1\text{H}$  and  $^{13}\text{C}$  NMR spectra of *syn* **66**

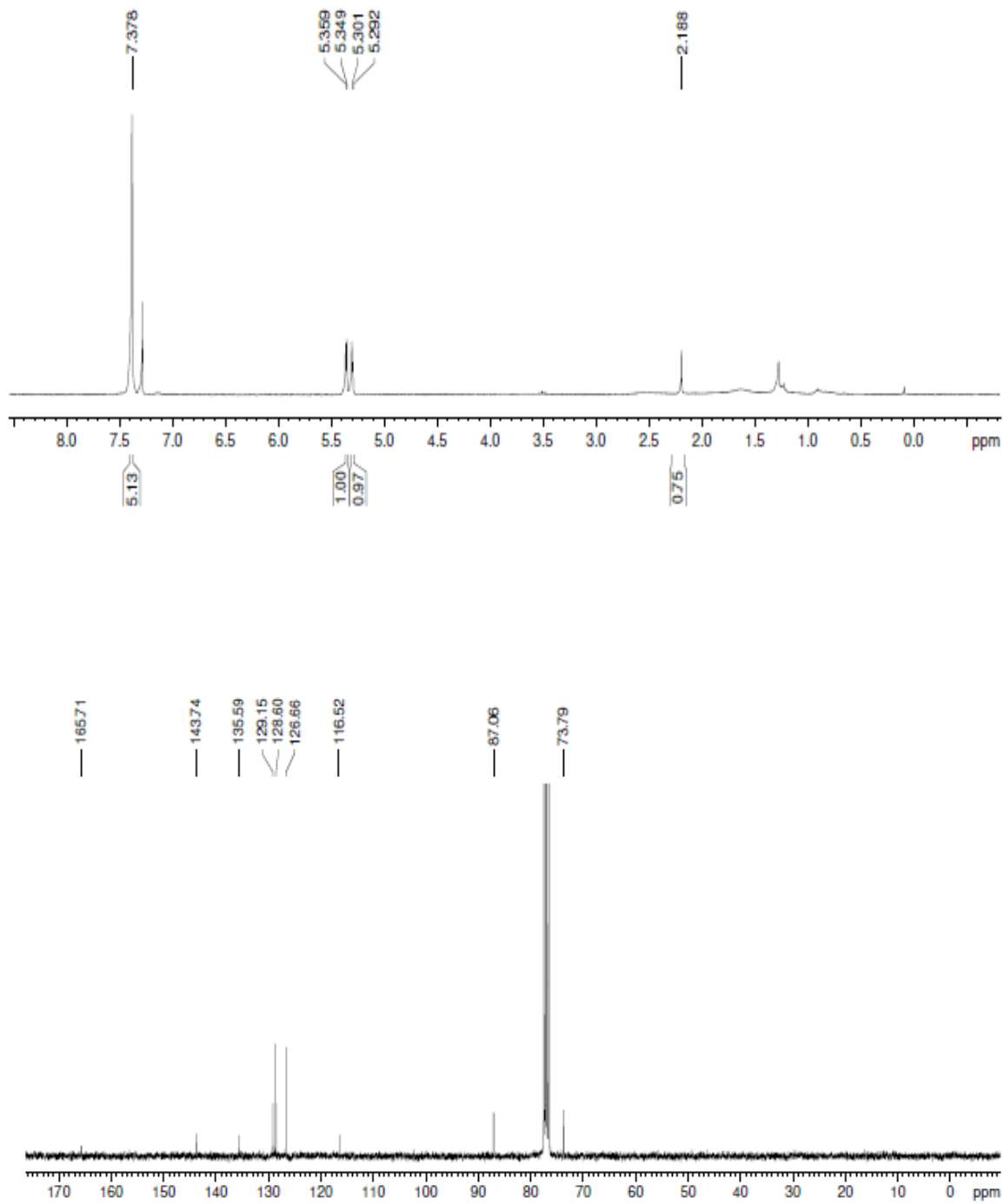


**Figure 25:**  $^1\text{H}$  and  $^{13}\text{C}$  NMR spectra of *anti* 66

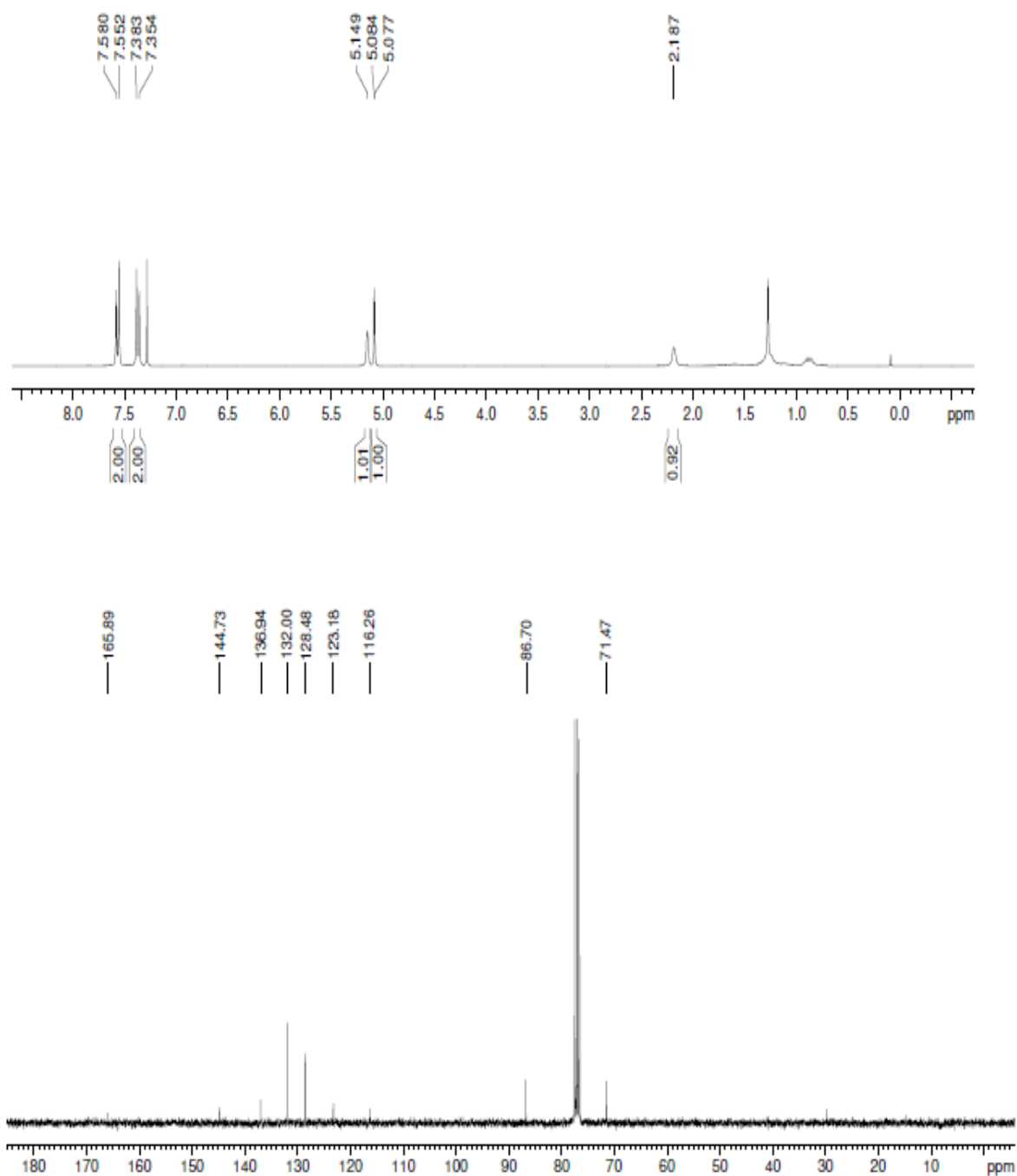


**Figure 26:**  $^1\text{H}$  and  $^{13}\text{C}$  NMR spectra of *syn* 63



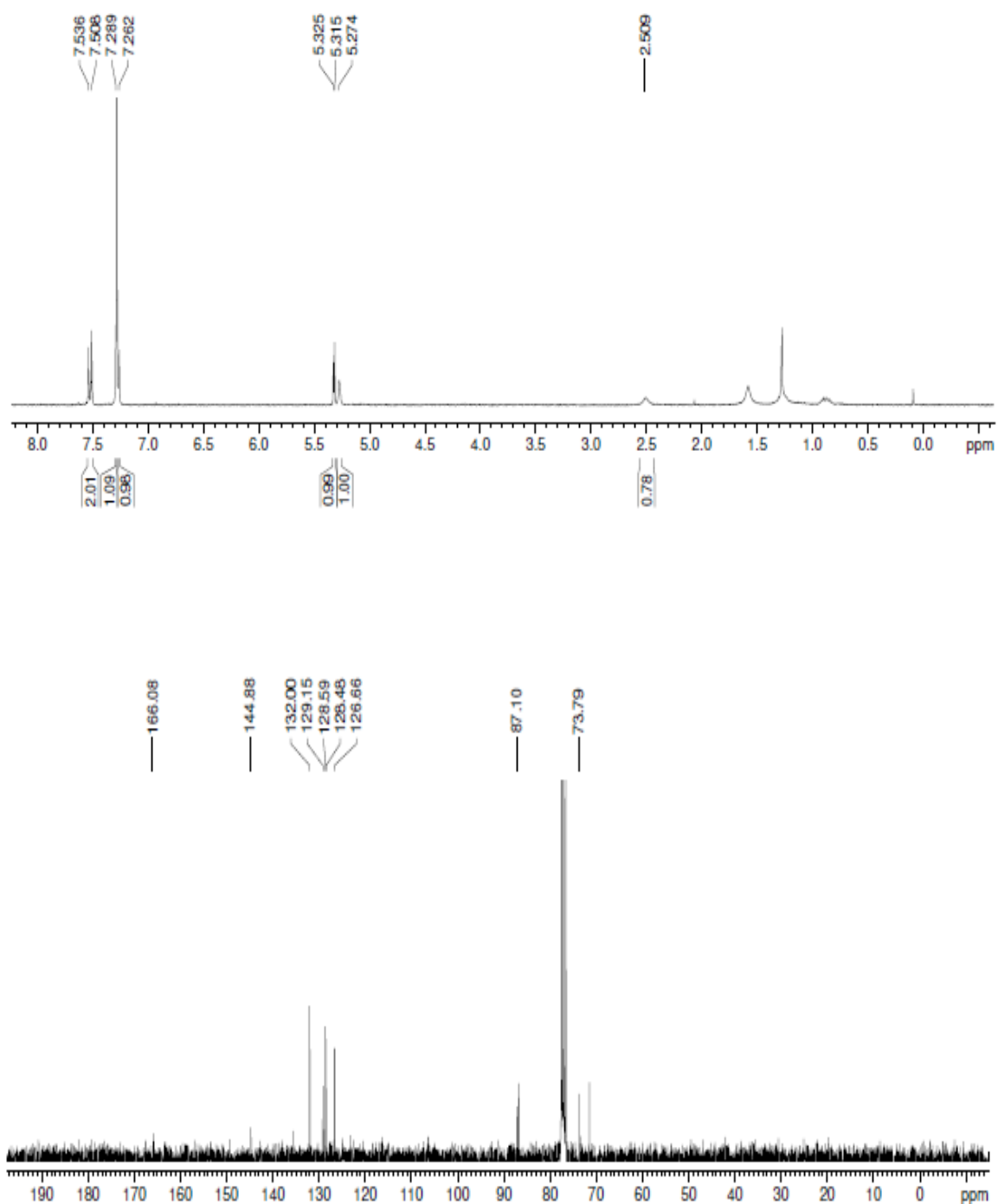


**Figure 27:**  $^1\text{H}$  and  $^{13}\text{C}$  NMR spectra of *anti* 63

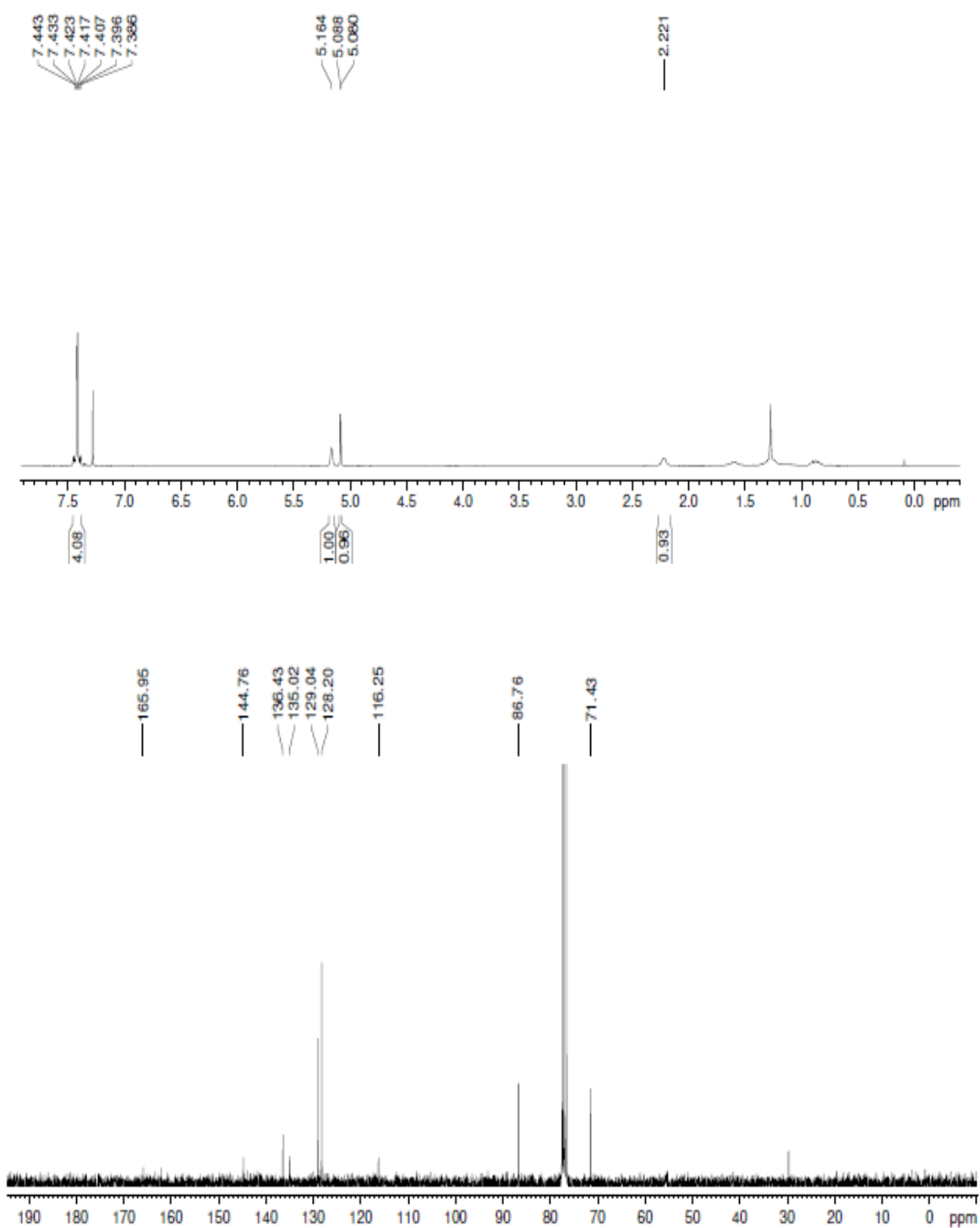


**Figure 28:**  $^1\text{H}$  and  $^{13}\text{C}$  NMR spectra of *syn* **64**

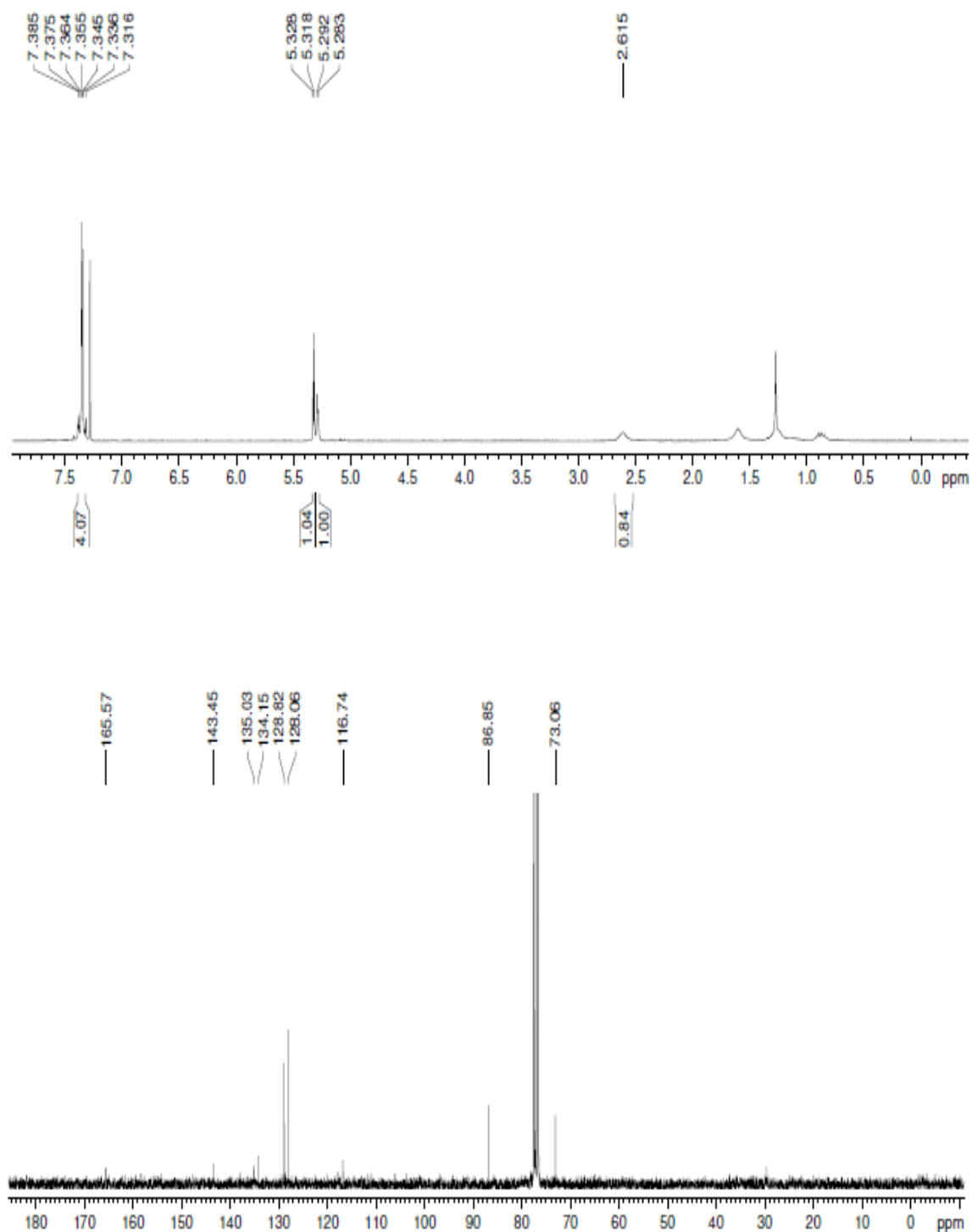


**Figure 29:** <sup>1</sup>H and <sup>13</sup>C NMR spectra of *anti* 64

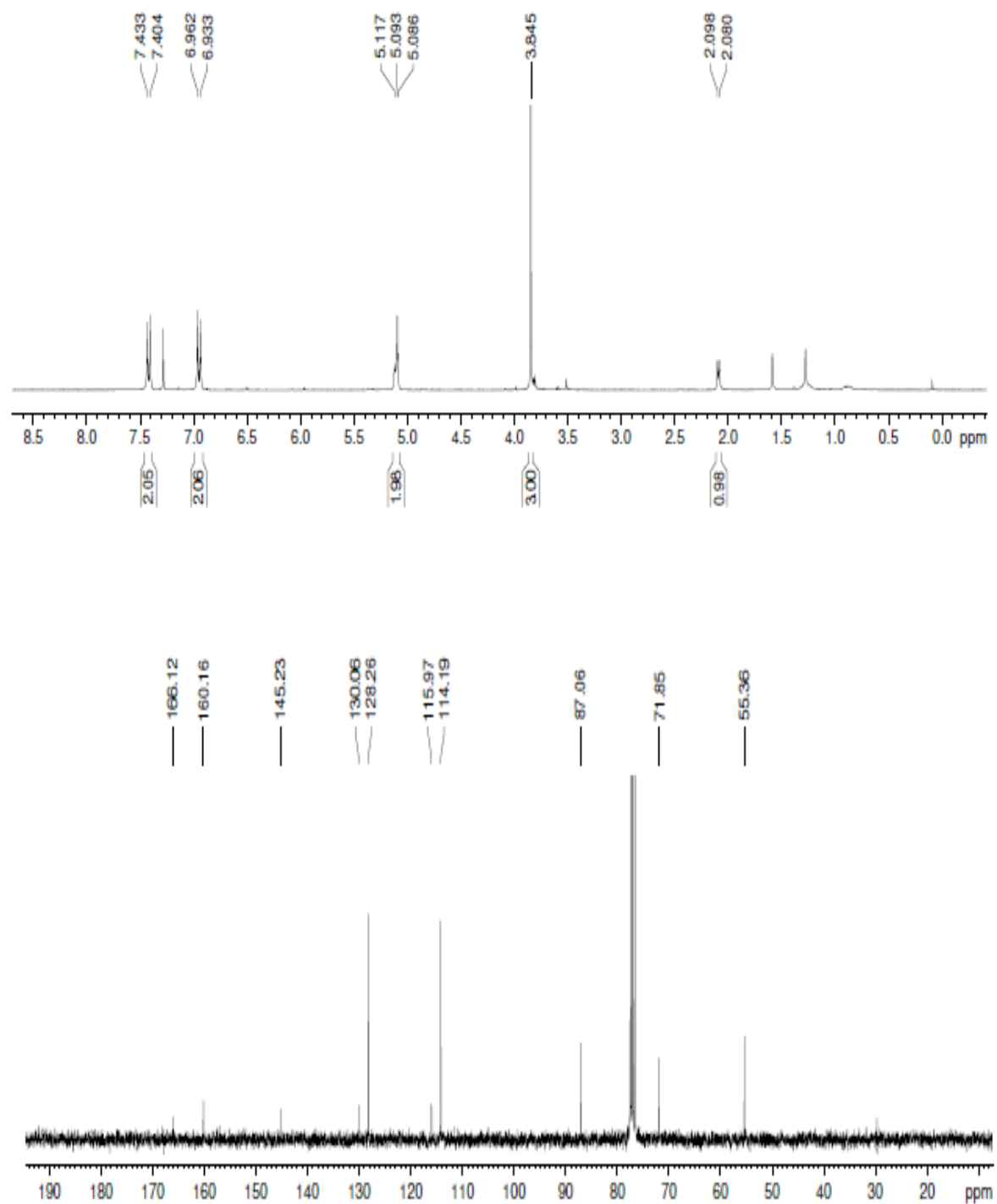


**Figure 30:**  $^1\text{H}$  and  $^{13}\text{C}$  NMR spectra of *syn* 65

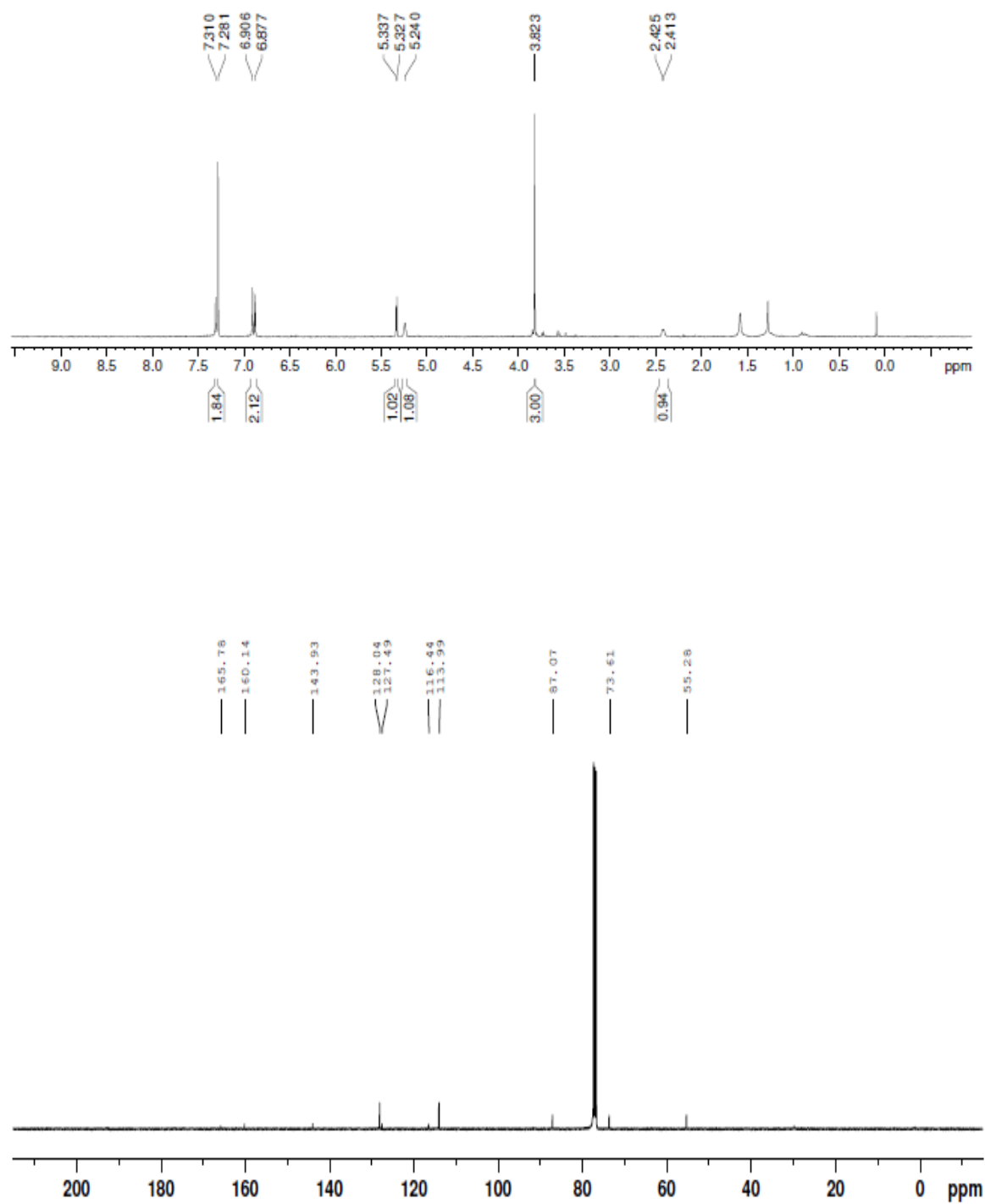


**Figure 31:**  $^1\text{H}$  and  $^{13}\text{C}$  NMR spectra of *anti* **65**